Spring 2019

The Use of Multi-Targeting Natural Products for the Treatment of Cancer

Wesley Taylor

THE USE OF MULTI-TARGETING NATURAL PRODUCTS FOR THE TREATMENT OF CANCER

by

Wesley Taylor

Bachelor of Science
The University of Alabama, 2016

Submitted in Partial Fulfillment of the Requirements

For the Degree of Master of Science in

Chemical Engineering

College of Engineering and Computing

University of South Carolina

2019

Accepted by:

Ehsan Jabbarzadeh, Director of Thesis

Melissa Moss, Reader

Mark Uline, Reader

Cheryl L. Addy, Vice Provost and Dean of the Graduate School

DEDICATION

I would like to dedicate this thesis to my wonderful wife, Morgan, whose support has been invaluable throughout my graduate studies.

ACKNOWLEDGEMENTS

I would like to thank my friends and family who have encouraged and supported my pursuit of this degree. I would also like to thank my advisor, Ehsan Jabbarzadeh, who has not only been an excellent mentor and teacher, but who has also been very accommodating in allowing me to pursue my career while writing this thesis. Additionally, I would like to thank the members of my thesis committee, Drs. Melissa Moss and Mark Uline, for their flexibility in scheduling and for their willingness to serve on the committee. I would like to extend special thanks to Drs. Sara Moghadam and Maria Yanez who helped generate data for this thesis in addition to proofreading my work and providing moral support throughout my time at The University of South Carolina. Finally I gratefully acknowledge support from the National Institutes of Health (NIH/NIBIB AR063338 and NIH/NIAMS EB026813) and the National Science Foundation (NSF 1631439).

ABSTRACT

The paradigm shift in cancer treatments from traditional chemotherapeutics to targeted therapies has rapidly improved prognoses for patients for whom cancer was once a death sentence. This is especially true in the case of targeted immune therapies which activate the body's own natural defense system to fight cancer. Despite these advances, however, cancer remains the second leading cause of death in the United States. The promise of targeted therapeutics has faced significant hurdles in providing effective cancer treatments, namely the limited percentage of susceptible cancers for each treatment, high cost burden, high toxicities, and significant risk of treatment induced resistance. As a result, targeted therapies are often combined into a cocktail of multiple drugs, including other targeted therapeutics and chemotherapies. These hurdles have led to a resurgence of interest in natural products to treat cancer. Natural products tend to be cheap, safe to use, and capable of targeting multiple cellular pathways at once. Multi-targeting natural products which simultaneously affect multiple cellular processes including angiogenesis, metastasis, immune response, and apoptosis are uniquely positioned to provide a robust treatment for cancer when used alone or in combination with current targeted therapeutics.

This study investigates the anticancer properties of two natural products, clusianone and deacetylnemorone. The compounds were screened against 60 cancer cell lines to determine the growth inhibitory properties of the compounds. Both compounds

were found to inhibit cancer cell growth across all nine of the tissue types screened at doses of 10 μM or less. Clusianone subsequently induced cell death in 25 of the cell lines screened at 100 μM concentrations, while deacetylnemorone only induced cell death in one melanoma cell line SK-MEL-5 at 10 μM. Clusianone was further shown to target tubulin polymerization and induce dose dependent apoptosis in non-small cell lung cancer. The compounds were additionally assayed in vitro to determine their effects on angiogenesis, macrophage polarization, and cancer cell invasion. Both compounds were shown to reduce tube formation between endothelial cells, a crucial step in angiogenesis, and inhibit cancer cell invasion into cell free gaps. Finally, clusianone was shown to increase the expression of TNF-α and IL-6 in THP-1 derived macrophages, suggesting polarization to an M1, anticancer state. The multi-targeting nature described may allow these compounds to simultaneously induce cell death directly in tumor cells, starve tumors by reducing their blood supply, limit the invasion of cancers into healthy tissue, and stimulate the immune system to attack cancer cells. This multipronged attack would provide treatments which are less susceptible to resistance when used alone in addition to enhancing the effects of targeted therapies when used in combination. Clusianone and deacetylnemorone are therefore promising drug leads for anticancer therapy.

TABLE OF CONTENTS

LIST OF TABLES

LIST OF FIGURES

LIST OF ABBREVIATIONS

ABC.....ATP-binding cassette

ABCB1.....ATP binding cassette B1

ALDH..... Aldehyde dehydrogenase

ALK (C1156Y)..... Anaplastic lymphoma kinase C1156Y

ATCC..... American Type Culture Collection

ATRA..... All-Trans Retinoic Acid

BAA.....BODIPY-aminoacetate

BAAA .....BODIPY-aminoacetaldehyde

BCA.....Bicinchoninic acid

BCRP..... Breast cancer resistance protein

BRAF.....B-rapidly accelerated fibrosarcaoma

BSA ..... Bovine serum albumin

CAR-T cell .....Chimeric antigen receptor T-cell

CD133..... Cluster of differentiation 133

CD24..... Cluster of differentiation

CD243..... Cluster of differentiation 243

CD44..... Cluster of differentiation 44

cDNA ..... Complementary deoxyribonucleic acid

CNS..... Central nervous system

COSY ..... H-H correlation spectroscopy

CSCs ..... Cancer stem cells

CT ..... Cycle threshold

DAPI .....4’,6-diamidino-2-phenylindole, dihydrochloride

DEAB ..... Diethylaminobenzaldehyde

DHC .....Dihydrocapsaicin

DMSO ..... Dimethyl sulfoxide

DOX ..... Doxorubicin hydrochloride

EDTA ..... Ethylenediaminetetraacetic acid

EGM-2 ..... Endothelial cell growth medium-2

ELISA ..... Enzyme-linked immunosorbent assay

EMT ..... Epithelial-mesenchymal transition

epCAM ..... Epithelial cell adhesion molecule

ER ..... Endoplasmic reticulum

ESA ..... Epithelial specific antigen

FACS ..... Fluorescence-activated cell sorting

FBE .....Fetal Bovine Essence

FDA ..... Food and Drug Administration

FdUrd .....5-fluoro-2’-deoxyuridine

GAPDH .....Glyceraldehyde 3-phosphate dehydrogenase

GI50 .....Growth inhibition of 50%

HA .....Hyaluronan

HAS ..... Heat stable antigen

HMBC ..... Heteronuclear multiple bond correlation

HRP ..... Horseradish peroxidase

HSQC ..... Heteronuclear single quantum coherence

HTS ..... High throughput screening

HUVEC ..... Human umbilical vein cells

IL-6 ..... Interleukin-6

JAK3 ..... Janus kinase 3

LC50 ..... Lethal concentration of 50%

LC-MS ..... Liquid chromatography-mass spectrometry

MDR ..... Multiple drug resistance

MDR1 ..... Multidrug resistance protein 1

MEK ..... Mitogen-activated protein kinase/extracellular signaling regulated kinases

MEM ..... Minimum essential medium

MET ..... Mesenchymal-epithelial transition

MS ..... Mass spectrometry

mTOR ..... Mechanistic target of rapamycin

MTS ..... 3-(4,5-dimethylthiazol-2-yl)-5-(3-carboxymethoxyphenyl)-2-(4-sulfophenyl)-2H-tetrazolium

NCI-60 ..... National Cancer Institute-60

NIH ..... National Institutes of Health's

NMR ..... Nuclear magnetic resonance

NPs ..... Natural products

Oct4 ..... Octamer-binding transcription factor

PARP ..... Poly (ADP-ribose) polymerase

PBS ..... Phosphate buffered saline

PD-1 ..... Programmed cell death protein 1

P-gp ..... P-glycoprotein 1

PI ..... Propidium iodide

PI3K ..... Phosphoinositide 3-kinase

PMA 12-myristate 13-acetate

PMSF ..... Phenylmethylsulfonyl fluoride

PTEN ..... Phosphatase and tensin homolog

RIPA ..... Radio-immunoprecipitation assay

RNA ..... Ribonucleic acid

RPMI ..... Roswell Park Memorial Institute

rT-PCR ..... Real time-polymerase chain reaction

SDS ..... Sodium dodecyl sulfate

SP ..... Side population

STAT3 ..... Signal transducer and activator of transcription 3

TAMs ..... Tumor associated macrophages

TBS ..... Tris buffered saline

TBST ..... TBS with Tween

TGF-ß ..... Transforming growth factor beta

TGI ..... Total growth inhibition

TICs .....Tumor initiating cells

TMB .....Tetramethylbenzidine

TNFα ..... Tumor necrosis factor alpha

TOF-MS.....Time of flight mass spectrometry

VEGF .....Vascular endothelial cell growth factor

CHAPTER 1

INTRODUCTION

The treatment of cancer has been revolutionized by the advent of targeted therapies. These therapies take advantage of our ever-evolving understanding of cancer biology and cellular pathways, by specifically interacting with key cancer associated proteins. This represents a dramatic shift from traditional chemotherapeutics, which were used to induce cell death in a wide range of cancer cell types through a variety of mechanisms, from causing DNA damage to interfering with microtubule function. Targeted therapies have expanded the universe of suitable cancer treatments from the primarily cytotoxic molecules of traditional chemotherapies to a range of therapies which may induce cell death, activate the immune system to attack cancer cells, or inhibit the formation of new vasculature to the tumor environment. Due to the targeted nature of these therapies, they can be tailored to very specific cancer morphologies, increasing efficacy in applicable patients.

Despite these advances, however, cancer remains the second leading cause of death in the United States[1]. The results gleaned from the clinical use of targeted therapies have been disappointing due to the major setbacks associated with their use. One major hurdle is the cost associated with the treatments. The low population of patients treatable with each developed therapy in combination with the expense of drug development can lead to prohibitive treatment cost to the patient. This is particularly

apparent in the case of the chimeric antigen receptor T-cell (CAR-T cell) therapy tisagenlecleucel, which is made by isolating a patient's T-cells and genetically engineering them to target cancer cells when re-introduced into the body. This personalized treatment, while effective, costs approximately $475,000[2].

Another major setback for targeted cancer treatments is the limited number of patients treatable with each developed therapy. As targeted therapeutics are engineered to affect a specific molecule, tumors with little expression or limited reliance on the target protein of a particular therapy cannot be effectively treated with that therapy. For example, the anti-programmed cell death protein 1 (PD-1) therapy nivolumab, is a targeted therapy which blockades the immune checkpoint process leading to cancer cell evasion from the immune system. However, this therapy has been shown to be ineffective at treating cancers with low mutational burden or low immunogenicity[3].

Arguably one of the most problematic hurdles faced by targeted therapies is acquired resistance to treatment. Many of these therapies are initially effective for applicable patients but quickly lose efficacy as the patient is treated. This could be due to increased expression of cancer stem cells, upregulation of unrelated cellular survival pathways, or alterations in the structure or expression of the target protein in response to the treatment. Targeted therapies from kinase inhibitors to angiogenesis inibitors, such as sorafenib and bevacizumab, have been limited by the development of resistance[4-6]. As a result of these challenges, targeted therapies are often combined with other unique targeted therapies or traditional chemotherapeutics to increase their efficacy and limit

the occurrence of treatment resistance. This thesis investigates the potential of natural compounds to be used in these cancer treatment cocktails.

Natural products possess the unique ability to influence multiple cellular targets simultaneously. As a result, these compounds are suggested for use in conjunction with targeted therapy/chemotherapeutic mixtures synergizing with multiple components of the cocktail, affecting unrelated cancer related pathways, and reducing the possibility for developed resistance. In the following chapters, the potential of natural products for the treatment of cancer is evaluated. In Chapter 2, a literature review is provided to give a brief background on the use of natural products to treat cancer. Specifically this review details the use of multi-targeting natural products to target cancer stem cells, inhibiting the invasion, metastasis, and drug resistance of cancer. Following this literature review, two specific compounds which were screened for anti-cancer properties from a library of natural products are presented. Chapter 3 details the use of the abietane diterpenoid, deacetylnemorone, to simultaneously inhibit cancer cell growth, inhibit cancer cell invasion, inhibit angiogenesis, and re-sensitize treatment resistance cancers to chemotherapy. Chapter 4 discusses the acylphloroglucinol, clusianone, a natural compound capable of inducing apoptosis in non-small cell lung cancer, inhibiting angiogenesis, and modulating the immune system. Potential mechanisms of action for clusianone are also discussed in this chapter. Finally, the findings of this study are summarized in Chapter 5.

CHAPTER 2

THE USE OF NATURAL PRODUCTS TO TARGET CANCER STEM CELLS[1]

2.1 ABSTRACT

The cancer stem cell hypothesis has been used to explain many cancer complications resulting in poor patient outcomes including induced drug resistance, metastases to distant organs, and tumor recurrence. While the validity of the cancer stem cell model continues to be the cause of much scientific debate, a number of putative cancer stem cell markers have been identified making studies concerning the targeting of cancer stem cells possible. In this review, a number of identifying properties of cancer stem cells have been outlined including properties contributing to the drug resistance and metastatic potential commonly observed in supposed cancer stem cells. Due to cancer stem cells' numerous survival mechanisms, the diversity of cancer stem cell markers between cancer types and tissues, and the prevalence of cancer stem cell markers among healthy stem and somatic cells, it is likely that currently utilized treatments will continue to fail to eradicate cancer stem cells. The successful treatment of cancer stem cells will rely upon the development of anti-neoplastic drugs capable of influencing many cellular mechanisms simultaneously in order to prevent the survival of this evasive subpopulation. Natural compounds represent a historically rich source of novel,

[1] Taylor, W.F. and Jabbarzadeh, E. 2017. *Am J Cancer Res.* 7: 1588-1605.
Reprinted here with permission of publisher.

biologically active compounds which are able to interact with a large number of cellular targets while limiting the painful side-effects commonly associated with cancer treatment. A brief review of select natural products that have been demonstrated to diminish the clinically devastating properties of cancer stem cells or to induce cancer stem cell death is also presented.

2.2 INTRODUCTION

Modern chemotherapy, radiotherapy, and other antineoplastic regimens have made the treatment of many solid tumors possible and have given hope to those diagnosed with cancer. However, the prognosis for many cancer patients remains bleak due to the high rate of cancer recurrence and multiple drug resistance (MDR) seen after initial chemotherapy treatments. Metastatic cancers affecting multiple organ systems are particularly difficult to treat and oftentimes demand the partial or complete surgical resection of multiple tissues. Cancer stem cells (CSCs) potentially explain many of the shortcomings of established chemotherapy treatments.

CSCs are distinguished as a small population of tumor cells which are able to form phenotypically diverse tumors, as wells as self-renew and differentiate. They are described as belonging to a group of tumor initiating cells (TICs) which may or may not possess stem-like characteristics, but debate remains as to how large a proportion of TICs are indeed stem-like. Additionally, it is not clear whether or not the plasticity of tumor cells allows any cell to become stem-like and gain the capability to recapitulate heterogeneous tumors. The role of CSCs in tumor formation was first identified by Bonnet and Dick in the late 90s [7]. In this paper, the $CD34^{+}/CD38^{-}$ subpopulation of cells from acute

myeloid leukemia were shown to form tumors in immunodeficient NOD/SCID mice with higher efficiency than the $CD34^+/CD38^+$ subpopulation. The ability of CSCs to asymmetrically divide, allowing the CSC to self-renew as well as differentiate to produce a heterogeneous tumor containing multiple cell phenotypes, was also identified. Since this discovery, the CSC hypothesis has been tested rigorously, and evidence that CSCs play a crucial role in tumor development for many different cancers has been reported. These include breast carcinoma[8, 9], colorectal carcinoma [10], head and neck squamous cell carcinoma [11], hepatocellular carcinoma [12, 13], lung carcinoma [14], ovarian adenocarcinoma [15], glioblastoma [16], and pancreatic carcinoma [17] among others.

According to the CSC model, cancer recurrence after treatment is due to the superior resistance of CSCs to cellular toxins and insults. While current treatments are capable of eradicating the bulk of the tumor mass, the lingering CSCs are able to form new, fully developed tumors from a small number of cells or even a single cell. CSCs are thought to resist treatment through several cellular mechanisms including the overexpression of drug efflux pumps, quiescence, and detoxifying enzymes[18]. A high population of CSCs within a tumor has subsequently been linked to MDR and a poorer prognosis for cancer patients [19]. Furthermore, the cellular machinery of CSCs has been shown to allow for epithelial-mesenchymal transition (EMT), a process by which epithelial cells lose their cell-to-cell and/or cell-to-matrix adhesion and can survive in a migratory state [20]. By undergoing EMT, migrating to other organs, and reattaching by mesenchymal-epithelial transition (MET), CSCs are hypothesized to initiate the formation of metastatic tumors.

Current methods for the treatment of cancer have been demonstrated to be insufficient in eliminating CSC populations from a number of cancer types. $CD133^+$ glioma CSCs have been shown to resist radiation therapy to a higher degree than their $CD133^-$ counterparts [21]. Breast CSCs exhibit a similar resistance to radiotherapy in addition to common chemotherapy treatments [22, 23]. Furthermore, the CSC population in residual breast cancer tumors has been shown to increase significantly following chemotherapy treatments, nearly doubling the tumorigenic potential of the residual cancer cells in immunodeficient SCID mice [23]. Treatments targeting a specific molecule or surface marker are likely to fail to eliminate CSCs due to the multiple survival pathways activated in CSCs in addition to the ambiguity of CSC markers across different tissue types, the presence of commonly used CSC markers in healthy tissues, and the often required combination of markers used to denote CSC populations. Treatments capable of reducing CSC populations will therefore require the development of novel, diverse, and multi-targeted approaches for cancer treatment. Due to the numerous, still poorly understood characteristics of CSCs, the discovery of CSC targeting therapies will likely be the result of opportunistic screening of new or known compounds against CSC populations.

Natural products may be the key to discovering novel treatments demanded by the difficulty of treating CSCs. Natural products (NPs) have been a historically rich source of biologically active compounds for the pharmaceutical industry. The value of NPs in medicine is a result of their ability to influence multiple signaling pathways simultaneously while producing diminished, benign side effects. The success of these compounds, especially as they relate to cancer treatment, has led researchers to

investigate the effect of a number of NPs on CSCs. Figure 2.1 summarizes the role of CSCs in cancer formation, metastasis, and relapse in addition to the potential role of natural products in their treatment. In this review, properties distinguishing CSCs as well as properties which give rise to the drug resistance associated with CSCs are identified. A brief review of select NPs which have been shown to target CSCs is also provided.

2.3 IDENTIFYING CANCER STEM CELLS

One of the major challenges facing cancer stem cell research is accurately defining which tumor cell subpopulations are stem like. The gold standard for identifying CSCs remains the ability of a small number of cells to generate a fully developed tumor when injected into immunocompromised mice, but the cost, time, and labor associated with animal studies have led to the search for markers of stem like cancer cells. Many putative CSC markers have been proposed and subsequently identified as targets for chemotherapeutics. However, the expression of these markers has been shown to be inconsistent across CSCs from different tissues and tumor phenotypes [24, 25]. Additionally, many of the reported CSC markers are possessed by healthy stem cells and even non-cancerous, non-stem-like cells, posing a challenge to the development of targeted therapies based upon these markers.

Oftentimes, a combination of supposed CSC markers is required to denote the CSC population. For example, a common population of cells within breast cancer that has been deemed breast cancer stem cells are $CD44^+/CD24^-/ESA^+$ [8]. The most notable among these putative markers are the surface proteins CD44 and CD133 which have been used to identify CSCs in a wide array of cancer types. In addition to these supposed markers,

certain properties of CSCs have also been use to distinguish them from the rest of the tumor population. For example, cells known as the side population (SP) have been shown to possess a high percentage of TICs [13, 15, 16]. Tumors cells within the SP are distinguished by their ability to exclude Hoechst 33342 fluorescent stain which is typically assessed via flow cytometry.

Investigators have attempted to isolate populations of CSCs using these properties combined with flow cytometric techniques or selective growth environments. Using these purified populations of CSCs, their tumorigenic properties and specific responses to drug candidates can be better investigated. Low purity of isolated populations, the ability of CSCs to differentiate into phenotypically diverse populations, and disagreement over which markers should be used to identify CSCs still pose major hurdles to many of these techniques. A brief review of common CSC markers and characteristics used to identify or isolate CSC populations is provided below.

2.3.1 CD44

Cluster of differentiation 44 (CD44) is a very commonly utilized marker for CSCs. CD44 proteins are integral membrane glycoproteins which play a role in cell attachment to the extracellular matrix by binding to hyaluronan (HA). CD44 is often used in combination with other markers to denote CSCs; however, in cases such as head and neck squamous cell carcinoma, CD44 has also been used alone to identify cancer cells capable of self-renewal and differentiation [11]. The expression of this marker has been used as a putative marker for cancer stem cells in such tissues as breast [8], ovarian [26], pancreatic [27], and bladder [28] along with many others. CD44 regulates the growth, migration, and

invasion characteristic of CSCs in addition to modifying the extracellular matrix of tissues to support new tumor formation [29, 30]. Interestingly, cells expressing CD44 also produce a higher amount of the cytokine transforming growth factor beta (TGF-ß) which has been shown to aid EMT [31]. Further, HA-CD44 binding activates protein kinase C_e, which in turn phosphorylates the stem cell maintenance transcription factor, Nanog. Nanog then begins a signaling cascade which results in the upregulation of ATP binding cassette B1 (ABCB1), a drug efflux pump, contributing to MDR [30]. Reducing the population of CD44 expressing cells in tumor populations, therefore, has the potential to diminish the CSC population and limit invasion, metastases, and drug resistance in a broad spectrum of cancers.

2.3.2 CD133

Cluster of differentiation 133 (CD133) is a pentaspan surface membrane protein that is also commonly used as an indicator of CSCs. Interest in this marker as an indicator of CSC was generated by its original use as a hematopoietic stem cell marker [32]. CD133 has been identified as a CSC marker in glioblastomas [31] as well as colorectal [10], ovarian [33, 34], hepatocellular [12], lung [14], and pancreatic [35] cancers. CD133 is localized to membrane protrusions and microvilli, but little is known about the function of this protein in cells or CSCs in particular. It is apparent that while CD133 can be used to distinguish CSC populations, it may not play a direct or critical role in cancer formation or CSC maintenance. A study demonstrating this point showed that a $CD133^+$ colon cancer population was able to differentiate and self-renew even when CD133 expression had been knocked down [36]. What is clearer is that CD133 has been positively correlated with

poor outcomes for cancer patients. A meta-analysis of 603 gastric cancer patients from 8 different studies revealed that CD133 overexpression was linked to lymph node metastasis, distant metastasis, higher drug resistance, an increased relapse rate, and a lower 5-year survival rate [37]. The widespread presence of CD133 in putative CSC populations across numerous tissues, coupled with the poor prognosis of patients overexpressing CD133, validates this marker as a dependable marker for CSCs as well as a potential cancer drug target.

2.3.3 CD24

Cluster of differentiation (CD24) is yet another surface marker used to demarcate CSC populations. CD24 is a notable CSC marker as both its presence [17] and absence [9, 38] has been used to denote CSC phenotypes depending upon the tissue. CD24 is a surface expressing glycoprotein, also known as heat stable antigen (HSA), which was initially identified as a marker for hematopoietic subpopulations, typically B-cells. Numerous functions have been suggested for this protein, including signaling and cell attachment, and its expression can be seen in various cell types, most commonly acting as a marker of differentiation for hematopoietic and neuronal stem cells. CD24 is often seen in the context of adaptive immune response in which its expression can be seen in pre or immature-B cell populations or in activated T-cells [39]. The function of CD24 in tumor cells may be explained by the association of the marker with P-selectin, a molecule expressed by platelets and vascular endothelium, which may play an important mechanistic role in cancer cell adhesion and metastasis. In addition to acting as positive or negative marker for CSCs, depending upon the tissue of origin, the expression of CD24 has also been

associated with poor prognosis, larger tumors, and lymph node metastasis in a range of cancers, demonstrating its influence on clinical outcomes [40-42].

2.3.4 ESA OR EPCAM

Epithelial specific antigen (ESA), also known as epithelial cell adhesion molecule (epCAM) has been used to identify CSCs from breast [9], colorectal [43], and pancreatic [17] cancer. As the name implies, ESA is a surface marker typically expressed on epithelial cells, which regulates cell-to-cell adhesion. ESA is overexpressed in a majority of epithelial cancers, such as colorectal cancer, and as a result it has been the subject of numerous studies and targeted chemotherapy strategies. ESA has further been linked to the migratory and invasive capabilities of breast cancer and is highly expressed in breast cancer metastases [44]. By disrupting the expression of ESA, the migration and invasion of cancer cells in vivo can be diminished. The upregulation of this transmembrane glycoprotein, as a result, may play a role in the metastatic potential of proposed CSCs.

2.3.5 ALDH ACTIVITY

Increased aldehyde dehydrogenase (ALDH) activity has been used to identify CSCs with little technical difficulty. ALDH can refer to any number of enzymes classified as aldehyde dehydrogenases which act to catalyze the oxidation of aldehydes entering or produced within the body. By oxidizing aldehydes, these enzymes transform potentially deleterious compounds into carboxylic acids, preparing them for cellular metabolism. In this way they act to detoxify the cell. ALDH enzymes are highly expressed in liver cells, but their expression has also been used to distinguish numerous progenitor cells including hematopoietic stem cells [45] and neural stem cells [46] among others. ALDH enzymes are

therefore theorized to contribute to stem cells' robust ability to survive chemical stresses throughout the body. The cytoprotective effect of ALDH enzymes utilized by these stem cell populations, however, can also be used to protect CSCs from chemotherapy treatments.

ALDH activity has been used to identify CSCs of various tissues including colon [47], breast [48], head and neck squamous cell carcinoma [49], ovarian [50], and lung [51]. ALDH1 is commonly proposed to be the source of ALDH activity in CSCs, and its expression has been widely used as a CSC marker. However, unspecific ALDH activity can also be utilized to categorize cells as CSCs using the ALDEFLUOR assay. The ALDEFLUOR assay contains BODIPY-aminoacetaldehyde (BAAA) which enters intact, viable cells and is oxidized by ALDH enzymes producing fluorescent BODIPY-aminoacetate (BAA). This fluorescence can be detected using fluorescent microscopy or flow cytometry. The non-cytotoxic nature of ALDEFLUOR additionally enables sorting of live CSC populations via fluorescence-activated cell sorting (FACS). Identification of CSCs using ALDH activity assays is a powerful tool for cancer researchers due to this ability to separate viable subpopulations combined with the association of ALDH activity with MDR.

2.3.6 HOECHST 33342 EXCLUSION

Hoechst 33342 is a stain capable of permeating intact cell membranes, which produces blue fluorescence when bound to nuclear DNA. This property is used to visualize nuclei, similar to 4',6-diamidino-2-phenylindole, dihydrochloride (DAPI), while maintaining cell viability. Stem cells and other cells overexpressing drug efflux pumps possess the unique ability to exclude this stain, and as a result Hoechst 33342 exclusion

has been used to label various progenitor cells such as hematopoietic stem cells [52]. The drug efflux pumps responsible for Hoechst 33342 dye exclusion may further contribute to MDR in cancer cells. Hoechst 33342 excluding cells, also known as the side population (SP), of tumors have therefore been investigated as a source of drug resistant CSCs. SP cells have been shown to exhibit stem-like properties in hepatocellular [13], lung [53], ovarian [15], breast [8] and other cancers as well as exhibiting enhanced drug resistance. Like the ALDEFLUOR assay, segregation of hypothesized CSCs using Hoechst 33342 exclusion can be combined with FACS techniques to isolate a viable CSC populations based upon a characteristic associated with MDR.

2.3.7 EMT CAPABILITY

Epithelial-mesenchymal transition (EMT) is the process undergone by epithelial cells in which the cells alter their morphology, lose their polarity, and break cell-cell or cell-matrix adhesions. In this way, the cells gain mobility and invasive potential. EMT is an essential process during development and wound healing, allowing epithelial cells to produce a population of mobile cells able to migrate to target locations and reestablish basal and apical polarity once there [20]. CSCs are hypothesized to possess enhanced EMT capability, enabling the cells to survive in the absence of cellular adhesion in addition to enhancing their resistance to apoptosis. CSCs having undergone EMT are thought to then reattach and produce metastatic tumors or circulate throughout the body in a dormant state, only to become active years later and cause distant cancer relapse to occur. The ability of CSCs to undergo EMT can be investigated by determining the expression of EMT related proteins such as Twist, Snail, or N-cadherin [54].

More commonly, however, EMT capability is assessed by removing any opportunity for cellular attachment. This can be accomplished through the use of non-adherent well plates, stirred bioreactors, serum-free growth conditions, or encapsulation in hydrogels. When in these conditions, cells without EMT capability will die leaving only cells that have undergone the transition. The remaining cells often grow in what are referred to as tumorspheres which have been shown to be enriched in CSCs in numerous tissues [55-57]. A major drawback of using these selective growth environments is the relatively low purity of CSCs in the resulting population. Further, CSCs within tumorspheres of a large enough size are likely to differentiate into phenotypically diverse cells. Still, drug discovery efforts directed at limiting the EMT capability of CSCs should be encouraged as this ability lies at the heart of the spread and recurrence of cancer that plagues many patients.

2.4 DRUG RESISTANCE IN CANCER STEM CELLS

While resistance to chemotherapy treatments is not necessary to define CSCs, drug resistance is commonly associated with CSC populations. In fact, when resistance to a drug is induced, an increase in the percentage of cells possessing CSC markers has been observed [58]. Resistance to specific chemotherapy agents in cancer cell lines is typically promoted in vitro by exposing the cells to gradually increasing doses of the drug or by exposing the cells to several cycles of clinically relevant chemotherapy doses followed by drug free media to mimic the treatment patients actually receive. The enrichment of CSCs following chemotherapy regimens observed both in vitro and in clinical studies [19] has enormous implications on drug discovery efforts and future cancer treatment. Without

the ability to target and kill CSCs, chemotherapy treatments will continue to leave patients at risk for tumor recurrence and developed drug resistance. The following proteins and properties of CSC are thought to contribute to drug resistance in CSCs and therefore represent ideal targets for future chemotherapy or chemotherapy sensitizing drug discovery efforts. It is important to note, however, that healthy stem cells share many of the properties imparting drug resistance to CSCs, and as a result targeting these properties may lead to unwanted side-effects on otherwise healthy tissues.

2.4.1 ABC TRANSPORTERS

ATP-binding cassette (ABC) transporters are transmembrane proteins that serve a crucial cytoprotective role for healthy stem cells throughout the body. The function of these proteins is to pump toxic compounds from the cell body before their deleterious effects can occur. These pumps are able to act on a large variety of compounds including many chemotherapeutic agents. The expression of ABC transporters has been used to indicate CSC phenotypes in multiple tissues and also plays a role in developing the multiple drug resistance (MDR) typical of CSCs [59]. Members of the ABC transporter family that appear to be highly expressed in CSCs include, but are not limited to, ABCB1, ABCG2, and ABCB5 [60]. The expressions of these proteins have been suggested as markers for CSCs, but the lack of appropriate antibodies makes their detection more difficult than previously discussed markers. The ability of the SP to exclude Hoescht 33342 is a result of ABC transporters, specifically ABCG2, making SP isolation an indirect method of CSC isolation based upon ABC transporter expression [60].

Many of the ABC transporter proteins have been "discovered" multiple times in the context of chemotherapy resistance leading to confusion in their identification. For example, ABCG2 is often referred to as breast cancer resistance protein (BCRP) alluding to its ability to confer MDR to breast tumor cells. ABCG2 expression has been identified in the drug resistant subpopulations of many cancer models including K562 chronic myeloid leukemia cells [61] and MCF7 breast adenocarcinoma to name a few [62]. The cell lines in these experiments were made resistant through selection with various chemotherapies such as doxorubicin.

ABCB1 is another ABC transporter with multiple aliases. ABCB1 has been referred to by the names multidrug resistance protein 1 (MDR1), cluster of differentiation 243 (CD243), and most commonly P-glycoprotein 1 (P-gp). ABCB1 contributes to the efflux of many widely used chemotherapeutic agents including anthracyclines, vinca alkaloids, and taxanes making it a highly clinically relevant MDR protein[63]. Reduction of the expression of ABCB1 has been shown to lead to an increased chemotherapy sensitivity of colorectal CSCs in addition to MDR cell lines of differing origin[63]. By targeting ABC transporters, the unique resistance of CSCs can theoretically be reversed, sensitizing them to traditional chemotherapy treatments.

2.4.2 ALDH ENZYMES

Another strategy CSCs employ in order to exhibit MDR is the rapid metabolization of the chemotherapy agents they are subjected to. As mentioned previously, the presence of ALDH enzymes and their activity is a commonly used marker to identify CSCs. ALDH enzymes exert their effect by oxidizing aldehyde groups of drug molecules, preparing

them for future cell metabolism and thus detoxifying the cell. ALDH enzymes may also play a role in the differentiation of healthy and malignant stem cells. Inhibition of ALDH activity in $ALDH^{hi}/CD44^{+}$ putative breast CSCs convincingly resulted in a loss of MDR [64]. Interestingly, the inhibition of ALDH activity using diethylaminobenzaldehyde (DEAB) further sensitized these CSCs to radiation therapy. By eliminating ALDH activity from tumors, the breakdown of chemotherapeutic agents within the tumor will be slowed resulting in a more effective treatment. Cytotoxic compounds which do not act as substrates for ALDH enzymes or that reduce their activity may have a unique ability to induce apoptosis in CSCs and act as more effective long-term treatments.

2.4.3 PRO-SURVIVAL SIGNALING AND STEM CELL MAINTENANCE

CSCs hijack many of the pro-survival signaling cascades and maintenance proteins seen in healthy stem cells. In this way, CSCs have a tendency to survive cellular stresses capable of eliminating differentiated cancer cells in a similar fashion to non-malignant stem cells. For example, mechanistic target of rapamycin (mTOR) and signal transducer and activator of transcription 3 (STAT3) play a role in the maintenance and proliferation of healthy and cancer stem cells. The activation of phosphatase and tensin homolog (PTEN) and subsequent inhibition of mTOR and STAT3 results in a significant decrease in CSC viability and overall tumor drug resistance [65].

The stem cell maintenance proteins Wnt, Hedgehog, and Notch are also upregulated in CSCs. These molecules play a major role in maintaining the stem-ness of CSCs and activating the expression of stem cell related transcription factors such as octamer-binding transcription factor (Oct4) and Nanog as well as influencing EMT [66]. Stem

cell maintenance proteins such as these ensure CSCs will continue to asymmetrically divide, allowing the CSC phenotype to persist in a number of harsh conditions. Dysregulation of these pathways is hypothesized to promote gradual CSC differentiation leading to decreased tumor viability in response to chemotherapeutics, making them an attractive target for the treatment of both bulk tumors and CSCs.

2.4.4 QUIESCENCE

Cellular quiescence is defined by a reduced occurrence of mitotic divisions within a cell population. Quiescence is recognized as a trait of most somatic stem cells, allowing them to survive in a state of relative dormancy and reduce the accumulation of DNA mutations over time [67]. While debate remains as to whether or not chemotherapy agents have a diminished effect on quiescent cells, experiments on leukemia stem cells have shown that forcing these cells out of their dormant state results in increased drug sensitivity [68]. The hypothesis behind this pathway for MDR is that diminished cellular metabolism, failure to proceed throughout the entirety of the cell cycle, and lack of DNA multiplication allows CSCs to avoid activating the targets of many chemotherapeutic toxins. Quiescence of CSCs not only potentially influences MDR, but also enables CSCs to remain dormant at the site of the original lesion or migrate throughout the body for years before attaching and initiating new tumors. Targeting the quiescence of CSCs has the potential to increase the efficacy of current therapeutic methods against CSCs within the original tumor as well as prevent CSCs from entering dormant states capable of initiating new tumors in patients in remission.

2.5 NATURAL PRODUCTS TARGETING CANCER STEM CELLS

Natural products (NPs) have played an important role in medicine for much of recorded human history. The earliest recorded use of medicinal plants dates back approximately 5000 years to a list of Sumerian drug recipes written on a clay tablet, but there is evidence that Neanderthals may have used plants for medicinal purposes as far back as 60,000 years ago [69, 70]. Even today many people in the world rely on medicinal plants for their healthcare needs. It is estimated that 70-95% of people in most developing countries use traditional medicine for their primary healthcare needs [71]. Traditional Chinese and Ayurvedic medicine have historically served as primary healthcare for many people in developing nations, and both systems have drawn the attention of pharmocognosists from around the world.

Active compounds from various organisms have had great success as pharmaceuticals. This is especially true in the case of cancer chemotherapeutics. Between 1981 and 2006, 63% of anticancer drugs being used came from NPs, were inspired by NPs, or were synthesized from a natural pharmacophore [72]. The most profitable chemotherapy drug in history, taxol (or paclitaxel), is a natural product derived from the bark of the Pacific Yew Tree [73]. Taxol was discovered through a random screening of approximately 15,000 species of plants [49], but targeted screening of known medicinal plants for anticancer properties has also been historically successful. For example, the vinca alkaloids vincristine and vinblastine have been used clinically in cancer therapies for over 50 years [74]. These compounds were isolated from the rosy periwinkle, Catharanthus roseus, a plant used in both traditional Chinese medicine and Ayurvedic medicine.

Bacteria have also been a source of successful anticancer agents. Anthracyclines, such as doxorubicin, are isolated from certain Steptomyces bacteria and have been used to treat breast cancer for decades [75].

With advances in technologies such as high throughput screening (HTS) and combinatorial chemistry in the 90's, the cancer related drug discovery efforts of many pharmaceutical companies shifted to targeted therapies [76]. These targeted, receptor specific therapies relied upon small synthetic molecules or antibodies that could act as "magic bullets" to treat specific cancer cells. Combinatorial chemistry has allowed vast libraries of new chemical entities to be generated synthetically which can be tested against disease related targets. Thousands of compounds from combinatorial chemistry libraries can be analyzed every day using HTS [77]. In addition, advances in proteomics and genomics have enabled researchers to attempt to model molecules that can interact with specific biological targets. The initial success of these targeted therapies including Gleevec and Herceptin led many to believe that traditional NP based drug discovery had become obsolete [51].

However, the limited number of successful drug candidates from targeted therapies, the relatively small number of cancers successfully treated with new therapies, and the higher risk of cancer developing a resistance to treatment created a renewed interest in natural product drug discovery in the late 2000's [52]. The limited efficacy of targeted therapies is of increased likelihood in CSCs, due to the lack of agreed upon universal CSC markers and the many survival mechanisms which they employ. Numerous NPs and their derivatives have shown early clinical success or have received FDA approval

for the treatment of cancer since the recent renewal in their interest [52, 78]. Despite the obstacles facing the screening of NPs using HTS, they have shown many advantages over synthetic chemical entities. Natural products are thought to possess "privileged structures" that are specialized to interact with biological targets allowing them to influence multiple cellular pathways simultaneously. This ability is crucial in combatting cancer and CSCs, as the robust survivability of cancer is often the result of many different mechanisms. Additionally, the chemical character and diversity of NPs is more favorable than that of synthetic molecules. When compared to synthetic libraries, NP libraries tend to have more chiral centers, higher steric complexity, fewer heavy atoms, more solvated hydrogen-bond donors and acceptors, and a larger variety of molecular properties [54]. Furthermore, historic use of a medicinal plant from which a NP is isolated can speak to the safety of compound for human consumption and the potential to limit side-effects.

The continued ability of natural compounds to compete with synthetic chemical entities has shown that NP based drug discovery is still relevant and capable of advancing the treatment of cancer. It is likely that the successful screening of NPs for cancer killing potential can be successfully applied to screening for CSC targeting agents. A few promising NPs have been utilized to target CSCs in vivo and in vitro. Figure 2.1 depicts the role that such NPs may play in preventing cancer metastasis and recurrence. These compounds may have the potential to sensitize CSCs to conventional treatments, directly induce cell death in CSCs, force CSCs to differentiate, or prevent CSCs from entering a dormant and more resistant state. A brief review of these compounds can be found

below. The reader of this review is directed to other reviews for a more comprehensive list of NPs capable of targeting CSCs [18, 79, 80].

2.5.1 POLYPHENOLS

Many natural products used as pharmaceuticals can be classified as polyphenols. Polyphenols are structurally defined by the presence of aromatic benzene rings bonded to hydroxyl groups, but they encompass a number of structurally diverse compounds. These subgroups include flavonoids, stilbenes, tannins, lignans, and phenolic acids among others. Polyphenols of various groups have been demonstrated to regulate inflammation, angiogenesis, cell growth, invasiveness, and apoptosis in vitro [81]. As a result, they have been studied extensively in the context of cancer prevention and metastasis. Recently, these investigations have been extended to determine the effect of polyphenols on CSCs. The polyphenols resveratrol and curcumin are notable examples of NPs that have been shown to exhibit cytotoxic effects on CSCs.

2.5.1.1 RESVERATROL

Resveratrol is a polyphenolic stilbene derivative most commonly found in the skin of grapes and berries. It has undergone extensive examination for its anti-inflammatory and antioxidant properties in addition to many other useful biological properties. These attributes give resveratrol the attractive potential to act as a cancer chemopreventative. Resveratrol has been shown to induce apoptosis and promote S-phase arrest of select cancer cells. This potential was demonstrated in Hep G2 hepatocyte carcinoma cells in vivo at concentrations ranging from 10 to 50 µM [82]. At concentrations higher than 50µM, however, resveratrol induced G_1/G_0 arrest which was confirmed in a separate study using

a number of ovarian cancer cell lines [82, 83]. Resveratrol has further been shown to induce cell death through a non-apoptotic mechanism at concentrations between 50 and 100 μM in a ovarian cancer cell lines [83]. This variety of mechanisms demonstrates the ability of resveratrol, like other NPs, to influence numerous biological mechanisms simultaneously making it an attractive anticancer agent.

Resveratrol may also be able to eliminate CSC populations from tumors. The compound has been shown in a study by Shankar et al to induce caspase-3/7 activated apoptosis in $CD44^+/CD24^+/ESA^+$ pancreatic CSCs at 10 to 30 μM concentrations. The study also found that 10 to 20 μM resveratrol was able to inhibit both stem cell maintaining factors, such as Nanog and Oct-4, as well as anti-apoptosis proteins of the Bcl-2 family in the pancreatic CSCs. Additionally, EMT proteins, such as Snail and Slug, as well as the EMT capability of the pancreatic CSCs in non-adherent conditions was inhibited in response to 10 to 20 μM of resveratrol. Further, the expression of the drug efflux pump ABCG2 was inhibited after administration of 10 to 30 μM of resveratrol, potentially sensitizing the cells to conventional chemotherapy treatments. The apparent ability of resveratrol to target CSCs and act as a chemopreventative and anti-inflammatory drug was further demonstrated using a mouse tumor model. The frequency of tumor formation in $Kras^{G12D}$ mice, spontaneous pancreatic tumor forming mutants, was significantly diminished when treated with resveratrol for 10 months [84]. The ability of resveratrol to induce apoptosis in CSCs as well as reduce their tumorigenic potential in vivo was additionally supported in a $CD24^-/CD44^+/ESA^+$ model of breast cancer stem cells. In this study, apoptosis was induced in the breast CSCs through a FAS mediated pathway after incubation with 50 or 100 μM

resveratrol. The tumorigenic potential of the cancer stem cells was significantly diminished in female nude mice through the administration of either an oral gavage or intraperitoneal injection of 22.4 kg/body weight of resveratrol, giving significant evidence that resveratrol is able to disrupt tumor formation by targeting CSCs [85].

While resveratrol exhibits extremely promising anticancer effects in preclinical studies in vivo and in vitro, resveratrol has failed to translate this success to clinical trials. This is due, in large part, to extremely low bioavailability, high effective dosages, and the rapid metabolism of resveratrol to glucuronide, sulfate, and hydroxylate conjugates [86, 87]. These conjugates, once absorbed into the bloodstream fail to provide the same health benefits as free resveratrol. As a result, there have been efforts to engineer resveratrol formulations or drug delivery systems aimed at increasing the bioavailability of resveratrol. These include formulations to stabilize resveratrol in the body, formulations to increase the aqueous solubility of resveratrol, and encapsulation of resveratrol in various lipids, micelles, or polymer structures with the aim of sustained, concentrated, and/or targeted release [86, 87].

2.5.1.2 CURCUMIN

Curcumin is another polyphenol which has been thoroughly investigated for its anticancer properties. This compound is a major component of turmeric, a spice widely used in Indian and many Middle-Eastern cuisines. Curcumin has been shown to exhibit an anti-inflammatory effect and promote apoptosis in cancer cells [88]. It has been used in clinical trials demonstrating its safety at high doses and activity against pancreatic

neoplasms in human patients despite its low bioavailability [89]. The antitumor properties demonstrated by curcumin have led to investigations of its potential to target CSCs.

Curcumin has been used to inhibit the formation of breast cancer mammospheres in vitro by 50% and 100% using 5μM and 10μM concentrations, respectively, demonstrating the ability of curcumin to inhibit CSC's ability to undergo EMT [90]. An analogue of curcumin, GO-Y030, was demonstrated to induce apoptosis, diminish tumorsphere formation, and inhibit STAT3 phosphorylation in $ALDH^+/CD133^+$ colon CSCs when used at 2 to 5μM concentrations. The ability of this analogue to target tumor initiating cells was further demonstrated using a NOD/SCID mouse model. When given a 50 mg/kg intraperitoneal injection of GO-Y030, the average tumor weight resulting from a xenograft implantation of 1×10^5 CSCs was diminished by 58.10% [91]. Curcumin has also been suggested as a supplement to current chemotherapy treatments. Curcumin in combination with FOLFOX, a commonly prescribed combination of leucovorin calcium, fluorouracil, and oxaliplatin, was able to decrease the viability and diminish EMT of colon CSCs to a higher extent than FOLFOX alone [92].

While curcumin shows great potential as an anticancer agent and has been used in a number of clinical trials against cancer, it suffers similar shortcoming to resveratrol. Namely, the rapid metabolism and excretion of curcumin, along with its hydrophobicity, results in low bioavailability which has been demonstrated using mouse models [93, 94]. Numerous drug delivery studies have been conducted to increase the bioavailability of curcumin including the use of adjuvants to interfere with metabolism, encapsulation in liposomes and nanoparticles, and the use of more stable structural analogues [95].

2.5.2 FLAVONOIDS

Flavonoids are a major class of polyphenolic secondary metabolites found in numerous medicinal plants. They are derived from flavone which contains two phenyl rings and one heterocyclic ring. Flavonoids are commonly found compounds throughout the plant kingdom, and as a result, they are widespread throughout the human diet. Due to their abundance in fruits, vegetables, nuts, spices, and herbs, a flavonoid rich diet has been suggested as a feasible means of cancer chemoprevention [96]. Certain flavonoids including, quercetin and kaempferol, have been implicated as apoptosis inducers, antioxidants, inflammation regulators, and angiogenesis inhibitors. Further, certain flavonoids have been shown to have an effect on heat shock proteins, multiple drug resistance, adhesion, metastasis, and angiogenesis [97]. The high number of CSC related properties which seem to be affected by flavonoids have led to their investigation as CSC targeting agents. A review of one such flavonoid, quercetin, is presented below.

2.5.2.1 QUERCETIN

Quercetin is a flavonol secondary metabolite found throughout many species of plants. Quercetin is a known anti-inflammatory agent and anti-oxidant which has been demonstrated to induce programmed cell death in many malignant cancer cell lines. Quercetin has been shown to interfere with a number of cellular pathways associated with the formation and maintenance of human cancers including down regulating P53, inhibiting tyrosine kinase, inhibiting heat shock proteins, and inducing type II estrogen receptor expression [98]. Quercetin has further drawn attention as a potential CSC targeting therapeutic.

Not only has quercetin been shown to inhibit the proliferation of $CD133^+$ colon CSCs at a concentration of 75µM, but it also increases the sensitivity of these cells to doxorubicin (Adriamycin). In fact, when combined with 50 µM quercetin, doxorubicin doses were more effective at inhibiting CSC proliferation in vitro than doxorubicin doses three times more concentrated but lacking quercetin [99]. This finding demonstrates the potential of quercetin and other natural products to enhance the use of other chemotherapeutics to eliminate CSC populations. The use of lower doses of chemotherapeutic agents in combination with natural products such as quercetin may result in diminished off target toxicity while also inducing apoptosis in CSCs, improving patient outcomes, lowering the risk of cancer recurrence, and preventing metastasis formation.

Other CSC models have been targeted using quercetin including $CD44^+/CD133^+$ prostate CSCs. At a concentration of 20 µM, quercetin lowers the viability of prostate tumor spheroids grown in non-adherent flasks as well as diminish the migratory, invasive, and colony forming potential of $CD44^+/CD133^+$ prostate CSCs [100]. In this same publication, quercetin was shown to synergize with epigallocatechin gallate, a catechin found in tea, synergistically amplifying the above effects on these prostate CSCs. As is the case with many other NP's, however, quercetin's poor solubility, poor permeability, and instability result in diminished bioavailability [101]. The relatively high dose of quercetin required to elicit a biological response in combination with these issues warrant further drug delivery efforts to increase the lifetime and concentration of the compound at the site of the neoplasm.

2.5.3 ALKALOIDS

Alkaloids are a class of pharmacologically active organic compounds distinguished by the presence of nitrogen and aromatic rings in the chemical structure. Alkaloids are produced throughout the plant kingdom, but are usually found in higher plants [102]. Many alkaloids have been used throughout history in the medical field from quinine for the treatment of malaria to vinblastine for the treatment of multiple carcinomas. Several alkaloids have been used clinically in the treatment of cancer with great success, demonstrating their importance in the field. A small group of alkaloid compounds have even been shown to differentiate between healthy and cancerous DNA, inhibiting in vitro cancer DNA synthesis while leaving healthy DNA unaffected and resulting in a potential cancer treatment with diminished side-effects [103]. New investigations on alkaloids are still being conducted showing further antineoplastic, anti-metastatic, and MDR inhibiting potential [82]. These results suggest a potential for alkaloids to eliminate CSCs, and indeed, a number of compounds belonging to the alkaloid family have been shown to target CSCs in vitro and in vivo. Three promising anti-CSC alkaloids, dihydrocapsaicin, piperine, and berberine, are presented in the following sections.

2.5.3.1 DIHYDROCAPSAICIN

Capsaicin is the secondary metabolite and alkaloid responsible for the hotness of many species of pepper. Dihydrocapsaicin (DHC), a saturated derivative of this compound, has exhibited numerous anti-neoplastic properties. DHC has been shown to induce dose-dependent and catalase regulated autophagic cell death in colon and breast cancer cells when used at concentrations between 50 and 400 μM [104]. However, when

autophagic cell death was inhibited through treatment with the inhibitor 3-methyladenine, DHC instead induced caspase-3 activated apoptosis in these cell lines. Further, when apoptosis was inhibited by the addition of peptide zVAD, autophagic cell death was enhanced. This ability to promote separate modes of cell death is a useful tool in targeting CSCs due to the many cell death evading pathways active in CSCs. This ability further highlights the potential of NPs to influence multiple cellular mechanisms and produce a robust cytotoxic effect on cancer cells.

A review of CSC related patents revealed that DHC is further hypothesized to exhibit a cytotoxic effect on neural CSCs [79]. In one of the patents collected in the review, US20090076019A1, a neurosphere assay was invented to screen potential drugs for activity against neural stem cells. As the percentage of putative CSCs are increased in cancer neurospheres, compounds capable of inducing cell death in these spheres can be thought of as agents targeting neural CSCs. DHC was identified in this patent as one of several lead compounds which showed an ability to target $CD133^{+}$ neural CSCs. The high IC_{50} values of DHC, however, limit its use as an effective chemotherapeutic agent, especially when one considers the low bioavailability common for many NPs. Further research is warranted to determine if DHC or an analogue can target any phenotype of CSCs with higher efficacy than what has been shown.

2.5.3.2 PIPERINE

Piperine is a promising antineoplastic alkaloid found in black and long pepper. The use of piperine has previously been suggested as a cancer chemopreventative, but it has also demonstrated the ability to induce cell cycle arrest, endoplasmic reticulum stress,

and apoptosis when exposed to colon cancer in vivo at concentrations between 75 and 150 μM [105]. The treatment of colon cancer cells with piperine has been shown to reduce the ability of the cells to form non-adherent spheres and colonies, suggesting the inhibiting effect of piperine on CSCs. The apoptotic effect of piperine has additionally been confirmed using prostate cancer cells [106].

The ability of piperine to target stem cells specifically has been investigated in a breast tissue model. After pre-treatment with 5 to 10 μM piperine, the mammosphere formation potential, ALDH expression, and Wnt signaling of unsorted breast tissue was significantly diminished [90]. Interestingly, the differentiated population of these cells was seemingly unaffected by the piperine treatment. The potential of piperine to target CSCs without affecting other cells is a fantastic example of the robust ability of NPs to influence molecular pathways while imparting only benign side effects. Piperine has additionally been suggested for use in combination therapies with compounds, such as resveratrol or curcumin, due to its ability to inhibit metabolic pathways. By slowing the glucuronidation of these compounds, piperine inhibits the metabolism and clearing of NPs and increases their bioavailability [107]. By inducing a cytotoxic effect on CSCs and increasing the efficacy of other compounds, piperine acts as an ideal complementary medication to other NP chemotherapies.

2.5.3.3 BERBERINE

Berberine is a tetracyclic, isoquinoline alkaloid found in the roots and stems of numerous plants. Berberine producing medicinal plants have been used as anti-inflammatories in Ayurvedic medicine for years, and the compound has been shown to

induce dose-dependent apoptosis, initiated by reactive oxygen species generation, in a broad spectrum of cancers [108, 109]. The apoptosis induced by berberine goes through an internal caspase-9 dependent pathway which results in a loss of mitochondrial membrane integrity. Like many natural products, the bioavailability of berberine is low in the body, limiting the potential of berberine as a drug. This obstacle is being overcome through the use of targeting liposomes as a drug delivery system [110]. This delivery system encapsulated berberine into liposomes which were engineered to deliver the compound directly to the mitochondria of $CD44^{+}/CD24^{-}$ breast cancer stem cells. Using this system, 1-50 μM of berberine was able to produce dose-dependent apoptosis in breast CSCs. The drug was further able to induce the expression of the pro-apoptotic protein Bax and activate caspase-9 and caspase-3 leading to apoptosis in CSCs isolated from MCF-7 mammospheres.

Additionally, berberine has been used to inhibit the expression of ABC transporters responsible for MDR in CSCs [84]. Diminishing MDR, especially in CSC populations, makes berberine an attractive complementary medicine when currently accepted cytotoxic agents are unable to kill cancerous cells. An in vivo mouse model in which MCF-7 breast CSCs were injected into female nude mice followed by an array of berberine treatments and formulations demonstrated this synergistic capability. A mixture of 10 mg/kg of berberine liposomes and 10 mg/kg of paclitaxel liposomes was able to reduce the average tumor size in these mice by 85.5% compared to the control after just 21 days [110]. In this way, berberine could be used to either target CSCs alone or in combination with traditional chemotherapy agents.

2.5.4 OTHER

Many other natural compounds which do not fit into the classifications of polyphenols, flavanoids, or alkaloids have shown promise in targeting CSCs. Retinoids are an example of these compounds. Vitamin A, also known as retinol, generates a number of biologically active retinoids, including All-Trans Retinoic Acid (ATRA). ATRA has found clinical success in the treatment of acute promyelocytic leukemia under the trade name Tretinoin. The drug is marked by its successful induction of remission coupled with relatively mild side effects [111]. The mechanism of action utilized by ATRA is through induction of cellular differentiation of leukemic and hematopoietic cells, and this differentiation induction has further been observed in other types of stem cells [112]. The differentiation potential of retinoids presents a unique potential for cancer treatment, namely differentiating CSCs into a cell population more sensitive to classic chemotherapeutic regimens. Additionally, ATRA acts as an inhibitor of ALDH activity, potentially reversing a cause of MDR in CSCs [64]. ATRA has thus been used to limit the tumorsphere formation ability and CSC percentage of breast cancer cells in vivo [113].

The lactone antibiotic brefeldin A is another NP that cannot be classified as a polyphenol, flavonoid, or alkaloid. It has shown anticancer potential in a number of cancer types including leukemia, colon, and prostate through p53 independent mechanisms [114, 115]. Brefeldin A is produced by certain fungal organisms and acts as a protein transport inhibitor, preventing proteins from traveling from the endoplasmic reticulum (ER) to the Golgi apparatus. Subsequently, brefeldin A initiates ER stress, potentially leading to its apoptotic effects. Recently, brefeldin A has been shown to preferentially induce cell death

in suspension cultures over adherent cultures of the human breast adenocarcinoma line MDA-MB-231. In the same publication, brefeldin A also down-regulated the expression of CD44, reduced the ability of the cells to form colonies in soft agarose, and reversed the EMT [116]. Preferential killing of putative CSCs and inhibition of colony forming potential was similarly reported in the human colorectal cancer line Colo 205 [117]. This preferential killing has the potential to diminish CSC populations while limiting the side effects typically associated with chemotherapy.

2.6 CONCLUSION

The cancer stem cell hypothesis, while still being investigated, presents explanations to many of the issues facing cancer treatment today. The CSC hypothesis explains the mechanisms underlying cancer recurrence, metastasis, and, to a degree, multiple drug resistance. Cancer treatments directed toward the eradication of CSCs could lead to higher survival rates and brighter prognoses for patients who fear cancer regression could occur at any time. Current cancer treatments are insufficient in regard to the eradication of CSC populations, likely due to the multitude of survival mechanisms utilized by CSCs and the lack of definitive, universal, single molecule targets that separate CSCs from healthy stem or somatic cells. Natural products have historically been an excellent source of bioactive compounds capable of targeting multiple pathways, and current investigations are underway to screen NPs for their effect on the CSC population of numerous cancer types. Many different NPs have exhibited a range of CSC inhibitory properties, and it is likely that more have yet to be discovered. As a result, NPs should continue to be screened as potential chemotherapy agents, complimentary treatments

for compounds already in clinical use, and cancer prevention molecules with special attention focused on their ability to target CSCs. Further, due to the limited bioavailability and rapid metabolism of many NPs, these drug discovery efforts must be coupled with continued efforts to engineer robust drug formulations and delivery systems.

2.7 ACKNOWLEDGEMENTS

Research reported in this publication was supported by the National Institute of Arthritis and Musculoskeletal and Skin Diseases of the National Institutes of Health under Award Number AR063338, and National Science Foundation under Award Number 1631439. The content is solely the responsibility of the authors and does not necessarily represent the official views of the National Institutes of Health and National Science Foundation.

2.8 FIGURES

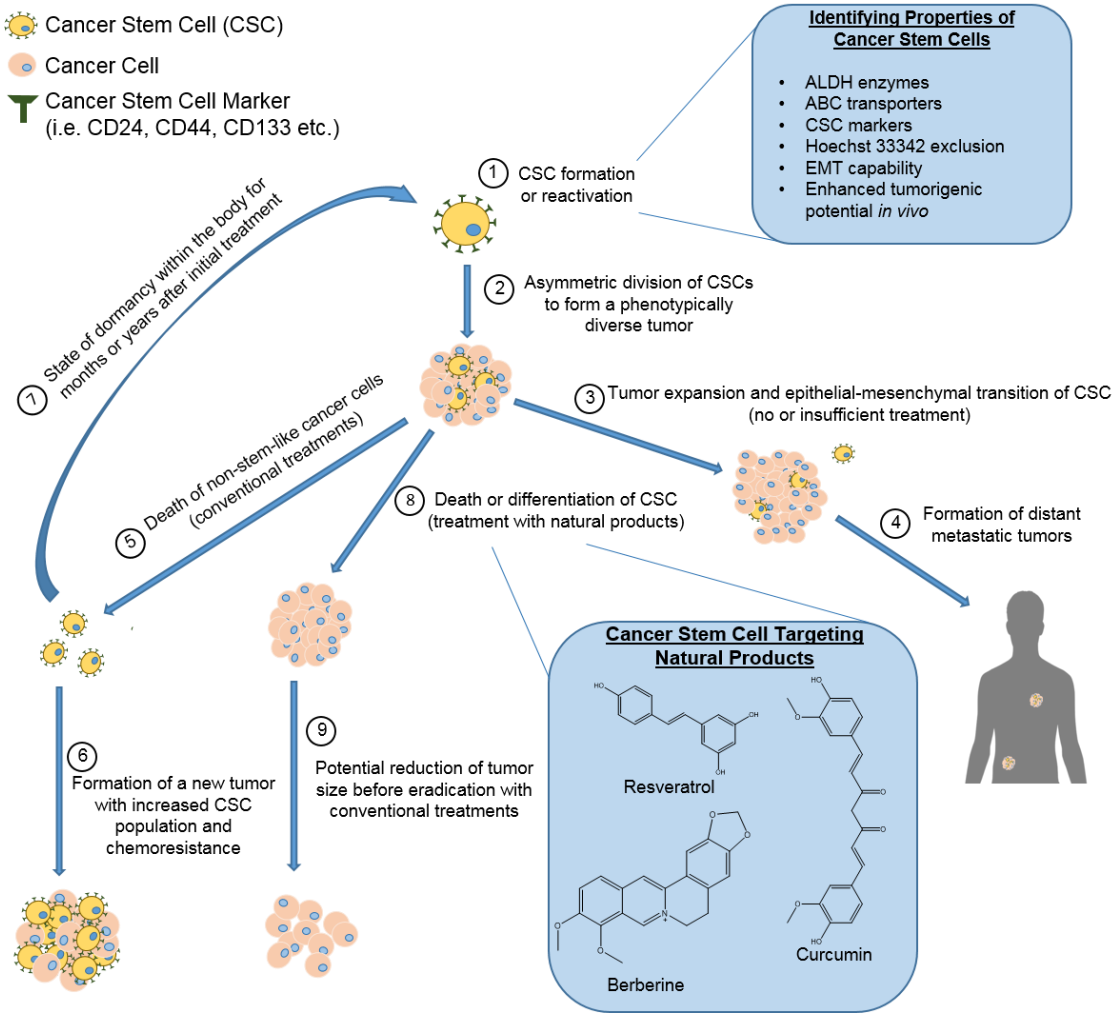

Figure 2.1: Illustration of the Cancer Stem Cell Model's explanation for tumor formation, metastasis, and recurrence and the potential of natural products in their treatment. Cancer Stem Cells (CSCs) are either formed upon carcinogenesis of somatic cells or stem cells, or they are activated after a period of dormancy (1). These CSCs then asymmetrically divide resulting in a phenotypically diverse tumor consisting of both CSCs and non-stem-like cells (2). Left untreated, the tumor will continue to grow and invade the surrounding tissue, and CSCs undergoing EMT may break off from the original tumor and travel to distant organs (3). The CSCs which reattach throughout the body can then initiate a new tumor, resulting in metastases (4). Using current treatment methods capable of inducing

cell death in the bulk of tumor cells, the CSCs are not destroyed due to their enhanced survival traits, such as quiescence and the expression of ALDH enzymes and ABC transporters (5). The remaining CSCs may then go on to recreate the original tumor, sometimes increasing the percentage of CSCs within the tumor and forming multiple drug resistant tumors (6). In other cases, the remaining CSCs will enter a state of dormancy within the body and remain undetected for long periods of time before reactivating and initiating the formation of a new tumor, thus resulting in cancer relapse in patients thought to be cancer free (7). As a result of these issues, new treatments are being investigated which can target CSCs. Natural products have shown the potential to induce cell death in CSCs, cause CSCs to differentiate, or sensitize CSCs to conventional chemotherapy treatments (8). Once the CSCs have been eliminated, the remaining tumor may diminish in size and can be subsequently eradicated through the use of conventional antineoplastic therapies (9).

CHAPTER 3

A MULTI-TARGETING ABIETANE DITERPENOID WITH GROWTH INHIBITORY AND ANTI-ANGIOGENIC PROPERTIES RE-SENSITIZES CHEMOTHERAPY RESISTANT CANCER[2]

3.1 ABSTRACT

Targeted therapies have become the focus of much of the cancer therapy research conducted in the United States. While these therapies have made vast improvements in the treatment of cancer, their results have been somewhat disappointing due to acquired resistances, high cost, and limited populations of susceptible patients. These hurdles often necessitate combining targeted therapies together, or using them in conjunction with chemotherapy in order to achieve an effective treatment. Using currently available treatments, an estimated 609,640 cancer related deaths will occur in the United States by the end of 2018[1]. Compounds which target more than one cancer related pathway are rare, but have the potential to synergize with multiple components of these cancer treatment cocktails, increasing the cocktail's efficacy and limiting resistance. Natural products, as opposed to targeted therapies, typically interact with multiple cellular targets simultaneously, making them a potential source of synergistic cancer treatments. One such natural product, deacetylnemorone, has been previously shown to inhibit

[2] Taylor, W.F., Moghadam, S.E., and Jabbarzadeh, E. 2019. To be submitted to *Scientific Reports*.

cancer cell growth, but little is known about its ability to target other cancer related pathways. In this study, deacetylnemorone was screened for its ability to inhibit cancer cell growth, synergize with existing chemotherapy, inhibit cancer cell invasion, and inhibit angiogenesis. The compound was found to inhibit cell growth in a broad spectrum of cancer cell lines and selectively induce cell death in SK-MEL-5 melanoma cells. Interestingly, the growth inhibitory properties of deacetylnemorone was stronger in FdUrd resistant HCT 116/200 colorectal cancer cells when compared to the parent cell line. The compound also enhanced the effect of FdUrd in HCT 116/200 cells when used at concentrations as low as 0.3 μM, suggesting the compound could be used to reverse acquired chemotherapeutic resistance. Furthermore, deacetylnemorone was able to inhibit the formation of vascular tubes between endothelial cells, a crucial step in angiogenesis, in addition to inhibiting the invasion of SK-MEL-5 melanoma cells, indicating the compound could inhibit the processes required for cancer metastasis. Combined, these results demonstrate that deacetylnemorone affects multiple cancer-related targets related to tumor growth, drug resistance, and metastasis. Thus, the multi-targeting natural product, deacetylnemorone, has the potential to enhance the efficacy of current cancer treatments as well as reduce commonly acquired treatment resistance.

3.2 INTRODUCTION

Despite continuing advances in the treatment of cancer, it remains the second leading cause of death in the United States according to the Centers for Disease Control and Prevention[1]. In recent years, there has been a shift in research efforts focusing on cancer drug discovery from cytotoxic chemotherapy agents, which induce cell death in

rapidly dividing cells relatively indiscriminately, to targeted therapeutics, which influence specific cancer-related pathways. Targeted therapies including immune modulating therapies, such as monoclonal antibodies[118], cytokines[119], dendritic cell therapies[120], chimeric antigen receptor T cells (CAR-T cells)[121], and immune checkpoint blockade therapies[122], as well as kinase inhibitors, such as cyclin dependent kinase inhibitors[4], tyrosine kinase inhibitors[5], and phosphoinositide 3-kinase (PI3K) inhibitors[123] have changed the landscape of cancer treatment. Targeted therapies such as bevacizumab, sorafenib, ziv-aflibercept, and vandetanib have also emerged to inhibit angiogenesis, a process of new blood vessel formation essential to wound healing, that is sometimes hijacked by cancer to feed growing and newly formed tumors[6, 124].

While these targeted therapies have led to a surge of improved prognoses, they have also come with drawbacks limiting their success in treating patients. For example, immune modulating targeted therapies, including sipuleucel-T and tisagenlecleucel, activate the immune system against cancer by isolating immune cells from the patient's body, altering their activity, and re-introducing the cells back into the patient[2, 125]. While these methods provide effective and innovative treatment, they can cost hundreds of thousands of dollars per injection[2]. Furthermore, this large price tag also comes with strong side effects, including neurotoxicity, high fever, and respiratory distress[126]. Other targeted therapies, such as the anti-programmed cell death protein 1 (PD-1) drug nivolumab are less patient-tailored but suffer from a high risk of developed resistance and a low population of susceptible patients[127]. Similarly, therapies targeting cancer cell growth, such as tyrosine kinase inhibitors, often suffer from acquired resistance following

the first few rounds of treatment. Angiogenesis targeting therapies come with their own set of complications as well. Like other targeted therapies, angiogenesis targeting therapies trigger treatment resistance, in part due to the plasticity of the tumor microenvironment manipulated by the tumor cells themselves[6]. Upregulation of pro-angiogenic factors[128], recruitment of pro-angiogenic cells[129], and increased pericyte coverage[130] has been observed in response to anti-angiogenesis treatments and may be responsible for anti-angiogenesis resistance. Additionally, angiogenesis-targeting therapies lead to increased hypoxia in the tumor microenvironment, resulting in increased tumor aggression and resistance to radiotherapy and chemotherapy[131, 132].

As a result of these challenges, targeted therapies are often administered in combination or in conjunction with chemotherapies in order to limit resistance and increase efficacy. Of course, angiogenesis-targeting therapies can also act against this combinatorial approach by limiting the drug delivery of other anti-cancer agents to the tumor[6]. The shortcomings of targeted therapies have led to a renewed interest in natural products for cancer treatment[76]. Compounds like natural products which are capable of targeting multiple cancer associated pathways may provide a more robust cancer treatment by limiting treatment acquired resistance, increasing the efficacy of multiple components of cancer therapy cocktails, and reducing the amount of drugs that are necessary to administer in order to achieve a positive treatment response.

In addition to influencing multiple biological targets, natural products are typically low cost and are associated with limited side effects. They have played an historically important role in cancer treatment, making up or inspiring approximately 60% of cancer

treatments between 1981 and 2006[72]. Before the advent of targeted therapies, cytotoxicity was the primary screening endpoint used to determine a natural product's potential as a chemotherapy agent. Now, however, natural products are investigated for numerous anti-cancer properties, such as their potential to induce cancer cell death, inhibit cancer cell growth and invasion, modulate the immune system, and inhibit angiogenesis to name a few. A select set of natural products have been identified that affect multiple cancer-related pathways simultaneously. For example, curcumin[133], emodin[134, 135], and astragaloside IV[136, 137], are thought to be capable of inducing apoptosis in cancer cells in addition to modulating the immune response to tumor formation. Curcumin[138] has also been suggested, along with resveratrol[139] and green tea catechins[140], as compounds that combine anti-proliferative and anti-angiogenic effects[141]. The widely used natural product derived chemotherapeutic, taxol, which imparts its cytotoxic effect by disrupting the microtubule cytoskeleton of cancer cells, may owe some of its success as an anticancer agent to an ability to inhibit angiogenesis through vascular endothelial cell growth factor (VEGF) suppression at low concentrations[142]. By affecting multiple cancer related pathways simultaneously, natural products may be able to synergize with multiple components of commonly used mixtures of targeted therapies and chemotherapeutics, enhancing their efficacy and limiting resistance. However, of the natural products that exhibit multi-targeted effects against cancer, many suffer from low bioavailability and low efficacy at low concentrations, necessitating the continued search for lead compounds.

Deacetylnemorone is a natural product of the abietane diterpenoid family that has been isolated from plants belonging to the genus *Salvia*. Like others from this class of natural compounds, deacetylnemorone has been shown to exhibit growth inhibitory properties in cancer cells, namely cervical and prostate cancer[143]. However, the anti-proliferative effect of this compound has not been widely established, nor has any mechanism of action been suggested. Furthermore, the effect of deacetylnemorone on other cancer related pathways has not been fully explored. Herein, the anti-proliferative effect of deacetylnemorone on multiple cancer tissue types, in addition to the effect of deacetylnemorone on angiogenesis and cancer cell invasion is studied. Cell cycle analysis was performed to gain insight into the compound's mechanism of action. Finally, the ability of deacetylnemorone to enhance the cytotoxic effect of chemotherapy in treatment-resistant cancer cells was determined.

3.3 MATERIALS AND METHODS

3.3.1 DEACETYLNEMORONE SOURCE AND IDENTIFICATION

The abietane diterpenoid, deacetylnemorone, was obtained through collaboration with the University of Basel. The structure of the compound, shown in Figure 3.1, was determined by 1D and 2D nuclear magnetic resonance (NMR) in addition to time of flight mass spectrometry (TOF-MS). NMR analysis of deacetylnemorone was conducted using dimethyl sulfoxide (DMSO) as the solvent and a Bruker Avance III-HD 400 MHz. ^{1}H-NMR, ^{13}C-NMR, H-H correlation spectroscopy (COSY), heteronuclear single quantum coherence (HSQC), and heteronuclear multiple bond correlation (HMBC) were performed for structural determinations. For mass spectrophotometry analysis,

deacetylnemorone was dissolved in methanol and analyzed using liquid chromatography-mass spectrometry on a Thermo Orbitrap Velos Pro. The generated spectra can be seen in Figures A.1 and A.2. A stock solution of deacetylnemorone in DMSO at a concentration of 20mM was used for all cell culture experiments.

3.3.2 NCI-60 SCREENING

Primary cytotoxicity screening of deacetylnemorone against 59 cancer cell lines was performed using the National Institutes of Health's (NIH) National Cancer Institute-60 (NCI-60) screening program[144]. This assay utilizes a Sulforhodamine B viability assay described by Shoemaker[145] to assess the growth percent of 60 immortalized cancer cell lines across 9 tissue types. One dose, 10 µM, of deacetylnemorone was tested. Only data generated from 59 cell lines was reported, as the HOP-92 non-small cell lung cancer cell line was excluded from the one dose screen. Growth percent between 0% and 100% in response to a compound can be interpreted as growth inhibition, and a negative percent growth is interpreted as cell death.

3.3.3 CELL CULTURE

MG-63 (osteosarcoma), SK-OV-3 (ovarian adenocarcinoma), MDA-MB-231 (breast cancer), HCT 116 (colorectal carcinoma), HCT 116/200 (FdUrd resistant subclone of HCT 116 cells), A2780ADR (doxorubicin resistant subclone of the ovarian carcinoma A2780), and HUVEC (normal human umbilical vein endothelial cells) were obtained and stored in liquid nitrogen until use. MG-63, SK-OV-3, MDA-MB-231, and HCT 116 cell lines were purchased from ATCC. A2780ADR cells were purchased from Sigma-Aldrich. HCT 116/200 cells were generously provided by Dr. Franklin G. Berger from the Center for Colon Cancer

Research, where they were originally cultured[146]. Human umbilical vein cells (HUVEC) were purchased from Lonza. The culture media used for MG-63 was minimum essential medium (MEM;Corning) supplemented with 10% Fetal Bovine Essence (FBE;VWR) and 1% penicillin/streptomycin solution (Corning). The culture media for SK-OV-3 cells was McCoy's 5A Medium (Sigma) supplemented with 10% FBE and 1% penicillin/streptomycin. The growth media for A2780ADR cells was Roswell Park Memorial Institute (RPMI) 1640 medium (Corning) supplemented with 10% FBE and 2mM L-glutamine (ThermoFisher). The growth media used for MDA-MB-231, HCT 116, and HCT 116/200 cells was RPMI 1640 medium supplemented with 10% FBE and 1% penicillin/streptomycin. The growth media for HUVEC cells was endothelial cell growth medium-2 (EGM-2; Lonza BulletKit). All cells were maintained at 37 °C and 5% CO_2.

3.3.4 MTS ASSAY

Cells were grown to approximately 80% confluency before being washed with phosphate buffered saline (PBS; Corning) and typsinized using a 0.25% trypsin, 2.21 mM Ethylenediaminetetraacetic acid (EDTA), and sodium bicarbonate solution (Corning). Trypsinized cells were suspended in culture media and centrifuged at 2500 rpm for 5 minutes. Cell viability was confirmed using trypan blue (Gibco). Cells were then seeded into 96 well plates (VWR). MG-63, SK-OV-3, and A2780ADR cells were seeded at a density of 2,000 cells/well. MDA-MB-231 cells were seeded at a density of 5,000 cells/well. HCT 116 and HCT 116/200 cells were seeded at a density of 4,000 cells/well. HUVEC cells were seeded at a density of 3,000 cells/well. For all cell types, 100 µL of cell culture media was used. The cells were then incubated for 24 hours at 37 °C and 5% CO_2 to allow for cell

attachment. After cell attachment, the culture media was aspirated and replaced with media containing deacetylnemorone. The vehicle control was 0.5% DMSO (Macron Fine Chemicals) in culture media. Doxorubicin hydrochloride (DOX;Sigma), and 5-fluoro-2'-deoxyuridine (FdUrd; Sigma), were used as positive controls. In combination studies, deacetylnemorone and FdUrd were added to the same culture media then added to the cells. At 48 and 72 hours, the cells were washed with PBS and culture media supplemented with 20% 3-(4,5-dimethylthiazol-2-yl)-5-(3-carboxymethoxyphenyl)-2-(4-sulfophenyl)-2H-tetrazolium (MTS) solution (Promega) was added to the cells. The cells were incubated for 2 hours, and the absorbance of each well at 490 nm was measured using a Spectramax 190 microplate reader.

3.3.5 CELL CYCLE ANALYSIS

The effect of deacetylnemorone on the cell cycle of SK-MEL-5 melanoma cells was determined using flow cytometry. First, cells were seeded into 6 well plates at a density of 250,000 cells per well suspended in 2 mL of media. The cells were allowed to attach overnight, then the media was replaced with media containing deacetylnemorone. The cells were trypsinized with 0.25% trypsin and collected along with the drugged media at 6, 12, 24, 48, and 72 hours of treatment with deacetylnemorone. The detached cells were centrifuged at 2500 rpm for 5 minutes and washed with ice cold PBS twice. After centrifuging and discarding the supernatant, the pellet was suspended in 1 mL of ice-cold PBS, which was then added dropwise to 3 mL of ice-cold 70% ethanol in deionized water. The cells were fixed in this condition at 4° for at least 24 hours. After fixation, the cells were centrifuged, the supernatant was discarded, and the pellet was suspended in

FxCycle PI/RNase Staining Solution (Invitrogen) for 15 minutes. The final cell suspension was analyzed using a BD LSR II flow cytometer. The percentage of cells in the sub-G1, G0/G1, S, and G2/M phases of the cell cycle were determined using the resulting histograms.

3.3.6 IN VITRO INVASION ASSAY

Cell migration of SK-MEL-5 melanoma cells was investigated by making a cell-free gap with a 2 well culture- insert for 24 well plates (IbiTreat, Martinsried, Germany). The insert was made up of two wells that were separated by a thin wall. In each of the two wells of the insert, 70 µl of cell suspension containing 6×10^4 cells was added. Cells were allowed to reach confluency for approximately 24 hours. The 2 well inserts were then removed and any resulting cell debris was washed with PBS. Fresh culture media containing either the vehicle control or deacetylnemorone was added to the cells, and the plates were incubated at 37 °C and 5% CO_2 for 24 hours. Images were taken at 6, 12, and 24 hours after the addition of the treated media using a phase contrast Nikon Eclipse Ti-E inverted microscope. Percent invasion was calculated by measuring the gap distance at each time point and using the formula

$$\text{invasion \%} = \frac{(W_0 - W_n)}{W_0} * 100\% ,$$

in which W_n is the width of the gap at the desired time point, and W_0 is the initial width zero right after forming a cell-free gap. One representative well was stained and imaged after the final time point. The media was first replaced with 400 µL of Cell Stain Solution (Cell Biolabs, Inc) and the plates were incubated for 15 minutes at room temperature.

Each well was washed with deionized water and allowed to air dry. Images were taken using a phase contrast inverted microscope (Invitrogen EVOS FL Auto Cell Imaging).

3.3.7 TUBE FORMATION ASSAY

Growth factor reduced BD Matrigel (Corning) was stored at -20 °C. Before use, the Matrigel was thawed on ice at 4 °C overnight. Next, 50 µL of Matrigel was added to each well of an ice-cold 96-well plate and incubated at 37 °C and 5% CO_2 for 30 minutes, allowing a gel to form. A suspension of 20,000 HUVEC cells in 100 µL of cell culture media treated with deacetylnemorone was added to each well. The vehicle control contained only HUVEC cells suspended growth media. The junctions, or tubes, between the endothelial cells were imaged using an Invitrogen EVOS FL Auto at 4x magnification and manually counted.

3.4 RESULTS

3.4.1 DEACETYLNEMORONE INDUCES CONCENTRATION DEPENDENT CELL DEATH IN IMMORTALIZED CANCER CELL LINES ALONE AND IN COMBINATION WITH FDURD

In order to determine the chemotherapeutic potential of deacetylnemorone, the compound was screened against 59 cancer cell lines using the NCI-60 cancer panel. This panel utilizes a sulforhodamine B cell viability assay to determine the percent growth of cells treated with a compound of interest for 48 hours compared to cells treated with a vehicle control. Only one concentration, 10 µM, of deacetylnemorone was screened (Figure 3.2). This concentration inhibited the cell growth of 55 of the 59 cell lines tested, including at least one cell line from each of the 9 tissue types investigated. Of the 55 cell lines whose growth was inhibited by deacetylnemorone, one melanoma cell line, SK-MEL-

5, exhibited cell death in response to 10 μM of the compound. The growth percent of SK-MEL-5 was -23.8% after 48 hours of treatment. While deacetylnemorone was capable of inhibiting the cell growth of each tissue type tested, it was particularly effective against melanoma, inhibiting the cell growth of four melanoma cell lines by at least 80%. This result suggested that the compound may be indicated for the treatment of melanoma.

To further assess the growth inhibition poperties of deacetylnemorone, a 3-dose MTS assay screen of 6 immortalized cancer cell lines was performed (Figure 3.3). The six cell lines examined were MG-63 (osteosarcoma), SK-OV-3 (ovarian cancer), MDA-MB-231 (breast cancer), HCT116 (colorectal carcinoma), HCT 116/200 (colorectal carcinoma), and A2780ADR (ovarian cancer). In each cell line tested, dose-dependent cell growth inhibition was observed. This inhibition was significant in each cell line at concentrations less than or equal to 150 μM after 48 hours of treatment with deacetylnemorone. Notably, the inhibitory effect of the compound was stronger in HCT 116/200 cells than it was in HCT 116 cells. The HCT 116/200 cell line was derived from the HCT 116 cell line through treatment with gradually increasing concentration of the chemotherapeutic agent FdUrd[146]. This treatment induced resistance to FdUrd in the cell line compared to HCT116 by selecting for a resistant variant of thymidylate synthase. By comparing the doxorubicin control groups from Figures 3.3D and 3.3E, it was observed that the HCT116/200 cell line had also developed a cross-resistance to doxorubicin. The high sensitivity of the chemotherapy resistant HCT 116/200 cell line to deacetylnemorone when compared to the parent cell line prompted an investigation of the combinatorial effect of deacetylnemorone with FdUrd (Figure 3.4). Three concentrations of

deacetylnemorone (3 μM, 30 μM, and 150 μM) were used to treat HCT 116/200 cells either alone or in combination with FdUrd. Each of these concentrations of deacetylnemorone significantly increased the growth inhibition of the 4μM FdUrd treatment. Both the deacetylnemorone-alone treatment and the combination treatment acted in a dose dependent manner.

3.4.2 DEACETYLNEMORONE DELAYS PROGRESSION OF THE CELL CYCLE THROUGH S AND G2/M PHASES.

Due to the growth inhibitory properties of deacetylnemorone, cell cycle analysis was performed on SKMEL5 melanoma cells exposed to the compound to gain insight into the mechanism of action. SKMEL5 cells were treated with deacetylnemorone for 72 hours, analyzing the DNA content of the cells at 6, 12, 24, 48, and 72 hours by propidium iodide (PI) staining followed by flow cytometry (Figure 3.5A). Using the generated histograms, the percentage of cells in the sub-G1, G0/G1, S, and G2/M phases of the cell cycle was determined (Figures 3.5B and 3.5C). Compared to the control, no increase in sub-G1 cells through the 72 hour treatment was observed, suggesting no apoptotic cell death was occurring. However, the treated group did exhibit a build-up of cells in the S-phase of the cell cycle through 24 hours of treatment, accompanied by a decrease in G0/G1 cells. This was followed by gradual decrease in S-phase cells and a subsequent increase in G2/M cells from 24 to 72 hours of treatment. These trends could be explained by a slowing down of progress through the cell cycle for the first 24 hours of treatment, followed by a gradual release of cells from the S-phase and G2-M phase between the 24

and 72 hour period. It is possible that higher concentrations of the compound could completely arrest progress through the cell cycle.

3.4.3 DEACETYLNEMORONE INHIBITS INVASION OF MELANOMA *IN VITRO*.

The effect of deacetylnemorone on melanoma cell invasion was also investigated. A cell free gap was created between two regions of SK-MEL-5 melanoma cells using 2-well cell culture inserts. When the culture inserts were removed, the cells were treated for 24 hours with 0.3 μM, 3 μM, and 30 μM of deacetylnemorone. At 6, 12, and 24 hours the percent invasion into the cell free gap was measured (Figure 3.6). At each time point, the percent invasion of melanoma cells decreased as the concentration of deacetylnemorone increased. The inhibition of melanoma cell invasion was significantly lower ($p < 0.05$) than the control when the cells were treated with 30 μM deacetylnemorone at each of the tested time points (Figure 3.6B). Both the movement of the cell front and the migration of single cells into the cell free gap was inhibited as the concentration of deacetylnemorone was increased (Figure 3.6A). Trypan blue cytotoxicity assays were also performed at each time point, revealing the inhibition of cancer cell invasion occurred at lower concentrations of deacetylnemorone than was toxic to the cells (Figure A.3).

3.4.5 DEACETYLNEMORONE INHIBITS TUBE FORMATION OF ENDOTHELIAL CELLS, A CRITICAL STEP OF ANGIOGENESIS.

The effect of deacetylnemorone on angiogenesis was investigated using a tube formation assay (Figure 3.7). The assay consisted of HUVEC endothelial cells grown on a Matrigel basement membrane in the presence of growth factors. Under these conditions, cellular projections called “tubes” will begin to form between the cells (Figure 3.7B). In

this study, tube formation was allowed to occur for 8 hours under control conditions or with growth media treated with deacetylnemorone. The number of tubes or junctions per field were manually counted in triplicate for the groups treated with the control (culture media alone), 0.3 μM deacetylnemorone, and 3 μM deacetylnemorone, and a dose-dependent decrease in tube formation between HUVEC endothelial cells was observed as the concentration of deacetylnemorone was increased (Figure 3.7A). The decrease for both the group treated with 0.3 μM deacetylnemorone and the group treated with 3 μM deacetylnemorone was significant ($p \leq 0.05$) when compared to the control treated group. A representative image of the cells treated with 0.3 μM and 3 μM deacetylnemorone can be seen in Figures 3.7C and 3.7D respectively. The toxicity of an 8 hour treatment of deacetylnemorone on HUVEC endothelial cells was also determined using the MTS assay. No significant difference ($p \leq 0.05$) in cell viability between HUVEC cells treated with the vehicle control and the HUVEC cells treated with up to 30 μM deacetylnemorone was observed (Figure 3.7E), indicating the compound was not cytotoxic to HUVEC cells at the concentrations used to inhibit angiogenesis.

3.5 DISCUSSION

Multi-targeting natural products may create renewed vigor in the use of natural compounds for the treatment of cancer. Targeted therapies hold great promise for the future of cancer treatment but have been accompanied by numerous shortcomings, including high rates of resistance, low rates of susceptible patients, and high cost. Natural products that attack multiple cancer-related pathways may limit therapy-induced resistance and provide robust treatment when in combination with currently available

therapies. Deacetylnemorone was examined in this study to determine its ability to interfere with multiple cancer-related pathways, including cancer cell growth and proliferation, cancer cell invasion, and angiogenesis.

The growth inhibitory properties of deacetylnemorone were first examined by submitting the compound to the NCI-60 one dose cytotoxicity screen. At 10 μM, deacetylnemorone exhibited growth inhibitory properties across all nine of the tissue types examined. Within each tissue type a range of activity was observed, from no growth inhibition at all to inducing cell death in one melanoma cell line. These results suggest that the growth inhibitory effects of deacetylnemorone are not tissue-type dependent. However, the compound did appear to have a strong effect on multiple cell lines isolated from melanoma. SK-MEL-5 is a melanoma cell line that exhibited a 23.8% reduction in cell viability after 48 hours of treatment with deacetylnemorone. As a result, it appears that at concentrations near 10 μM, deacetylnemorone is selective in inducing cell death. The growth inhibition and cytotoxicity results across the 59 cell lines tested in the NCI-60 screen were less potent than other compounds that have undergone NCI-60 screening, and thus further screening was not performed using the NCI-60 panel. However, dose-dependent growth inhibition was demonstrated independently using an MTS viability assay on MG-63, SK-OV-3, A2780ADR, MDA-MB-231, HCT 116, and HCT 116/200 cells. Each of the six cell lines tested exhibited a dose-dependent response in cell viability to deacetylnemorone. In each case, the viability of the cells treated with 150 μM of deacetylnemorone was significantly less than the control ($p \leq 0.05$). In the case of colorectal carcinoma (HCT 116 and HCT 116/200) and breast cancer (MDA-MB-231), a

significant decrease ($p \leq 0.05$) compared to the control group at 30 μM of deacetylnemorone was observed. This confirmed the selectivity noted in the NCI-60 screening.

Of particular interest was the seemingly greater sensitivity of the chemotherapy resistant HCT116/200 cells to deacetylnemorone compared with the parent HCT 116 cell line. Deacetylnemorone at 30 μM reduced the cell viability of HCT 116/200 after only 48 hours compared to the 72 hours needed for the parent cell line. The compound also reduced the cell viability of the HCT 116/200 cell line to a greater extent than the parent cell line at both the 30 and 150 μM concentrations. The compound may therefore be targeting a cellular pathway that is responsible for the treatment-induced resistance of HCT 116/200 cells or was co-selected with the cellular pathway responsible for the treatment-induced resistance such as the percentage of cancer stem cells within the population[147]. In order to further explore this interesting result, deacetylnemorone was used in combination with the chemotherapy agent FdUrd to treat HCT 116/200 cells. The cell viability of HCT 116/200 was significantly lower when deacetylnemorone was used in combination with FdUrd than when FdUrd was used alone. This effect occurred at as little as 3 μM deacetylnemorone, a concentration lower than the minimum required to reduce cell viability when deacetylnemorone was used on this cell line alone. It is likely that a synergistic rather than simply a combinatorial effect occurred when deacetylnemorone was used alongside the chemotherapy.

Next, cell cycle analysis was performed to gain insight into the mechanism of action for the cell growth inhibition of SK-MEL-5 melanoma cells. When compared to the

control, deacetylnemorone at 15 μM did not increase the percentage of cells in the sub G1 phase of the cell cycle, suggesting apoptotic cell death was likely not occurring. As a result, another mechanism of cell death, such as necrosis or autophagy, is likely responsible for any cell death observed at this dose[148]. Additionally, from 6 to 24 hours of incubation with deacetylnemorone, the percentage of cells in the G1 phase decreased with a corresponding increase in the S phase cells. After 24 hours, the percent of S-phase cells decreased and the percentage of cells in the G2/M phase increased. The increase in G2/M phase cells continued until 72 hours of incubation with deacetylnemorone, at which point the percentage of cells in the G2/M phase outnumbered the percentage of cells in the S-phase. This trend was not seen on cells treated with the vehicle control. These results suggest that deacetylnemorone may slow progression of the cell cycle through the S and G2/M phases. While the mechanism is unclear, this could be the result of DNA damage, inhibition of DNA synthesis, or inhibition of cell cycle regulating cyclins[149]

With the cancer cell growth inhibition properties of deacetylnemorone established, the effect of the compound on other cancer-related pathways was then examined. Deacetylnemorone was observed to reduce SK-MEL-5 invasion at a concentration as low as 0.3 μM after 24 hours of treatment. The decrease in invasion was concentration dependent, and the decrease became significant ($p \leq 0.05$) at 30 μM of the compound. Both the migration of the cell front and the invasion of single cells into a cell free gap between cell fronts were inhibited as deacetylnemorone was added to the cell culture media. The inhibition of cell front migration could be interpreted as an extension of the cell growth inhibition observed previously, as the cell front will migrate when the

cells divide. However, the decrease in single cells invading the cell free gap suggests that the cells were being inhibited from undergoing epithelial-mesenchymal transition (EMT). This process allows cancer cells to detach from their extracellular matrix, move freely within the body, and reattach in a new location, establishing metastatic growth[150]. Cancer cells undergoing this process may also be linked to innate chemotherapy resistance and an increased percentage of cancer stem cells[147]. The decrease of single cells in the cell free gap suggests a decrease in the number of cells that had migrated from one of the cell fronts. This inhibition is unique from cell growth inhibition and may lead to an ability of deacetylnemorone to inhibit the metastasis and chemotherapy resistance of melanoma. The final cancer-related pathway that was assayed for a response to deacetylnemorone was angiogenesis. At sub-cytotoxic concentrations of deacetylnemorone (0.3 and 3 μM), significantly less tube formation was observed between HUVEC endothelial cells. Tube formation is a crucial step in angiogenesis, which is required for both extended tumor growth and metastatic formation. By inhibiting the formation of tubes between endothelial cells, deacetylnemorone may cut off the blood supply to new and growing tumors and further inhibit metastasis.

3.6 CONCLUSIONS

Deacetylnemorone is a natural product of the abietane diterpenoid family. While limited growth inhibition studies have been performed to investigate the potential of this compound, it has remained an understudied lead compound for anti-cancer therapy. In this study, deacetylnemorone was shown to inhibit cell growth of a wide variety of cancer cell lines, induce non-apoptotic cell death in SK-MEL-5 melanoma, sensitize HCT 116/200

resistant colorectal carcinoma to chemotherapeutic treatment, inhibit the EMT and invasion of melanoma cells, and inhibit angiogenesis. These properties may give deacetylnemorone the ability to provide a robust, multi-targeted treatment for a range of cancers, which not only increases the efficacy of current cancer treatment combinations and reduces the risk of treatment-acquired resistance, but also re-sensitizes already resistant tumors to further chemotherapy use. Further examination is warranted to elucidate the mechanism by which each of deacetylnemorone's anti-cancer effects are produced in addition to translating these *in vitro* results *in vivo*. Additionally, the ability of deacetylnemorone to target cancer stem cells specifically should be investigated as a potential mechanism for the ability of the compound to inhibit cell growth in chemotherapy resistant cell lines and inhibit EMT. In summary, deacetylnemorone is a multi-targeted natural product which has the potential to enhance currently utilized cancer treatments when used in combination with chemotherapeutic, anti-angiogenic, and other targeted therapies.

3.7 FIGURES

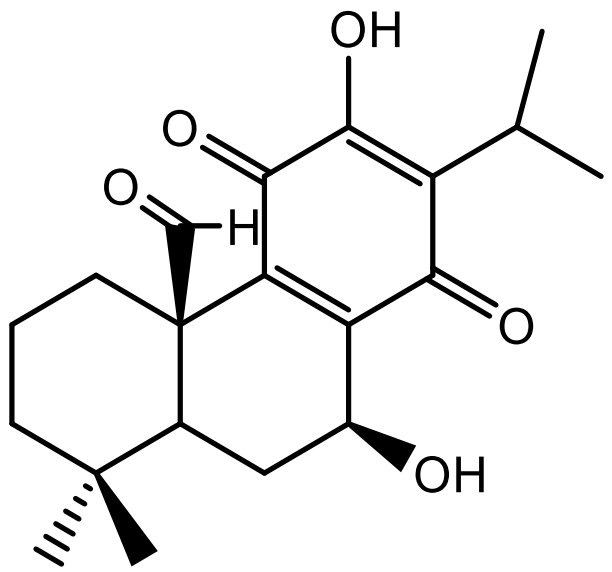

Figure 3.1: The structure of the abietane diterpenoid, deacetylnemorone.

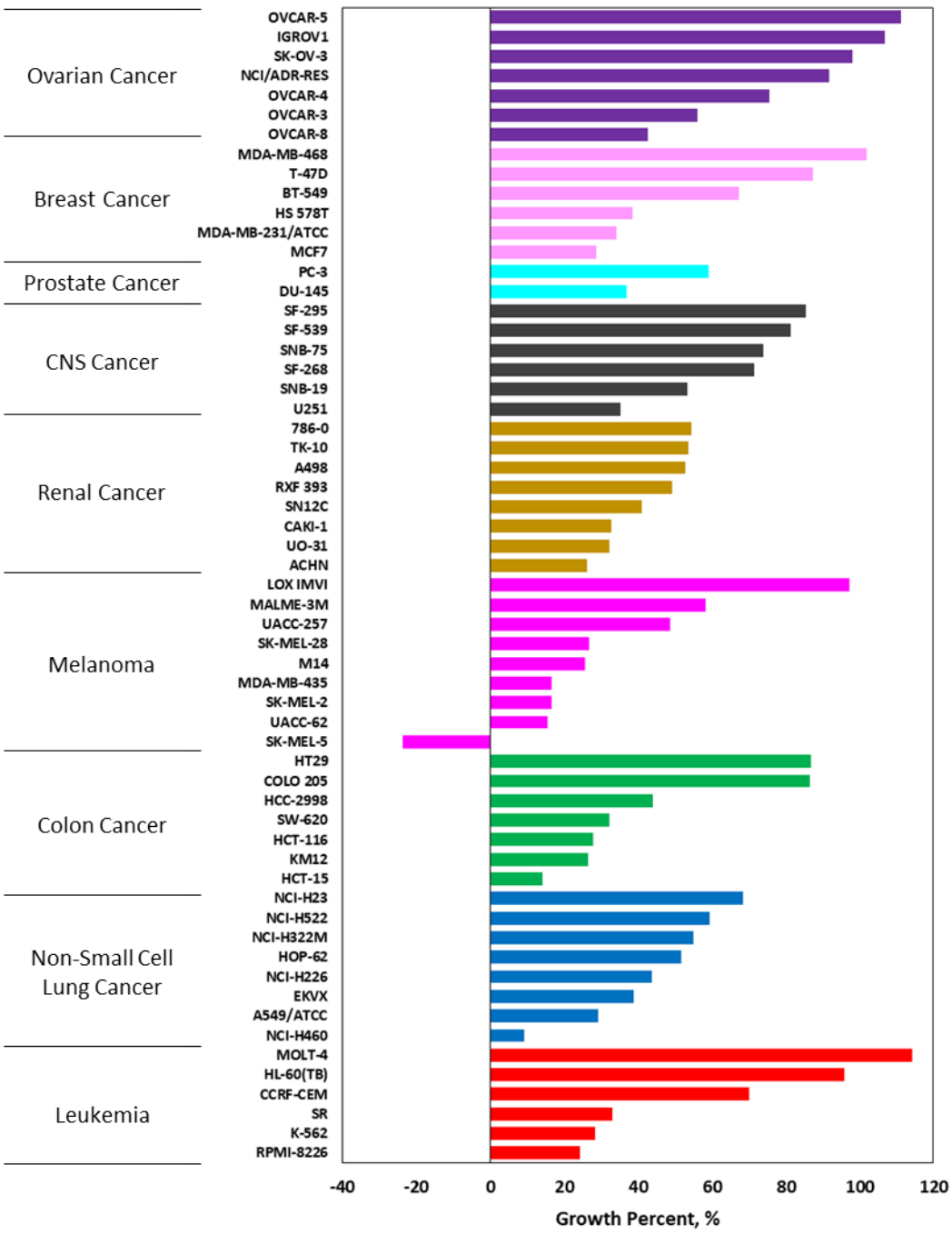

Figure 3.2: Waterfall plot of the growth percent of 59 cell lines in response to 10 µM of deacetylnemorone, determined by the NCI-60 one dose screening test. The tissue type of each cell line is denoted by color (Purple – Ovarian Cancer, Pale pink – Breast Cancer, Aqua – Prostate Cancer, Grey – CNS cancer, Gold – Renal Cancer, Bright Pink – Melanoma, Green – Colon Cancer, Blue – Non-small cell lung cancer, Red – Leukemia).

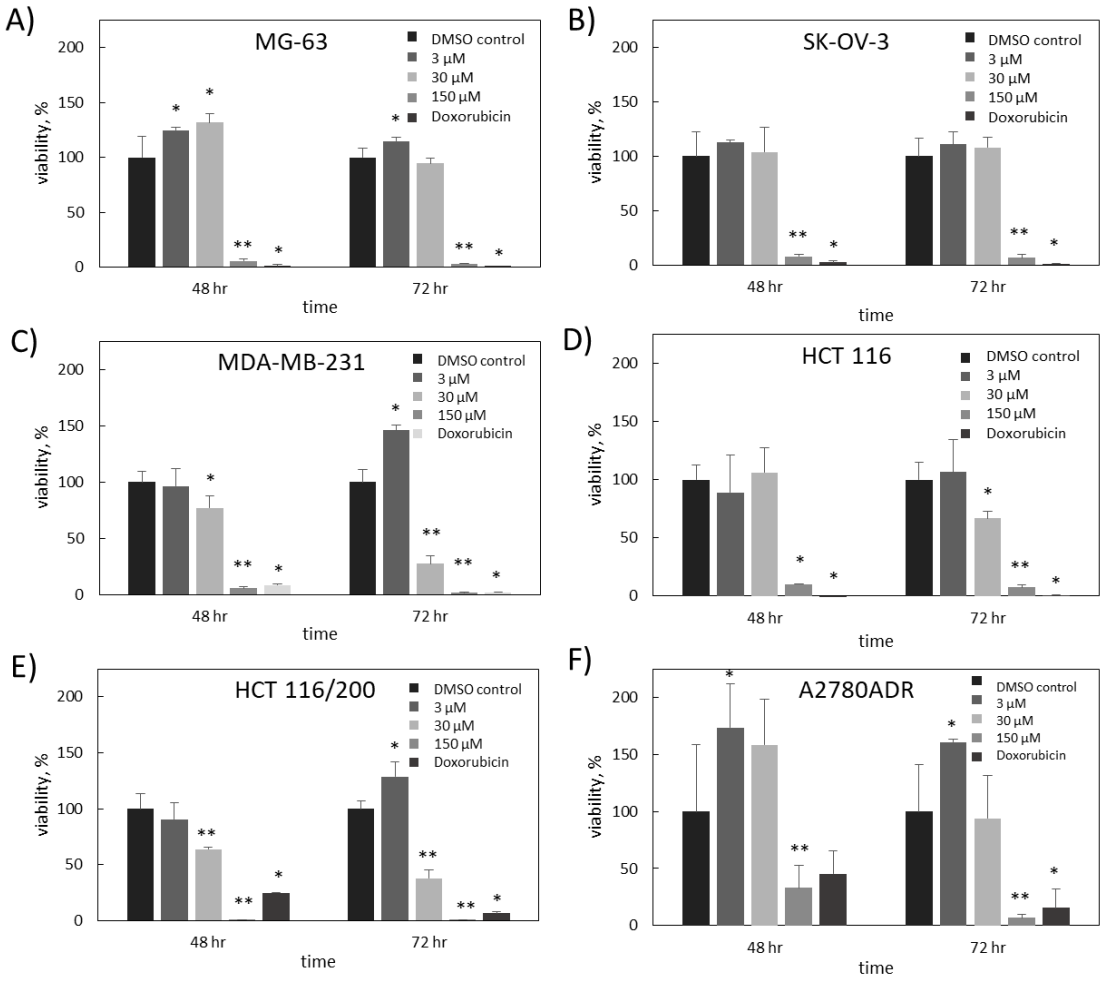

Figure 3.3: Percent viability of A) MG-63, B) SK-OV-3, C) MDA-MB-231, D) HCT 116, E) HCT 116/200, and F) A2780ADR cells in response to various concentrations of deacetylnemorone after 48 and 72 hours of exposure, as determined by the MTS cytotoxicity assay. For all cell lines except A2780ADR, the concentration of doxorubicin was 2 µM. For the A2780ADR cell line the concentration of doxorubicin was 1 µM. * denotes a significant difference ($p < 0.05$) from the control group. ** denotes a significant difference ($p < 0.05$) from the previous concentration in addition to the control group.

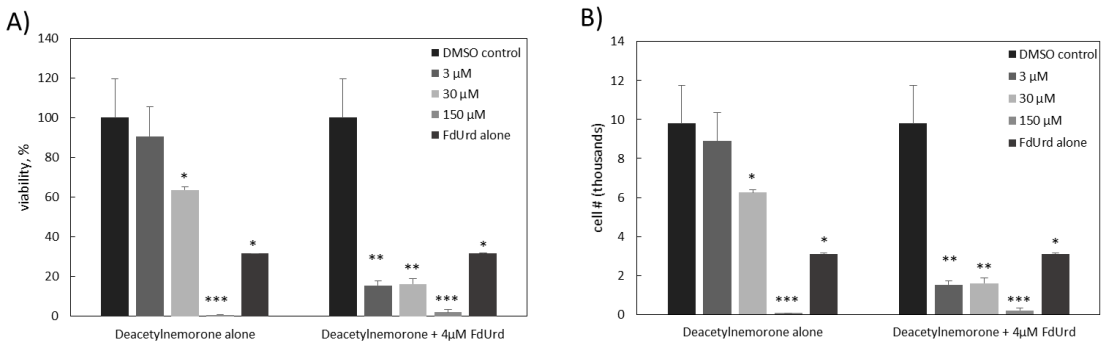

Figure 3.4: The A) percent viability and B) cell number of the HCT 116/200 cell line in response to a 48 hour exposure of various concentrations of deacetylnemorone, alone or in combination with the chemotherapy agent FdUrd, as calculated using the MTS assay. * denotes a viability significantly lower than the control. ** denotes a viability significantly lower than the 4 µM FdUrd treatment. *** denotes a viability significantly lower than both the 4µM FdUrd treatment and the preceding natural compound concentration. In all cases, significance is defined by a two tailed t-test with $p < 0.05$.

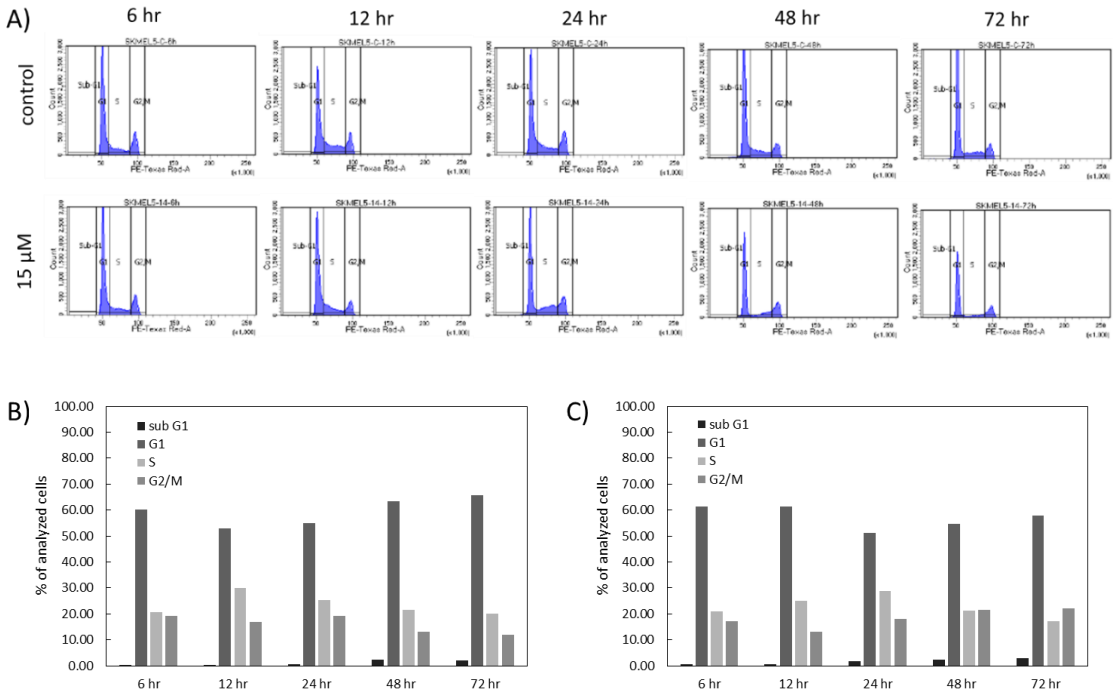

Figure 3.5: Histogram of propidium iodide expression as measured by flow cytometry for SK-MEL-5 cells treated with either a vehicle control or 15 µM of deacetylnemorone. The histograms A.) were divided into four sections representing the sub-G1, G0/G1, S, and G2/M phases of the cell cycle. The histograms were used to calculate the percentage of analyzed cells treated with B) the vehicle control and C) 15 µM deacetylnemorone.

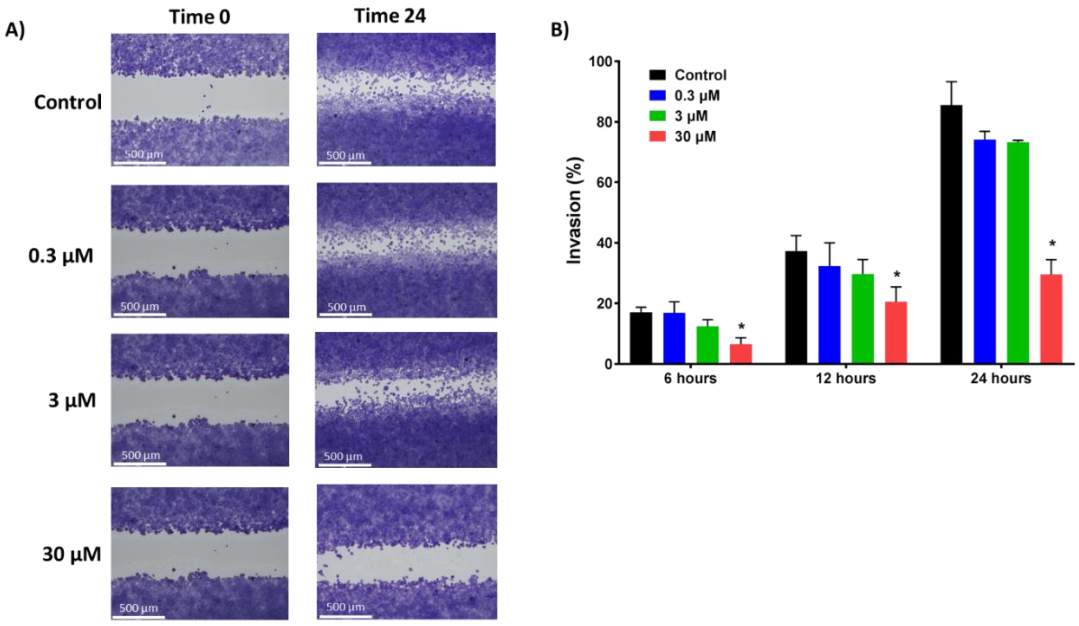

Figure 3.6: Invasion of SK-MEL-5 melanoma cells into a cell-free gap created using a 2-well cell culture insert when incubated with different concentrations of deacetylnemorone for 24 hours. A) A representative image of the cells at 0 and 24 hours after insert removal and the addition of deacetylnemorone. B) The percent invasion of the cells after 6, 12, or 24 hours. A significant difference, $p \leq 0.05$, from the control at the same time point is denoted by *.

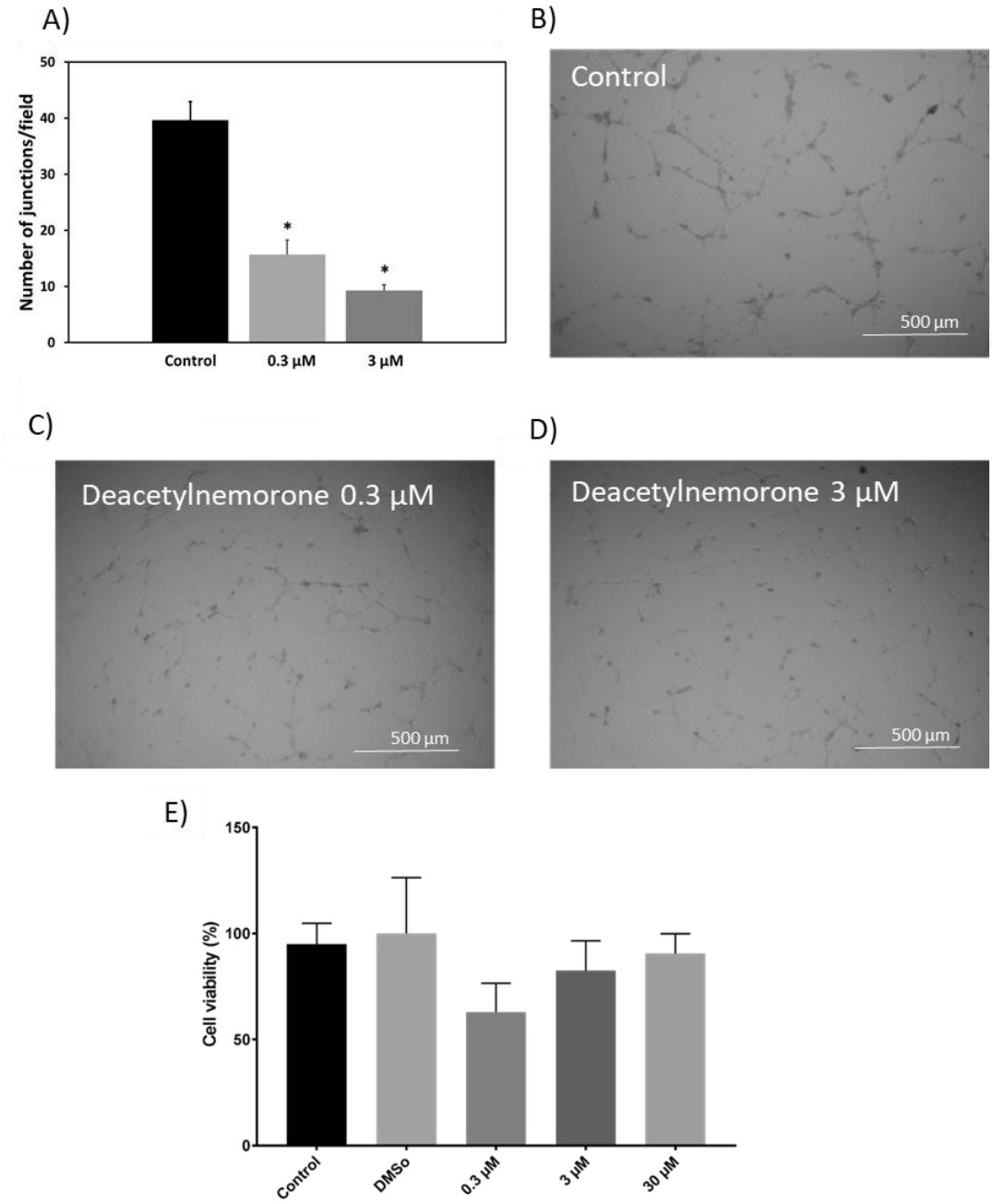

Figure 3.7: A) The average number of junctions, or tubes, formed between HUVEC endothelial cells after 8 hours of incubation on growth factor reduced BD Matrigel, where * represents a significant difference ($p < 0.05$) from the control group. A representative bright field image is shown for treatment with B) growth media alone, C) 0.3 µM deacetylnemorone, and D) 3 µM deacetylnemorone. E) The percent viability of HUVEC endothelial cells in response to 8 hours of incubation with various concentrations of deacetylnemorone as determined by an MTS assay. The control group was treated with culture media alone, and the DMSO group was treated with 0.05% DMSO in culture media.

CHAPTER 4

A MULTI-TARGETING NATURAL PRODUCT WITH CHEMOTHERAPEUTIC, IMMUNE-MODULATING, AND ANTI-ANGIOGENIC PROPERTIES[3]

4.1 ABSTRACT

Targeted therapies have changed the treatment of cancer, giving new hope to many patients in recent years, but also coming with serious hurdles. These hurdles have resulted in cancer remaining the second leading cause of death in the United States with over a quarter of these deaths coming as a result of lung and bronchus cancers. The shortcomings of targeted therapies including acquired resistance, limited susceptible patients, high cost, and high toxicities, has led to the necessity of combining these therapies with other targeted or chemotherapeutic treatments in order to reduce the required doses and increase efficacy. Natural products are uniquely capable of synergizing with targeted and non-targeted anticancer regimens due to their ability to affect multiple cellular pathways simultaneously. Compounds which provide an additive effect to the often combined immune therapies and cytotoxic chemotherapies, are exceedingly rare. Compounds of this nature would however provide a strengthening bridge between the two treatment modalities, increasing their effectiveness and improving patient

[3] Taylor, W.F., Moghadam, S.E., Yanez, M, and Jabbarzadeh, E. 2019. To be submitted to *Scientific Reports*.

prognoses. In this study, clusianone, a natural acylphloroglucinol, was investigated for its anticancer properties. While previous studies have suggested clusianone and its conformational isomers are anti-cancer agents, very few cancer types have been demonstrated to exhibit sensitivity to these compounds and little is known about the mechanism by which clusianone inhibits cancer cell growth. In this study, clusianone was shown to inhibit the growth of 60 cancer cell types and induce significant cell death in 25 cancer cell lines. The compound was further shown to modulate the immune system by polarizing macrophages to an M1 anti-cancer state. Mechanistic studies were also performed to demonstrate the effect of clusianone on non-small cell lung cancer, specifically. The compound was shown to induce G1 cell cycle arrest followed by apoptosis, as confirmed by flow cytometry and western blot analysis. Three direct targets of clusianone, namely tubulin polymerization, JAK3 kinase, and ALK (C1156Y) were identified. Clusianone was finally demonstrated to inhibit the invasion of non-small cell lung cancer and angiogenesis, suggesting an ability to prevent growth and metastasis of non-small cell lung cancer. The multi-targeted anticancer effect of clusianone on cancer cell growth, cancer cell invasion, immune regulation, and angiogenesis makes it a promising lead compound for drug discovery, especially as a combinatorial treatment alongside targeted therapies for lung cancer.

4.2 INTRODUCTION

In recent years, new hope has been given to patients diagnosed with cancer due to the emergence of targeted therapeutics[151]. However, due to the limitations of newly discovered targeted therapies, cancer remains the second leading cause of death in the

United States according to the Centers for Disease Control and Prevention[152, 153]. Of the approximately 610,000 deaths caused by cancer in 2018, over 25% will be due to lung and bronchus cancers, making them the deadliest cancer type in the United States[1]. The use of targeted therapies has represented a paradigm shift from traditional chemotherapeutics (often derived from multi-targeting natural products) to molecules and antibodies affecting specific cellular functions. Within the category of targeted therapies, immune modulating therapies have been the source of many novel treatments. Monoclonal antibodies[118], cytokines [119], dendritic cell therapies[120], chimeric antigen receptor T cells (CAR-T cells)[121], and immune checkpoint blockade therapies[122] are among the immune modulating treatments that have been approved by the Food and Drug Administration (FDA) for the treatment of cancer.

Each of these emerging technologies has led to an increase in treatment responses and survival times, however, major drawbacks have been identified for each. For example, the dendritic cell therapy, sipuleucel-T, which is made by isolating a patient's antigen presenting cells, then activating the cells with prostatic acid phosphate and granulocyte-macrophage colony-stimulating factor, and finally reintroducing the cells back into the patient has been shown to be effective in treating early metastatic castration-resistant prostate cancer. However, sipuleucel-T treatment is extremely costly due to the personalized nature of the treatment and often must be combined with other treatments, including radiation or chemotherapy, to successfully treat the patient[125]. CAR-T cell therapies, including tisagenlecleucel and axicabtagene ciloleucel, similarly function by isolating T cells from a patient and genetically engineering them to express

the chimeric antigen receptor to target cancer cells. While tisagenlecleucel holds much promise for the treatment of leukemia, as well as the distinction of being the first FDA approved gene therapy treatment in the United States, it also comes with a record setting $475,000 price tag[2]. In addition, CAR-T cell therapies have been associated with neurotoxicities and cytokine release syndrome, leading to high fever, hypotension, hypoxia, and respiratory distress[126]. Other immune regulating treatments, including immune checkpoint blockade therapies such as nivolumab, tend to be more cost effective but less personalized to each patient. Nivolumab acts by inhibiting the programmed cell death protein 1 (PD-1) checkpoint which reduces the immune surveillance evasion of cancer cells. This therapy has been shown to have a higher objective response rate and a prolonged progression-free survival compared to traditional chemotherapy in melanoma patients[3], yet the treatment is not effective in tumors with low mutational burden or lower immunogenicity. Additionally, resistance development is common even in settings with initially favorable responses[127]. As a result, these treatments are often used in combination with other therapies. Modulation of the activity of macrophages found within the tumor microenvironment has also garnered interest as a potential immune regulating cancer therapy, though the FDA has not currently approved a macrophage-targeted therapy[154].

Targeted therapies used to disrupt the unregulated growth signals of mutated proto-oncogenes or disrupt angiogenesis have similarly changed the landscape of cancer treatment despite being accompanied by major drawbacks. For many years, the first-in-line treatment for metastatic melanoma was the alkylating agent dacarbazine, until the

advent of the B-rapidly accelerated fibrosarcaoma (BRAF) inhibitor, vemurafenib. This targeted therapy increased the objective response rate to treatment from 5% to 48% in $BRAF^{V600E}$ mutant metastatic melanoma and paved the way for numerous BRAF and mitogen-activated protein kinase/extracellular signaling regulated kinases (MEK) inhibitors to be used in the treatment of the disease[155]. However, innate resistance to immune checkpoint blockade has been observed in 40–50% of metastatic melanoma patients, and BRAF/MEK inhibitors have only increased the median progression free survival of susceptible melanoma patients to 9–11 months due to the short lived efficacy [156]. Angiogenisis targeting therapies such as bevacizumab and sorafenib have been used to treat solid and metastatic tumor growth, but similarly suffer from acquired resistance, likely as a result of plasticity of the tumor microenvironment[6]. The disappointing performance of targeted therapies has led to a renewed interest in multi-targeting natural products[76].

Natural products have a long history of use as cancer therapies, either being used for or inspiring approximately 60% of cancer treatments used between 1981 and 2006[72]. These compounds tend to be safe and low cost in addition to targeting a number of cellular functions simultaneously. By targeting multiple cancer related pathways, natural compounds may be able to provide a robust, widely applicable treatment less susceptible to resistance. Natural products targeting the immune response in addition to inducing cancer cell death are uniquely positioned to synergize well with current treatment regimens. Compounds of this type may be able to limit the number of immune therapies and chemotherapies used in cancer treatment cocktails in addition to increasing their

efficacy. The number of compounds with combined chemotherapeutic and immune-modulatory effects is limited, and many of these compounds are classified as natural products[157]. Notable examples include astragaloside IV [136, 137], curcumin[133], emodin[134, 135], and total saponins of panax ginseng[158, 159]. These compounds have been demonstrated to induce apoptosis in cancer cells while simultaneously altering cytokine expression or macrophage polarization. However, the low bioavailability and limited efficacy of these compounds warrants further drug discovery efforts for multi-targeting compounds.

Clusianone and its configurational isomers are natural products that have been demonstrated to feature antimicrobial, anti-allergenic, schistosomicidal, and anti-inflammatory effects[160-163]. Additionally, these compounds have been shown to induce cell death in glioblastoma, as well as lung, melanoma, breast, prostate, renal, cervical, and tongue cancer[164-167]. Researchers have identified several potential molecular targets of clusianone, including microtubules, the mitochondrial membrane, cathepsins, and cyclins[164, 166-168]. It is likely that multiple molecules are targeted by clusianone due to the so-called "privileged structures" typically possessed by natural products. Limited *in vivo* studies have demonstrated the safety of a common configurational isomer of clusianone, 7-epiclusianone, *in vivo* in administrations of up to 300 mg/kg of body weight in female albino mice[160]. Additionally, the chemical synthesis of clusianone and its configurational isomers have been explored, allowing for a high availability of the compounds[169]. As a result, clusianone is a promising lead compound for multi-targeted cancer treatment. However, screening of clusianone across a wide range of cancers has not yet been reported. Additionally, only limited studies of the molecular targets of clusianone have

been performed, and the direct interaction of clusianone and its purported targets has yet to be determined. Finally, the effect of clusianone on the anticancer immune response has not been explored. To address these knowledge gaps, herein the combined anticancer and immune modulatory effects of clusianone are examined.

4.3 MATERIALS AND METHODS

4.3.1 CLUSIANONE SOURCE AND IDENTIFICATION

The acylphloroglucinol, clusianone, was obtained through collaboration with the University of Basel. We independently confirmed the identity of the compound by 1D and 2D nuclear magnetic resonance (NMR) in addition to time of flight mass spectrometry. For NMR analysis, clusianone was dissolved in dimethyl sulfoxide (DMSO) and analyzed using a Bruker Avance III-HD 400 MHz. ^{1}H-NMR, ^{13}C-NMR, H-H correlation spectroscopy (COSY), heteronuclear single quantum coherence (HSQC), and heteronuclear multiple bond correlation (HMBC) spectrums were generated. For mass spectrophotometry analysis, clusianone was dissolved in methanol and analysed using liquid chromatography-mass spectrometry (LC-MS) on a Thermo Orbitrap Velos Pro. NMR and mass spectrometry (MS) data can be found in Figures A.4 and A.5. For all cell culture experiments, clusianone was diluted in dimethyl sulfoxide (DMSO; Santa Cruz Biotechnology) at a concentration of 20 mM before being diluted into the cell culture media specified for each cell line.

4.3.2 CELL LINES AND REAGENTS

The non-small-cell lung cancer cell line, NCIH460, was purchased from the Development Therapeutics Program, Division of Cancer Treatment and Diagnosis tumor

repository. THP-1 human monocytic cells were obtained from American Type Culture Collection (ATCC). All cells were stored in liquid nitrogen until use. THP-1 cells were maintained in Roswell Park Memorial Institute (RPMI-1640) medium (Corning) supplemented with 10% Fetal Bovine Essence (FBE; VWR), and 0.05 mM 2-mercaptoethanol (Sigma-Aldrich). NCIH460 cells were maintained in RPMI-1640 media supplemented with 10% FBE and 2 mM L-glutamine (Sigma) in a 5% CO_2, 37°C, humidified incubator. THP-1 cells were differentiated into M0 macrophages by culturing the cells with 100 ng/ml of 12-myristate 13-acetate (PMA; Sigma) for 24 h. After differentiation, the cells were washed three times with serum free RPMI-1640 medium (Gibco) to remove non-differentiated cells.

4.3.3 NCI-60 CELL LINE SCREENING

Cytotoxicity screening was performed using the National Institute of Health's (NIH) National Cancer Institute-60 (NCI-60) screening program[144]. The screening of 60 cell lines was performed by the NIH using a Sulforhodamine B cell viability assay, as described by Shoemaker[145]. After sufficient activity was observed using one dose of clusianone (20 μM), the screening was repeated using a five-point dilution. Three concentrations, including the growth inhibition of 50% (GI50), total growth inhibition (TGI), and lethal concentration of 50% (LC50), were determined for each cell line in the screening assay using the five-dose data results.

4.3.4 IN VITRO INVASION ASSAY

Cell migration of NCIH460 cells was assessed by making a cell-free gap with a Culture-Insert 2 well 24 (IbiTreat) (Martinsried, Germany), consisting of two wells that

were separated by a wall. A total of 70 µL of cell suspension containing 6×10^4 NCIH460 cells was added to each well. Cell migration of THP-1 M0 macrophages was assessed in the same manner using 75 µL of cell suspension containing 100,000 cells per well. Cells were given 24 hours to attach and reach confluency. Culture inserts were then removed and any cell debris was washed with phosphate buffered saline (PBS; Corning). The samples were supplemented with different concentrations of clusianone in cell culture media and incubated at 37 °C and 5% CO_2 for 24 hours. Images were taken at different time intervals using a phase contrast Nikon Eclipse Ti-E inverted microscope. Quantification of the percent invasion was performed by measuring the gap distance using the following formula,

$$invasion\ \% = \frac{(W_0 - W_n)}{W_0} * 100\%$$

where W_n is the average of three gap width measurements at 6, 12, or 24 hours, and W_0 is the initial width of the cell-free gap. The media was removed and 400 µL of Cell Stain Solution (Cell Biolabs, Inc) was added to each well. The staining solution was incubated with the cells for 15 minutes at room temperature. The solution was then aspirated and discarded. Each stained well was washed with deionized water, then the water was discarded and the cells were allowed to dry at room temperature. Images were taken using a phase contrast inverted microscope (Invitrogen EVOS FL Auto Cell Imaging).

4.3.5 TUBE FORMATION ASSAY

Growth factor reduced BD Matrigel™ (Corning) was stored at -20°C long term. Before use, the Matrigel™ was thawed on ice at 4°C overnight. Next, 50 µL of Matrigel™ was added to each well of a pre-chilled 96-well plate and incubated at 37°C and 5% CO2

for 30 minutes until the Matrigel™ had formed a gel. A suspension of 20,000 human umbilical vein cells (HUVEC) in 100 µL of cell culture media dosed with clusianone was added to each well. The vehicle control consisted of only HUVEC cells and growth media. At the end of the 8 hour time point, the cells were stained Cell Stain Solution as outlined in the *in vitro* invasion assay protocol. The junctions, or tubes, connecting the endothelial cells were photographed using an Invitrogen EVOS FL Auto at 4x magnification and counted manually.

4.3.6 CELL CYCLE ANALYSIS

The effect of clusianone on the cell cycle of NCIH460 cells was determined using flow cytometry. The cells were seeded in 6 well plates at a density of 250,000 cells per well with 2 mL of media and were incubated overnight to allow the cells to attach. The media was then removed and replaced with media supplemented with clusianone. At 6, 12, 24, and 48 hours of treatment with clusianone the drugged media was collected and the cells were trypsinized with 0.25% trypsin (Corning). The detached cells were then combined with the media for each treatment and centrifuged at 2500 rpm for 5 minutes. The supernatant was discarded, and the pellet was washed and centrifuged with ice-cold PBS twice. The resulting pellet was suspended in 1 mL of ice-cold PBS, which was then added dropwise to 3 mL of ice-cold 70% ethanol in deionized water. The suspension was kept at 4°C for at least 24 hours to allow the cells to fix. Once all time points had been collected, the cells were again centrifuged and the resulting pellets were suspended in FxCycle PI/RNase Staining Solution (Invitrogen) for 15 minutes, then analyzed using a BD

LSR II flow cytometer. Propidium iodide (PI) expression was used to quantify the percentage of cells in the sub-G1, G0/G1, S, and G2/M phases.

4.3.7 ANNEXIN V/PI APOPTOSIS ASSAY

The ability of the clusianone to induce apoptosis in NCIH460 cells was determined using the FITC Annexin V/ Dead Cell Apoptosis Kit (Invitrogen). The cells were seeded in 6 well plates at a density of 200,000 cells with 2 mL of media per well and were incubated overnight to allow the cells to attach. The media was then removed and replaced with media supplemented with clusianone or a vehicle control, 0.3% DMSO in RPMI 1640 media supplemented with 10% fetal bovine essence and 2 mM L-glutamine. After 48 hours of incubation, the media was collected, and the cells were trypsinized with 0.25% trypsin. The detached cells were then combined with the media for each treatment and centrifuged at 2500 rpm for 5 minutes. The supernatant was discarded, and the pellet was washed with ice cold PBS, centrifuged, and resuspended in Annexin V buffer (Invitrogen) at 1,000,000 cells/mL. Next, 100 µL of the cell suspensions were added to flow cytometry tubes, and 5 µL of Annexin V/FITC antibody and 1 µL of PI working solution (Invitrogen) were added to each sample. The samples were incubated for 15 minutes at room temperature and analyzed using a BD LSR II flow cytometer.

4.3.8 WESTERN BLOTTING

The effect of clusianone on apoptosis related proteins in NCIH460 cells was assessed using western blotting. The cells were seeded in T-25 flasks (VWR) at a density of $1.5x10^6$ cells in 5 mL of media. The cells were allowed to attach for 24 hours. After the cells had attached, the media was replaced with media supplemented with either a

vehicle control or the designated concentration of clusianone. After 12 and 24 hours, one flask of each treatment group was selected, the media was removed and replaced with PBS, and the cells were detached by scraping. The cells were then centrifuged at 2500 rpm for 5 minutes and the supernatant was discarded. The cells were then lysed by suspending the pellet in Radio-immunoprecipitation assay (RIPA) buffer (CST) supplemented with phenylmethylsulfonyl fluoride (PMSF) (Sigma-Aldrich) at a concentration of 400 µL/ 10^7 cells. The suspension was incubated on ice for 5 minutes, briefly vortexed, and sonicated for 45 seconds. The suspension was then centrifuged at 14,000 g for 10 minutes at 4°C. The supernatant containing the extracted protein was collected. Protein concentration was determined by the bicinchoninic acid (BCA) assay following the manufacturer's protocol.

Protein extract was then diluted in RIPA buffer and 4x Laemmli sample buffer (Bio-Rad), heated at 95°C for 5 minutes, cooled, and briefly centrifuged. Approximately 50 µg of protein was loaded into each well of 12% Mini-Protean TGX Stain-Free Gels (Bio-Rad). The gels were electrophoresed in sodium dodecyl sulfate (SDS) running buffer (CST) at 70 V for approximately 90 minutes using a mini-protean tetra cell electrophoresis chamber (Bio-Rad). The proteins were transferred to a 0.2 µm pore size nitrocellulose membrane using Tris-Glycine transfer buffer (CST) in a Criterion wet blotter (Bio-Rad) at 70 V for 90 minutes. The membrane was washed with Tris buffered saline (TBS) (CST) and blocked with 5% milk (CST) in TBS for 1 hour. The membrane was then washed with TBST and treated with primary antibody diluted 1:1000 in 5% bovine serum albumin (BSA) in TBS with Tween (TBST) at 4°C overnight. All primary antibodies were purchased from CST and

were sourced from rabbit. The membrane was again washed with TBST before incubating the membrane in anti-rabbit horseradish peroxidase (HRP)-linked secondary antibody (CST) diluted 1:2000 in 5% milk in TBST for 1 hour. The membrane was washed with TBST a final time, then incubated with SignalFire reagent for 2 minutes and imaged using a BioRad ChemiDoc MP Imaging system. If a membrane was re-probed for a different protein, the membrane was stripped using Restore western blot stripping buffer (Thermo).

4.3.9 TUBULIN POLYMERIZATION ASSAY

Tubulin polymerization was assessed using the Tubulin Polymerization Assay Kit from Cytoskeleton as per the manufacturer's instructions. Clusianone was diluted in DMSO at 20 mM before being diluted to a 10x solution in General Tubulin Buffer. Paclitaxel was used as the positive control. Absorbance correlating to the extent of polymerization was recorded every minute for a total of one hour. Each experimental group was repeated in triplicate.

4.3.10 DISCOVERX KINASE PANEL

Clusianone was submitted to the DiscoverX KINOMEscan scanTK panel to determine its ability to directly inhibit the function of 135 tyrosine kinases. The assay is an active site-directed competition assay, which does not require the use of ATP to assess kinase function. One concentration of clusianone (20 µM) was tested in the panel, and the results were reported as the percent of remaining function for each kinase upon treatment with clusianone.

4.3.11 MACROPHAGE CYTOTOXICITY ASSAY

Macrophage viability in response to clusianone treatment was assessed using CellTitter 96 Aqueous Non-Radioactive Cell Proliferation assay (Promega). THP-1 cells were seeded into 96-well tissue culture plates at a density of 100,000 cells/well with a total volume of 100 µL of complete growth media (RPMI-1640 media supplemented with 10% Fetal Bovine Essence, and 0.05 mM 2-mercaptoethanol) with the addition of 100 ng/ml of PMA in each well. Cells were incubated for 24 hours at 37°C and 5% CO_2 to allow for cell differentiation to M0 macrophages. After differentiation, the cells were washed three times with serum free RPMI-1640 medium to remove non-differentiated cells. After cell differentiation, the cells were exposed to various concentrations of clusianone for 75 hours. Then, the cells were washed with PBS, and culture media supplemented 20% 3-(4,5-dimethylthiazol-2-yl)-5-(3-carboxymethoxyphenyl)-2-(4-sulfophenyl)-2H-tetrazolium (MTS) solution (Promega) was added to the cells. The cells were incubated for 2 hours, and the absorbance of each well at 490 nm was measured using a Spectramax 190 microplate reader.

4.3.12 ENZYME-LINKED IMMUNOSORBENT ASSAY (ELISA)

THP-1 cells were differentiated in a 24-well plate at a density of 300,000 cells/well with a total volume of 1.5 ml of culture media per well. After the 72 hours of treatment with clusianone the culture media was collected from all the experimental groups. The media was centrifuged at 2500 rpm for 5 min and stored at -20 °C. The concentrations of tumor necrosis factor alpha (TNFα) and interleukin-6 (IL-6) in the THP-1 media were evaluated using human IL-6 and TNFα tetramethylbenzidine (TMB) enzyme-linked

immunosorbent assay (ELISA) development kits (Peprotech) according to the manufacturer's protocol. Colorimetric changes were measured using a SpectraMax 190 microplate spectrophotometer at 450 nm with wavelength correction set at 620 nm. Standard curves for each cytokine were run in parallel to convert the absorbance to concentration in each group.

4.3.13 RNA EXTRACTION AND QUANTITATIVE REAL-TIME POLYMERASE CHAIN REACTION (RT-PCR)

Total RNA was isolated using the Gene Jet RNA Purification kit (Thermo Scientific) according to the manufacturer's instructions. The quantification of the ribonucleic acid (RNA) was measured using a Thermo Scientific Nanodrop 2000c spectrometer and considered pure if the ratio of absorbance at 260 nm/280 nm was ≥ 2. RNA isolates were stored at -20˚C until they were used for reverse transcription polymerase chain reaction (rt-PCR). The RNA was prepared as a template for complementary deoxyribonucleic acid (cDNA) synthesis using the iScript cDNA Synthesis kit (Bio-Rad). Quantitative rt-PCR analysis was performed with the synthesized cDNA and SYBER® Green PCR Supermix (Bio-Rad). Gene expression was normalized to the housekeeping gene glyceraldehyde 3-phosphate dehydrogenase (GAPDH) and the control group, non-treated THP-1 M0 macrophages (2-ΔΔC). Gene expression values were calculated by using the mean cycle threshold (CT) values of the samples. All primers (Table S1) were synthetized by Integrated DNA Technologies (Coralville).

4.4 RESULTS

4.4.1 CLUSIANONE INHIBITS CELL GROWTH AND INDUCES CELL DEATH IN A WIDE SPECTRUM OF CANCERS.

To determine the cytotoxic potential of clusianone (Figure 4.1), the compound was screened against the 60 cancer cell lines of the National Cancer Institute's NCI-60 cancer panel. This panel utilizes a Sulforhodamine B assay to quantify the total cellular protein present after 48 hours of treatment with a compound of interest. The panel screens 60 unique cancer cell lines across 9 different tissue types including leukemia, non-small cell lung cancer, melanoma, breast cancer, central nervous system (CNS) cancer, renal cancer, ovarian cancer, and prostate cancer. For each of the cell lines, the concentration of compound required to reduce the growth of cells to 50% that of the vehicle control (GI50), the concentration required to inhibit the growth of any amount of cells (TGI), and the concentration required to induce cell death of 50% of the seeded cells (LD50) was determined (Figure 4.2).

Clusianone inhibited the growth of all 60 cell lines in the NCI-60 cancer panel (Figure 4.2A) with an average GI50 of 2.7 μM. Clusianone did not, however, exhibit a high level of selectivity in inhibiting the growth of the cancer cell lines as the determined GI50 concentrations only ranged from 1.63 μM to 3.89 μM. The selectivity of clusianone was higher in completely inhibiting cell growth. The majority of TGI concentrations for cell lines within the panel were less than 10 μM, however, two leukemia cell lines continued to grow after 48 hours of incubation with 101 μM of clusianone, the highest concentration tested (Figure 4.2B). In addition to inhibiting the growth of many cancer cell lines,

clusianone exhibited an LD50 of less than 101 µM for 25 of the cell lines tested (Figure 4.2C). Interestingly, the cytotoxicity of clusianone varied widely within each tissue type, with the exception of leukemia, for which no LD50 under 101 µM was observed.

The full growth response data for each of the cell lines can be found in Table S2 As lung and bronchus cancers are projected to be responsible for over one quarter of all cancer-related deaths in the United States in 2018, the effect of clusianone on small cell lung cancer was investigated further. The non-small cell lung cancer cell line, NCIH460, was the most sensitive lung cancer cell line to clusianone. The GI50, TGI, and LD50 concentrations of the NCIH460 cell line were 2.6 µM, 6.2 µM, and 35µM, respectively (Figure 4.3).

4.4.2 CLUSIANONE INDUCES G1 ARREST FOLLOWED BY APOPTOSIS IN NCIH460 SMALL CELL LUNG CANCER CELLS

In order to gain insight into the mechanism of action of clusianone on NCIH460 small cell lung cancer cells, the cell cycle of the NCIH460 cells over 48 hours under exposure to clusianone was analyzed by quantifying the amount of PI bound to DNA within the cells using flow cytometry (Figure 4.4). When the NCIH460 cells were treated with 35 µM of the compound the number of cells in the G1 phase of the cell cycle increased at 12 and 24 hours of incubation when compared to the vehicle control, 0.2% DMSO in RPMI 1640 media supplemented with 10% fetal bovine essence. Additionally, a depletion of cells in the S and G2/M phases of the cell cycle occurred after 24 hours when compared to the control and persisted after 48 hours. The percent of cells in the S phase decreased at a rate faster than the percent of cells in the G2/M phase decreased when

exposed to clusianone, suggesting that cells were progressing from the S phase to G2/M phase, but they were unable to progress from the G1 phase to S phase when exposed to clusianone. At the 48-hour time point, the percentage of cells in the G1 phase decreased when compared to the percent of cells in the G1 phase at 24 hours when exposed to clusianone. As the percent of cells in the S and G2/M phases continued to decrease over this same time period, this decrease in G1 phase cells can be explained by the increase in sub G1 cells seen from 24 hours to 48 hours of incubation with clusianone. These sub G1 cells are hypothesized to be dead cells with cleaved DNA.

Annexin V/PI expression for the NCIH460 cells after 48 hours of incubation with 7.6 µM, 15 µM, 35 µM, and 61 µM clusianone was determined to evaluate whether the cells observed in the sub-G1 phase had undergone apoptosis (Figure 4.5). As the concentration was increased the number of live cells decreased, confirming the dose dependent cytotoxicity of clusianone on NCIH460 cells. In each of the clusianone-treated groups, the number of apoptotic and necrotic cells increased when compared to the vehicle control, 0.3% DMSO in RPMI 1640 media supplemented with 10% fetal bovine essence and 2 mM L-glutamine. The number of apoptotic, Annexin V positive cells increased as the concentration of clusianone was increased. Additionally, at lower concentrations, a population of PI positive and Annexin V low cells was observed (Figure 4.5B and Figure 4.5C). This suggests that at lower concentrations, a population of NCIH460 cells were in the process of exposing the Annexin V binding protein, phosphatidylserine, and therefore were in an earlier stage of apoptosis after 48 hours than were cells treated with a higher dose of clusianone.

We also determined the caspase activity of the NCIH460 cells to confirm the occurrence of apoptosis after exposure to clusianone. The quantity of inactive/full length and active/cleaved forms of caspases 7, 8, 3, and 9 present with the NCIH460 cells was determined using western blotting (Figure 4.6). After 12 and 24 hours of exposure to clusianone, the full length form of caspases 7 and 8 decreased as the concentration of clusianone was increased, but the cleaved forms of these caspases were not detected. No trend was apparent from the quantity of caspase 3 detected at either time point. However, the ratio of cleaved caspase 9 to full length caspase 9 increased dramatically for NCIH460 cells treated with 7.6 µM or 15 µM of clusianone for 12 or 24 hours. Additionally, a dose- and time-dependent increase in the ratio of cleaved Poly (ADP-ribose) polymerase (PARP) to full length PARP occurred under incubation with clusianone. The cleavage of caspase 9 and PARP further confirm that clusianone induces apoptosis in NCIH460 lung cancer.

4.4.3 CLUSIANONE INHIBITS ANGIOGENESIS AND CELL MIGRATION OF NCIH460 CELLS

After determining clusianone's ability to induce cell death at high concentrations, the ability of clusianone to inhibit cell migration of NCIH460 cells at low concentrations was assessed. A uniform cell gap was formed using a 2 well cell culture insert, and the cells were allowed to grow for up to 24 hours exposed to either a vehicle control or clusianone (Figure 4.7). After 24 hours, the cell-free gap had almost completely closed for cells treated with the vehicle control. In contrast, after 24 hours of incubation with clusianone the percent invasion of NCIH460 cells into the cell-free gap was significantly lower compared to the control for each concentration used, including 200 nM, a

concentration 10-times lower than the GI50 concentration. At each time point considered (6, 12, and 24 hours), a dose dependent decrease in invasion was observed.

Similarly, the ability of clusianone to inhibit angiogenesis was indirectly assessed. HUVEC endothelial cells were incubated with or without clusianone on a growth factor reduced BD Matrigel^{TM} basement matrix. Tube formation between the endothelial cells was assessed after 8 hours (Figure 4.8A). A dose dependent reduction of tube formation was observed when the cells were exposed to clusianone at concentrations between 0.2 and 20 µM (Figure 4.8B). The reduction of tube formation became significant ($p \leq 0.05$) at 20 µM clusianone. An MTS viability assay of HUVEC endothelial cells in response to clusianone for 8 hours revealed that the compound was not toxic at this time point (Figure 4.8C). No significant difference in viability was observed in these cells even at the highest concentration of 20 µM clusianone.

4.4.4 CLUSIANONE DIRECTLY TARGETS TUBULIN POLYMERIZATION, JAK3, AND ALK (C1156Y)

While the cytotoxic effect of clusianone on a number of cell lines has been previously reported, the direct effect of clusianone on its purported molecular targets has yet to be determined[164-167]. Due to the identification of microtubules as a potential target of clusianone in other lung cancer cell lines[167], the effect of clusianone on tubulin polymerization was investigated using the cytoskeleton tubulin polymerization assay (Figure 4.9). While the nucleation time, *i.e.,* the time required for tubulin to begin polymerizing, was not affected by the presence of clusianone, the rate at which the tubulin polymerized was significantly increased by 100 and 200 µM of clusianone (Figure

4.9A). The rate at which the tubulin polymerized is best represented by the Vmax value, which corresponds to the highest ratio of increase in the absorbance at 340 nm to time for each treatment group. We observed a dose dependent increase in Vmax, consistent with the increase in Vmax observed in the presence of the known microtubule stabilizing agent, paclitaxel[170].

To determine the ability of clusianone to target tyrosine receptor kinases, a common target of cancer therapeutics, the compound was screened using the DiscoverX scanTK kinase panel. This panel determines the ability of a compound to inhibit the activity of 135 different tyrosine kinases. A reduction of kinase activity to 30% or below is considered significant in this one dose screen. At a concentration of 20 µM, clusianone significantly inhibited two kinases, anaplastic lymphoma kinase C1156Y (ALK C1156Y) and janus kinase 3 (JAK3). The activity of ALK (C1156Y) and JAK3 were inhibited by 70% and 75% respectively. ALK (C1156Y) is a mutation of the ALK tyrosine kinase, which has been associated with acquired resistance to the targeted ALK inhibitor, crizotinab, used for the treatment of small cell lung cancer[171]. JAK3 is a kinase that plays a role in the immune response of several types of cells[172].

4.4.5 CLUSIANONE INCREASES THE EXPRESSION OF PRO-INFLAMMATORY CYTOKINES IN THP-1 MACROPHAGES

In order to determine the effect of clusianone on the immune response, the ability of clusianone to modulate macrophages was investigated. A shift in M0, naïve macrophages, to M1 polarized, pro-inflammatory and anticancer macrophages, is denoted by an increase in inflammatory cytokines, including TNFα and IL-6 among others.

We assessed the expression of these cytokines by THP-1 macrophages after 72 hours of incubation with clusianone (Figure 4.10). Both the gene expression of the cytokines and the concentration of the cytokine excreted into the cell culture media were determined by quantitative rtPCR (q-rtPCR) and ELISA, respectively. In order to ensure the concentrations of clusianone tested were safe for the macrophages, the viability and invasion capability of the macrophages under exposure to clusianone was tested and no significant changes were observed (Figure A.6). The gene expression of both TNFα and IL-6 increased as the concentration of clusianone was increased. At 20 μM of clusianone, the gene expression of both cytokines had increased 60–70 fold over the expression of the control, untreated macrophages. While a dose dependent increase in the presence of each cytokine in the media of the cells also occurred, this increase was not significant when compared to the control. These results indicate that the M0 macrophages may polarize to anticancer M1 macrophages in the presence of clusianone.

4.5 DISCUSSION

Natural products have been instrumental in the treatment of cancer and are currently garnering renewed interest as lead compounds for cancer therapies and complementary treatments due to the shortcomings of targeted therapeutics. Compounds which simultaneously affect immune regulation of cancer and induce cancer cell death may provide a uniquely well suited complementary treatment to current targeted therapy and chemotherapy regimens. Clusianone and its configurational isomers, particularly 7-epiclusianone, are natural products that have been shown to exhibit a wide array of biological effects. The anticancer effects of clusianone have been

previously investigated in a limited number of cancer cell lines[164-167], but the mechanism of action and the molecular targets of the compound have not been fully investigated, nor has its ability to modulate the immune response to cancer.

In this study, clusianone was demonstrated to inhibit the growth of cancer cells across 9 tissue types and 60 individual cancer cell lines. A growth inhibitory effect was observed for each cell line, but an LD50 less than the highest concentration tested was only observed in 25 of the 60 cell lines tested. These 25 cell lines were composed of cell lines from each tissue type tested excluding leukemia. In combination, these effects suggest that clusianone could be used to slow the progression of many variations of cancer, but it will not be cytotoxic to all types of cells. As clusianone is likely to be safe *in vivo* at relatively high concentrations[160] and the compound is selective in inducing cell death, clusianone has the potential to be safely used for the treatment of a diverse group of cancers. In particular, renal cancer, melanoma, central nervous system tumors, colon cancer, and non-small cell lung cancer appear to be sensitive to the cytotoxic effects of clusianone. It is unclear what factors determine the sensitivity of each cancer cell line to clusianone, and further study will be required to determine how to best predict sensitivity to clusianone within a particular cancer tissue. Clusianone's anticancer effects have the biggest potential for clinical impact, however, on non-small cell lung cancer due to the high rate of lung cancer related death in the United States, the ability of the compound to induce cell death in non-small cell lung cancer cell lines, and the ability of clusianone to inhibit an ALK tyrosine kinase mutation responsible for acquired resistance to treatment.

In order to further investigate the anticancer effect of clusianone on non-small cell lung cancer, additional experiments were performed on a lung cancer cell line which had exhibited sensitivity to the compound. The non-small cell lung cancer cell line that exhibited the greatest sensitivity to clusianone was NCIH460. Clusianone induced dose dependent cell death in this cell line with a GI50, TGI, and LD50 of 2.6 µM, 6.2 µM, and 35µM, respectively. We determined that cell death in the NCIH460 cell line occurred after 48 hours of treatment with 35 µM of clusianone. Cell cycle analysis revealed that the cell death was preceded by G1 phase arrest, and a subsequent reduction of S phase and G2/M phase cells. A similar G1 phase arrest has been observed after treatment of A549 lung cancer cells with 7-epiclusianone, suggesting that the configurational isomers have similar mechanisms of action for inducing cytotoxicity in lung cancer[167]. Furthermore, the cell death induced by clusianone in NCIH460 cells was shown to proceed through an apoptotic mechanism. As the concentration of clusianone was increased, more apoptotic cells were observed using flow cytometry. Apoptosis was confirmed by the cleavage of caspase 9 and PARP, which participate in the caspase cascade leading to cell death after mitochondrial depolarization has occurred[173, 174]. We also observed a decrease in full length caspase 7 and caspase 8 expression upon treatment of NCIH460 cells with clusianone. The decrease in full length caspase 7 was further evidence that the caspase cascade leading to apoptotic cell death had been activated. The decrease in full length caspase 8 in addition to the activation of caspase 9 suggested that both the extrinsic, receptor mediated apoptosis pathway and the intrinsic apoptosis pathway were

activated[174]. This finding is not conclusive, however, as no cleaved caspase 8 was detected at either 12 or 24 hours of incubation with clusianone.

In addition to inducing dose dependent apoptosis in non-small cell lung cancer, clusianone also inhibited the invasion of NCIH460, non-small cell lung cancer. Significant invasion inhibition was observed at a concentration as low as 200 nM. Further, clusianone was shown to significantly reduce the tube formation between HUVEC endothelial cells at a concentration of 20 μM. Tube formation is a critical step in the process of angiogenesis which is utilized by the wound healing process as well as by cancers to feed tumor growth[124, 175]. By inhibiting angiogenesis and tumor cell invasion, clusianone may act to inhibit continued tumor growth and metastasis of non-small cell lung cancer into healthy tissue. These effects were seen in concentrations less than the concentrations required to induce cell death, suggesting clusianone directly inhibits molecular targets associated with angiogenesis and invasion which were outside the scope of this study.

Mechanistic studies were however performed to elucidate the mechanism by which clusianone induces cell death in non-small cell lung cancer. For the first time, the direct effect of clusianone on cancer proliferation targets including microtubules and ALK (C1156Y) was determined. While 7-epiclusianone has been previously suggested to impact microtubule structure [167], the mechanism of this effect was unclear. This study demonstrated that clusianone acts by stabilizing and increasing the rate of polymerization of tubulin directly. This mechanism of action is one shared by chemotherapy agents, such as paclitaxel, though the concentration of clusianone required to impact the polymerization of tubulin was high compared to the concentration necessary to induce

growth inhibition or cell death on NCIH460 cells. As a result, it is likely that additional molecular targets are influenced by clusianone in order to impart its cytotoxic effects. We further determined that clusianone directly inhibits the function of two tyrosine kinases, ALK (C1156Y) and JAK3. While these molecular targets are not largely present within NCIH460 lung cancer, and thus are not likely to be involved with a mechanism of cell death, they do suggest clusianone may target non-small cell lung cancer cells with acquired resistance to kinase inhibitors.

Due to the increasing role of immune targeted therapies in lung cancer, the ability of clusianone to modulate the immune system within the tumor microenvironment was also investigated[176]. Macrophages are immune cells that play a role in T-cell activation in addition to engulfing pathogens and dead cells. Within the tumor microenvironment, tumor associated macrophages (TAMs) can be formed, which resemble macrophages polarized to an M2, anti-inflammatory state and aid in tumor growth and evasion from the immune system[177]. While some studies have suggested eliminating TAMs as a therapeutic strategy, others have hypothesized that polarizing macrophages to the M1 state within the tumor microenvironment will not only eliminate the tumor-supportive functions of TAMs but will also activate the immune system against the tumor[178]. In this study, clusianone was shown to increase the gene expression of TNFα and IL-6 within THP-1 derived macrophages, potentially polarizing the cells to an anticancer, pro-inflammatory M1 state. This regulation of macrophages suggests that clusianone might be a useful complementary treatment when combined with current first-in-line immune

therapies. This is especially true in the case of CAR-T cell therapy, in which macrophage dysfunction is the source of some of the most serious side effects[126].

Future studies will be required to determine the effectiveness of clusianone as a cancer therapy. More mechanistic studies should be performed to elucidate the primary targets for clusianone's cytotoxic and immune regulatory properties. Of particular interest to future studies should be the effect of clusianone on non-small cell lung cancer due the high mortality rates of this malignancy and the compound's ability to induce apoptosis and inhibit invasion of non-small cell lung cancer cell lines. With this information, the groundwork will be laid to perform *in vivo* determinations of the efficacy of clusianone in inducing cancer cell death and regulating the immune response. Special notice should be paid to the effect of clusianone on the polarization of macrophages within the tumor microenvironment in these *in vivo* experiments. Additionally, the synergistic effect of clusianone when combined with currently approved cancer immune therapies should be investigated.

Clusianone is a promising lead compound for anticancer therapies due to its combined apoptotic, anti-angiogenesis, anti-invasion, and immune-regulating properties. The natural product was shown to have three direct molecular targets in this study, with more targets likely undiscovered. The multi-targeting nature of clusianone stands to provide a complementary treatment to emerging targeted oncology therapeutics, which suffer from limited efficacy when used alone as well as toxicities and acquired resistance. Additionally, clusianone may combine growth inhibitory and cytotoxic effects on cancer cells with a modulation of the tumor microenvironment to oppose the formation and

spread of cancer when used alone. In summary, clusianone may provide a robust and multipronged treatment for cancer, especially non-small cell lung cancer.

4.6 FIGURES

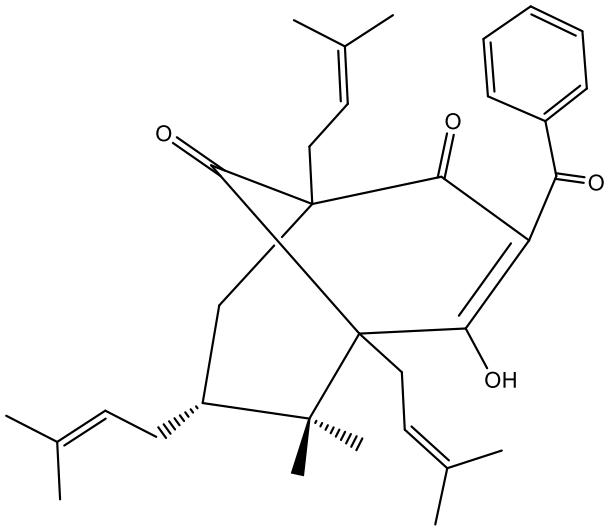

Figure 4.1: The structure of the polyprenylated acylphloroglucinol natural product, clusianone.

A)

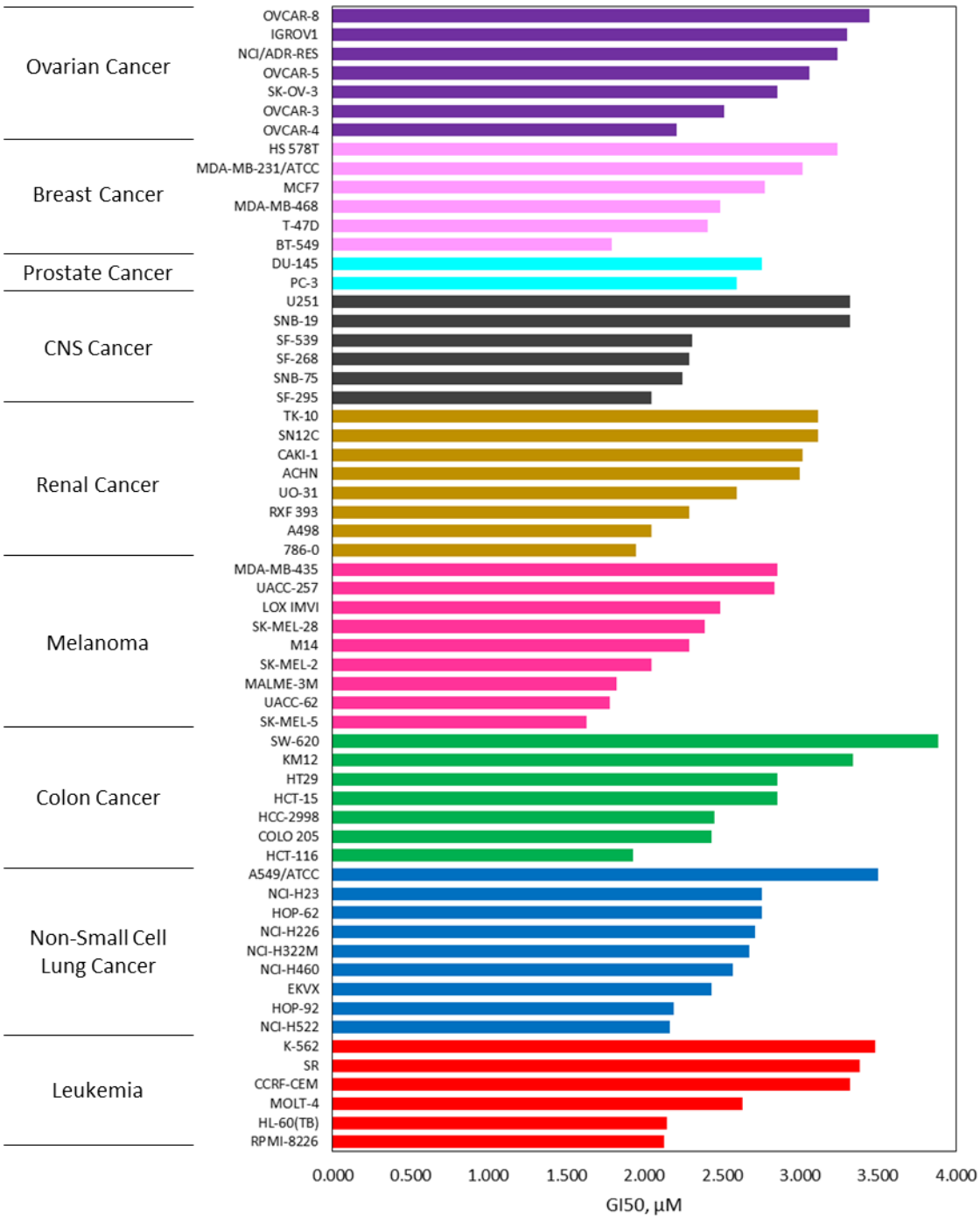
Ovarian Cancer
Breast Cancer
Prostate Cancer
CNS Cancer
Renal Cancer
Melanoma
Colon Cancer
Non-Small Cell Lung Cancer
Leukemia
OVCAR-8
IGROV1
NCI/ADR-RES
OVCAR-5
SK-OV-3
OVCAR-3
OVCAR-4
HS 578T
MDA-MB-231/ATCC
MCF7
MDA-MB-468
T-47D
BT-549
DU-145
PC-3
U251
SNB-19
SF-539
SF-268
SNB-75
SF-295
TK-10
SN12C
CAKI-1
ACHN
UO-31
RXF 393
A498
786-0
MDA-MB-435
UACC-257
LOX IMVI
SK-MEL-28
M14
SK-MEL-2
MALME-3M
UACC-62
SK-MEL-5
SW-620
KM12
HT29
HCT-15
HCC-2998
COLO 205
HCT-116
A549/ATCC
NCI-H23
HOP-62
NCI-H226
NCI-H322M
NCI-H460
EKVX
HOP-92
NCI-H522
K-562
SR
CCRF-CEM
MOLT-4
HL-60(TB)
RPMI-8226
0.000
0.500
1.000
1.500
2.000
2.500
3.000
3.500
4.000
GI50, µM

B)

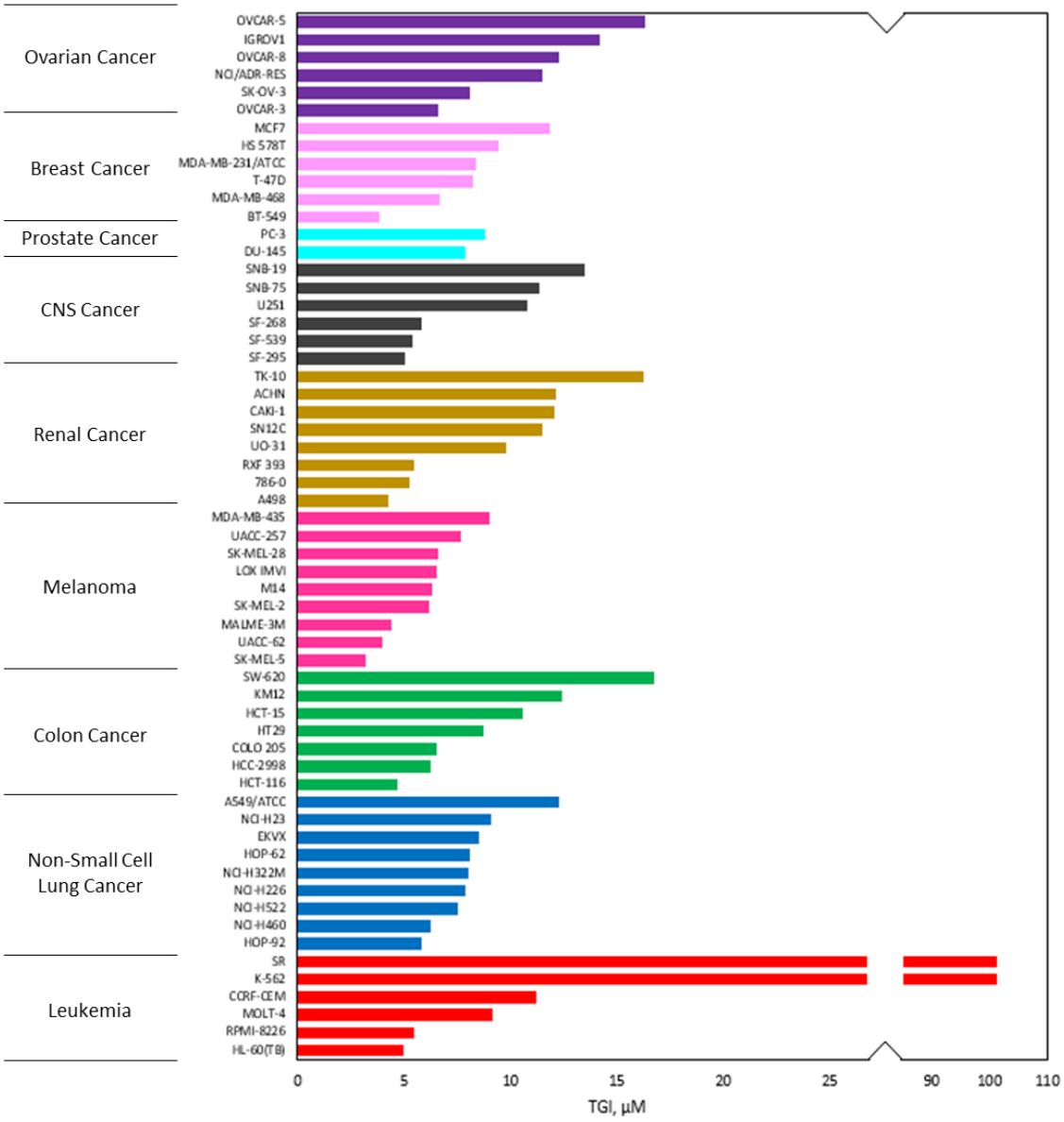
Ovarian Cancer
Breast Cancer
Prostate Cancer
CNS Cancer
Renal Cancer
Melanoma
Colon Cancer
Non-Small Cell Lung Cancer
Leukemia
OVCAR-5
IGROV1
OVCAR-8
NCI/ADR-RES
SK-OV-3
OVCAR-3
MCF7
HS 578T
MDA-MB-231/ATCC
T-47D
MDA-MB-468
BT-549
PC-3
DU-145
SNB-19
SNB-75
U251
SF-268
SF-539
SF-295
TK-10
ACHN
CAKI-1
SN12C
UO-31
RXF 393
786-0
A498
MDA-MB-435
UACC-257
SK-MEL-28
LOX IMVI
M14
SK-MEL-2
MALME-3M
UACC-62
SK-MEL-5
SW-620
KM12
HCT-15
HT29
COLO 205
HCC-2998
HCT-116
A549/ATCC
NCI-H23
EKVX
HOP-62
NCI-H322M
NCI-H226
NCI-H522
NCI-H460
HOP-92
SR
K-562
CCRF-CEM
MOLT-4
RPMI-8226
HL-60(TB)
0
5
10
15
20
25
90
100
110
TGI, µM

C)

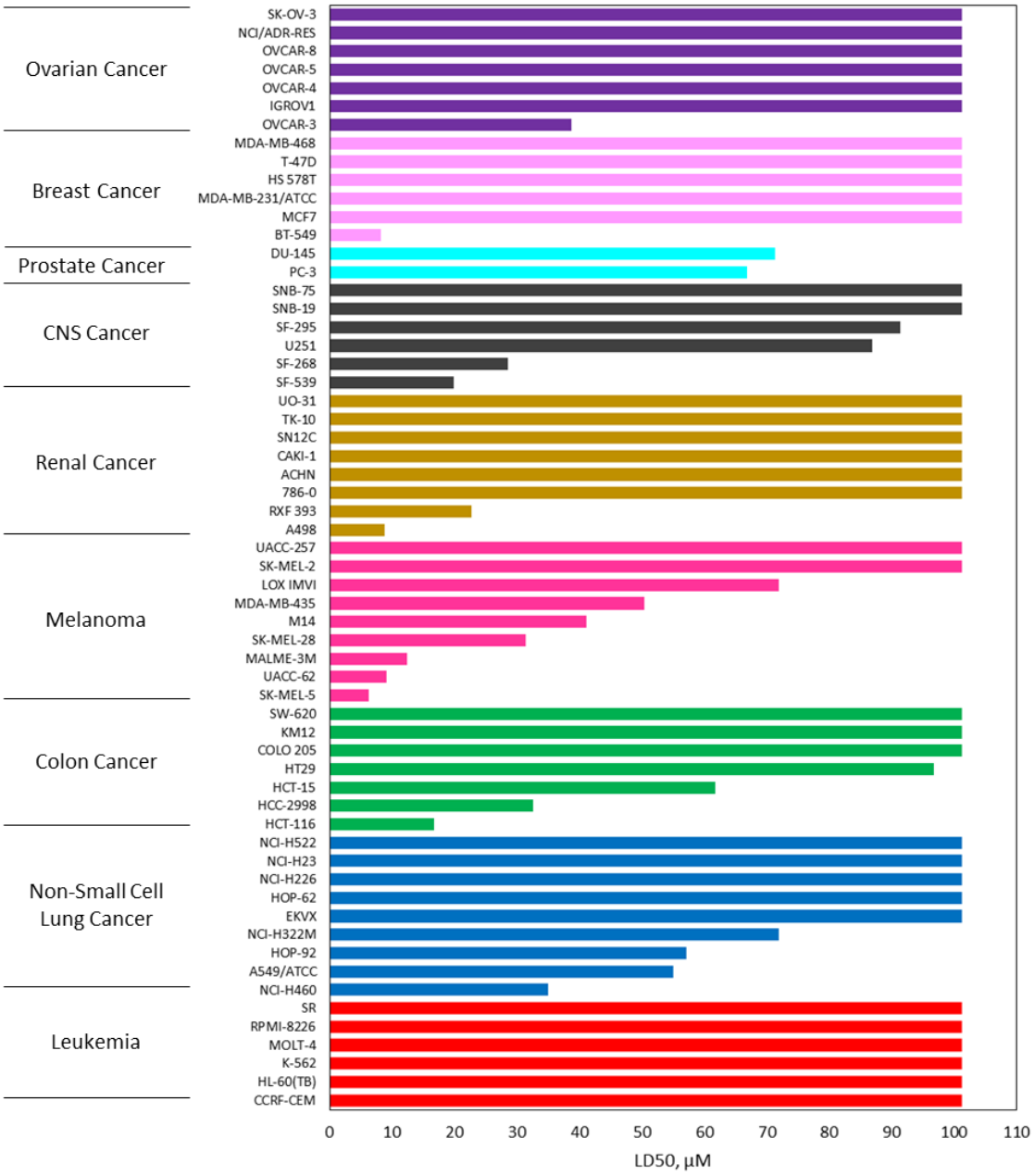

Figure 4.2: Waterfall plot of the A) GI50, B) TGI, and C) LC50 of clusianone for 60 cell lines as determined by the NCI-60 five dose screening assay. The tissue type of each cell line is denoted by color (Purple – Ovarian Cancer, Pale pink – Breast Cancer, Aqua – Prostate Cancer, Grey – CNS cancer, Gold – Renal Cancer, Bright Pink – Melanoma, Green – Colon Cancer, Blue – Non-small cell lung cancer, Red – Leukemia). The GI50, TGI, and LC50 was set to 100 µM if the true concentration was higher than what was tested in the five dose screen.

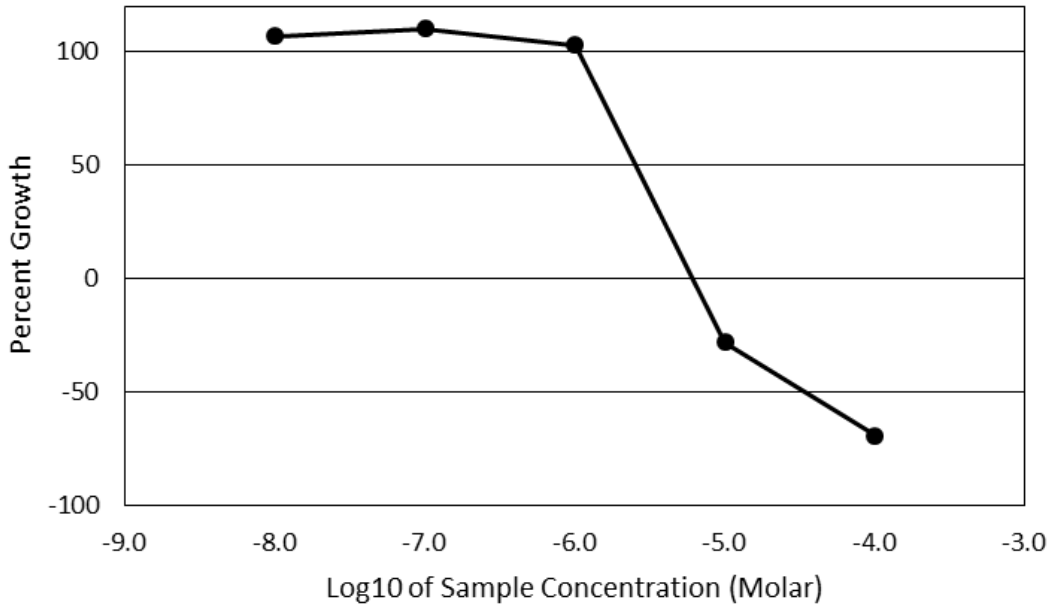

Figure 4.3: Percent growth of NCIH460 non-small cell lung cancer cells after 48 hours of treatment with clusianone in the NCI-60 panel. The NCI-60 panel is a sulforhodamine B based screening method of 60 immortalized cancer cell lines. The GI50, TGI, and LD50 concentrations of clusianone for the NCIH460 cells were determined to be 2.6 µM, 6.2 µM, and 35µM, respectively.

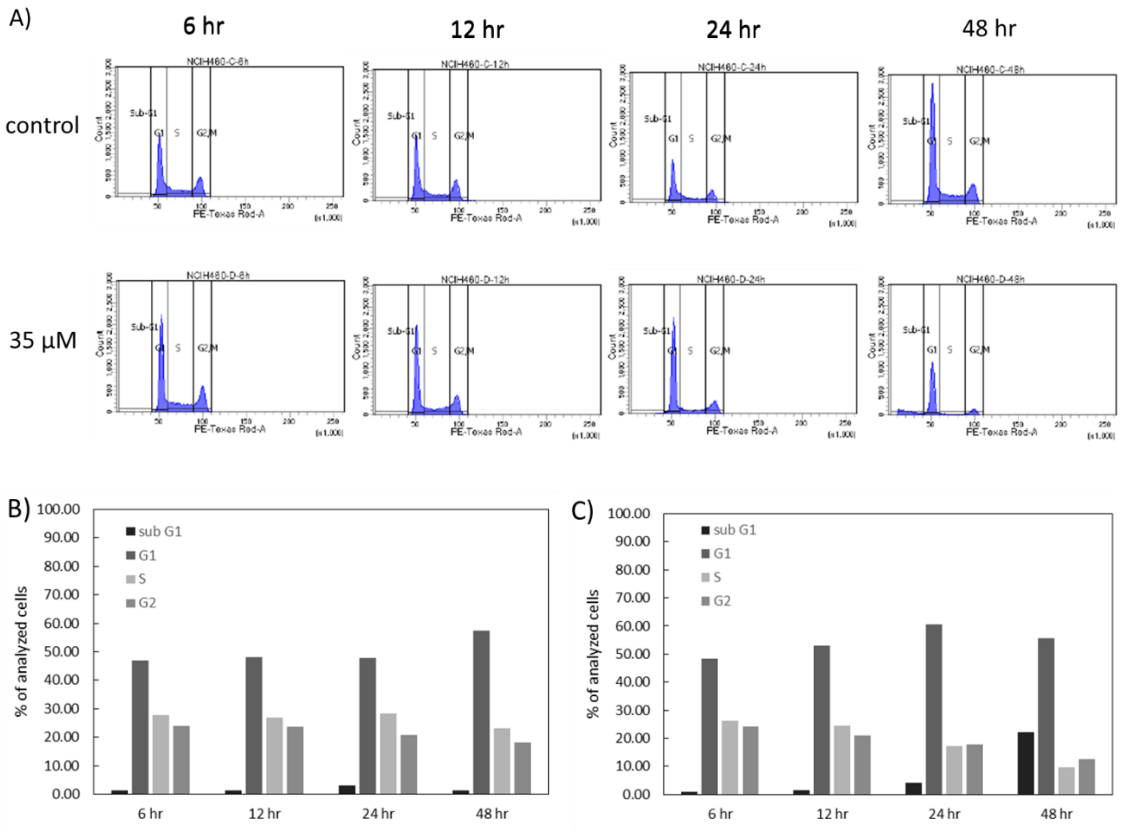

Figure 4.4: Cell cycle flow cytometry experiment showing the A) histogram of propidium iodide expression of NCIH460 cells after four different time points of treatment with either a vehicle control or clusianone. The histograms were divided into 4 regions representing the sub-G1, G1/G0, S, and G2/M phases of the cell cycle. The percentage of cells in the sub-G1, G1/G0, S, and G2/M regions is shown for both B) the cells treated with the vehicle control and C) the cells treated with 35 µM of clusianone.

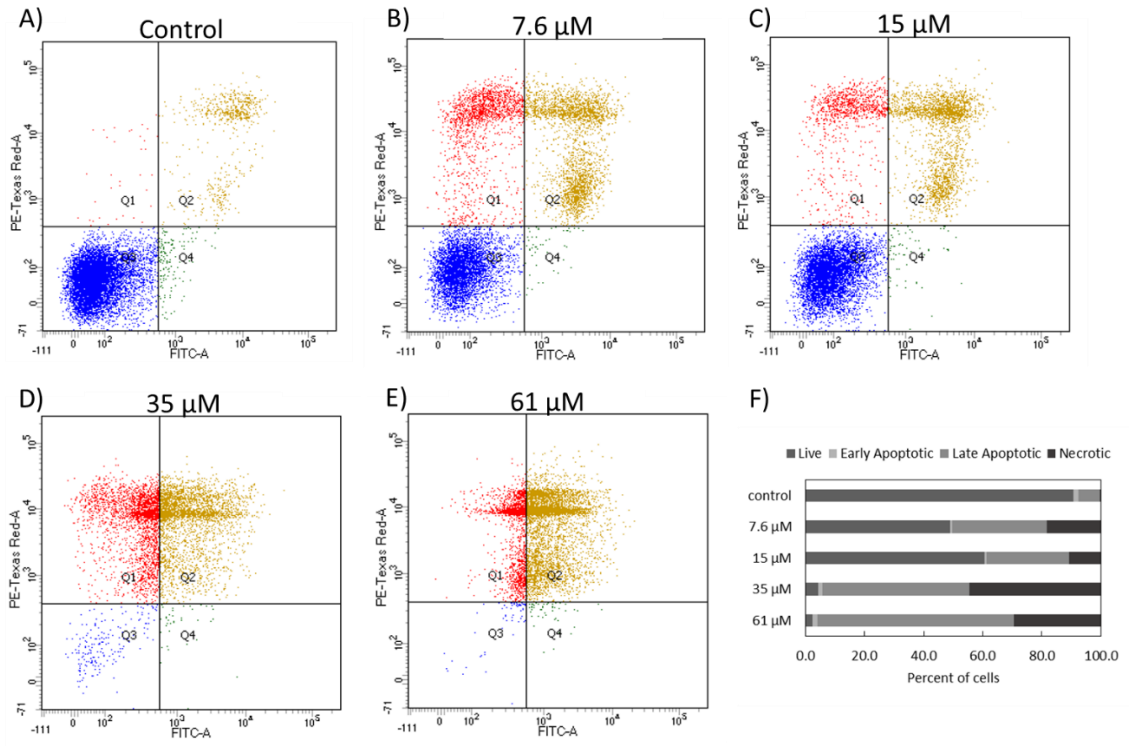

Figure 4.5: Annexin V/propidium iodide expression of NCIH460 cells exposed to A) a vehicle control, B) 7.6 µM clusianone, C) 15 µM clusianone, D) 35 µM clusianone, or E) 61 µM clusianone for 48 hours. The expression scatterplots were divided into four quadrants representing double negative cells, annexin V positive cells, propidium iodide positive cells, and double positive cells. Double negative cells were considered live cells, annexin V positive cells were considered early apoptotic cells, propidium iodide cells were considered necrotic, and double positive cells were considered late apoptotic cells. The divided histograms were used to express the percentage of cells that were live, early apoptotic, late apoptotic, or necrotic within each treatment group F).

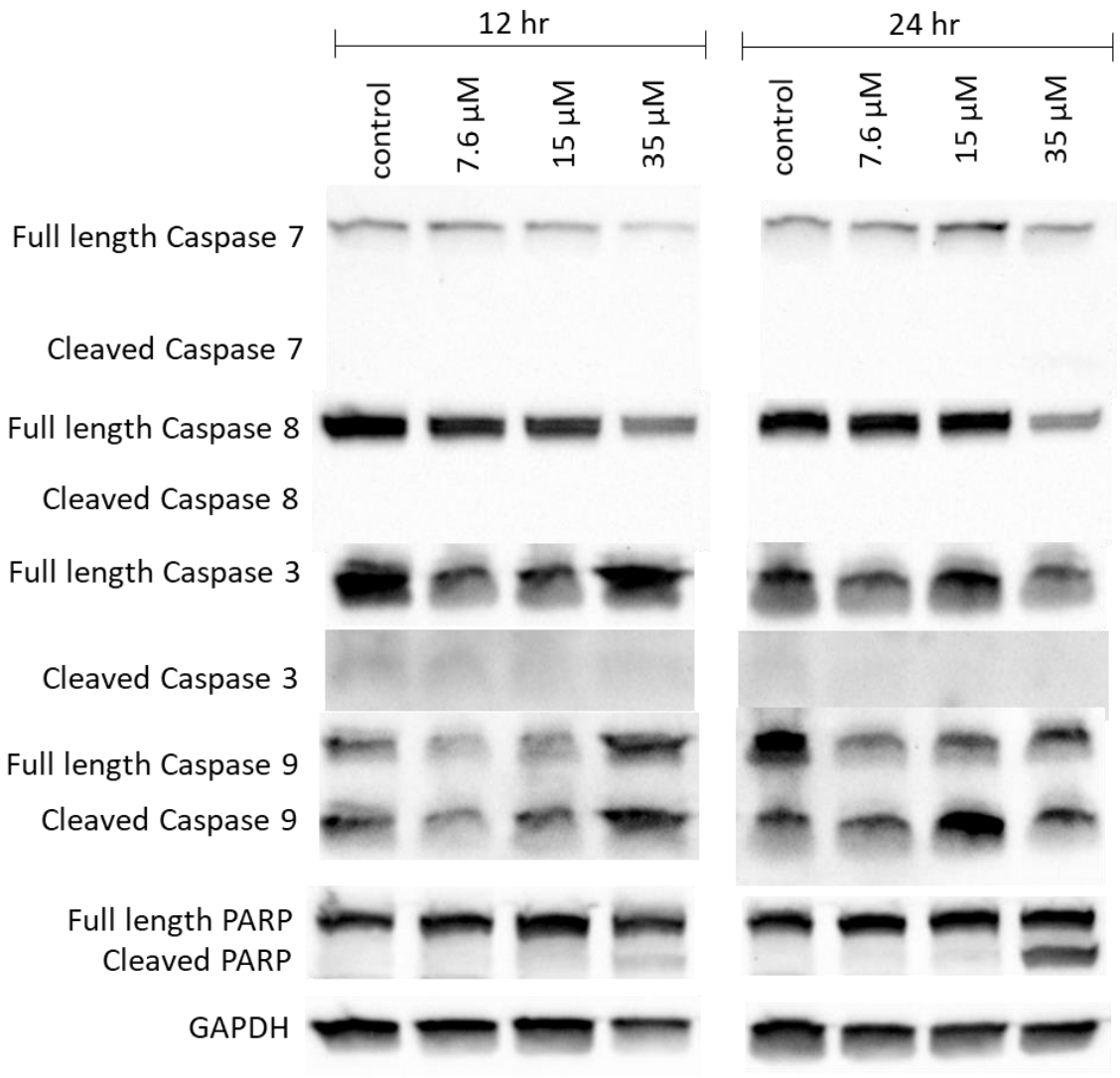

Figure 4.6: Expression of apoptosis-related proteins in NCIH460 cells after treatment with clusianone as determined by electrophoresis followed by western blot analysis. Cells were treated with clusianone for 12 or 24 hours before loading 50 µg of isolated protein into each well.

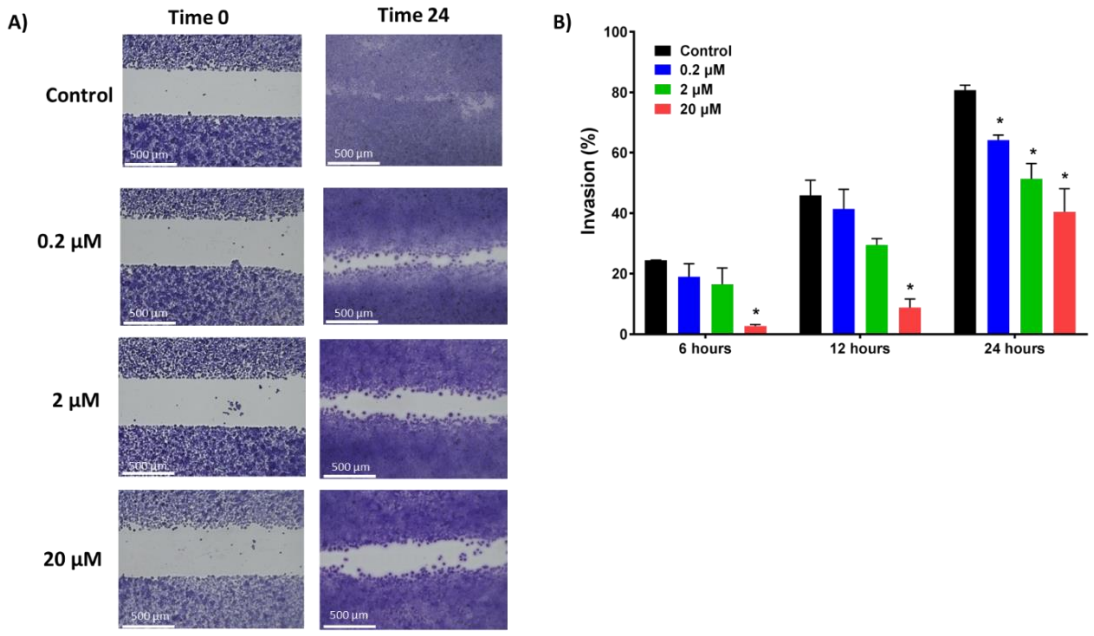

Figure 4.7: Invasion of NCIH460 cells into a cell free gap created using a 2 well cell culture insert consisting of two wells that were separated by a wall. After the cells reached full confluency, the culture insert was removed and the cells were treated with either a vehicle control or clusianone for 24 hours. A) Representative images of each treatment group after 24 hours in addition to B) graphs depicting the % invasion of each treatment group after 6, 12, and 24 hours. All data are statistically presented as the mean ± standard error. Multiple *t*-tests were performed using Graph-Pad Prism 7.03 (La Jolla, CA, USA) to determine the significance between each experimental group. P values of less than 0.05 were considered to be significant. (* denotes significant difference compared to the control group in the same time point.)

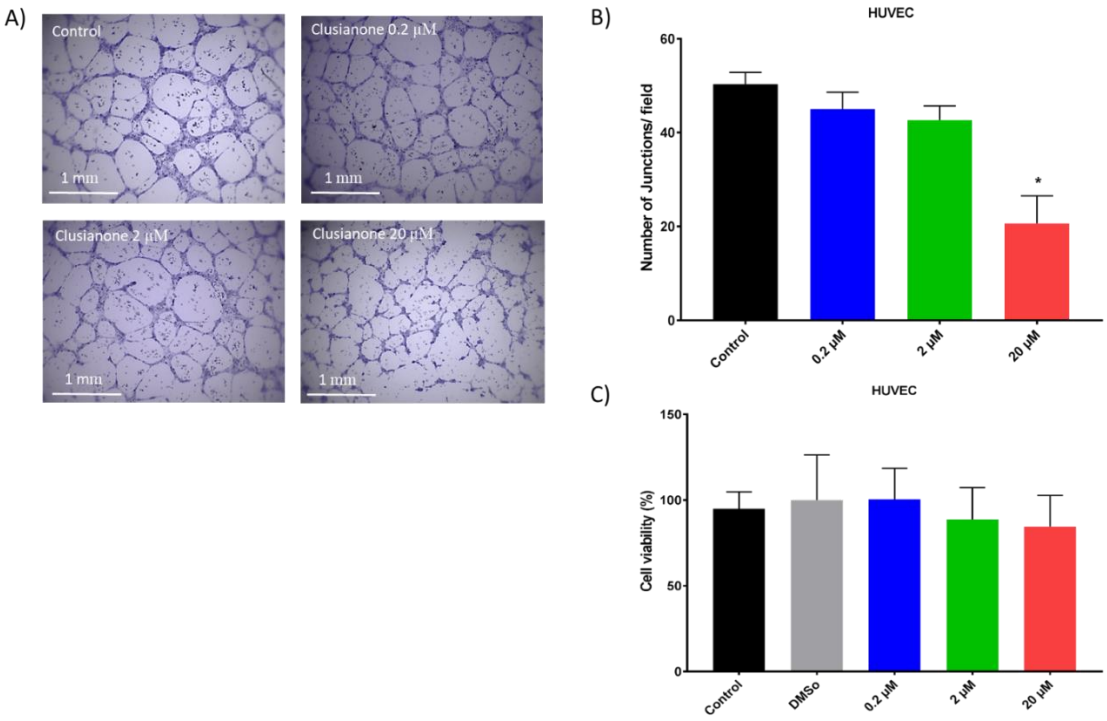

Figure 4.8: Tube formation between HUVEC endothelial cells after 8 hours of incubation on growth factor reduced BD Matrigel™ with or without clusianone. A representative image of the cells treated with the vehicle control, 0.2 µM, 2 µM, and 20 µM clusianone is shown in part A). The average number of junctions counted per field is graphed in part B). The viability of HUVEC cells after 8 hours of incubation with clusianone as determined by MTS assay is shown in part C).

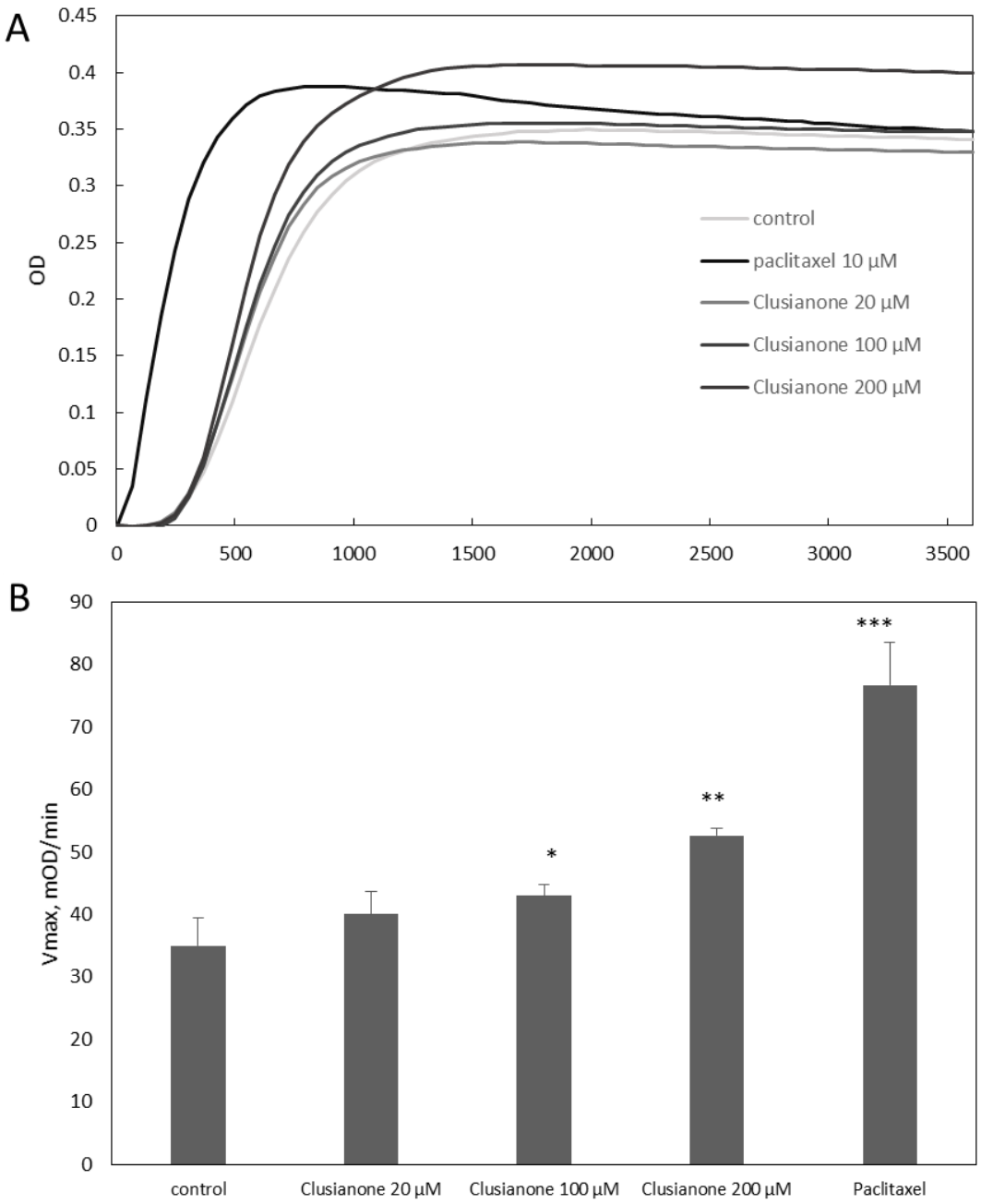

Figure 4.9: The extent of tubulin polymerization when exposed to clusianone as determined by absorbance at 340 nm for 1 hour. A) The average absorbance of three repetitions of the tubulin polymerization assay treated with clusianone, paclitaxel, or a vehicle control, and B) the average calculated Vmax for each treatment group (* represents $P \leq 0.05$ compared to the control, ** represents $0.05 \leq P \leq 0.01$ compared to the control, and *** represents $0.01 \leq P \leq 0.001$).

Target	EJhyh1
Gene Symbol	%Ctrl @
ABL1(E255K)-phosphorylated	86
ABL1(F317I)-nonphosphorylated	58
ABL1(F317I)-phosphorylated	66
ABL1(F317L)-nonphosphorylated	98
ABL1(F317L)-phosphorylated	73
ABL1(H396P)-nonphosphorylated	71
ABL1(H396P)-phosphorylated	80
ABL1(M351T)-phosphorylated	65
ABL1(Q252H)-nonphosphorylated	84
ABL1(Q252H)-phosphorylated	87
ABL1(T315I)-nonphosphorylated	53
ABL1(T315I)-phosphorylated	69
ABL1(Y253F)-phosphorylated	79
ABL1-nonphosphorylated	80
ABL1-phosphorylated	88
ABL2	100
ALK	68
ALK(C1156Y)	30
ALK(L1196M)	41
AXL	80
BLK	95
BMX	98
BRK	92
BTK	70
CSF1R	73
CSF1R-autoinhibited	64
CSK	96
CTK	87
DDR1	86
DDR2	61
EGFR	88
EGFR(E746-A750del)	88
EGFR(G719C)	97
EGFR(G719S)	98
EGFR(L747-E749del, A750P)	90
EGFR(L747-S752del, P753S)	70
EGFR(L747-T751del,Sins)	96
EGFR(L858R)	95
EGFR(L858R,T790M)	71
EGFR(L861Q)	97
EGFR(S752-I759del)	93
EGFR(T790M)	72
EPHA1	100
EPHA2	82
EPHA3	94
EPHA4	86
EPHA5	82
EPHA6	84

Target	EJhyh1
Gene Symbol	%Ctrl @
EPHA7	99
EPHA8	100
EPHB1	97
EPHB2	89
EPHB3	86
EPHB4	92
EPHB6	69
ERBB2	59
ERBB3	93
ERBB4	100
FAK	85
FER	97
FES	92
FGFR1	100
FGFR2	90
FGFR3	94
FGFR3(G697C)	100
FGFR4	85
FGR	85
FLT1	90
FLT3	85
FLT3(D835H)	100
FLT3(D835V)	89
FLT3(D835Y)	87
FLT3(ITD)	88
FLT3(ITD,D835V)	87
FLT3(ITD,F691L)	82
FLT3(K663Q)	90
FLT3(N841I)	100
FLT3(R834Q)	60
FLT3-autoinhibited	45
FLT4	99
FRK	96
FYN	98
HCK	97
IGF1R	83
INSR	71
INSRR	99
ITK	100
JAK1(JH1domain-catalytic)	75
JAK1(JH2domain-pseudokinase)	87
JAK2(JH1domain-catalytic)	76
JAK3(JH1domain-catalytic)	25
KIT	76
KIT(A829P)	86
KIT(D816H)	96
KIT(D816V)	80
KIT(L576P)	73
KIT(V559D)	80

Target	EJhyh1
Gene Symbol	%Ctrl @
KIT(V559D,T670I)	85
KIT(V559D,V654A)	97
KIT-autoinhibited	78
LCK	100
LTK	70
LYN	84
MERTK	87
MET	86
MET(M1250T)	92
MET(Y1235D)	76
MST1R	94
MUSK	95
PDGFRA	46
PDGFRB	69
PYK2	91
RET	83
RET(M918T)	100
RET(V804L)	100
RET(V804M)	97
ROS1	68
SRC	90
SRMS	73
SYK	97
TEC	100
TIE1	100
TIE2	95
TNK1	97
TNK2	96
TRKA	93
TRKB	54
TRKC	100
TXK	95
TYK2(JH1domain-catalytic)	83
TYK2(JH2domain-pseudokinase)	92
TYRO3	96
VEGFR2	58
YES	85
ZAP70	78

Figure 4.10: Inhibition of 135 tyrosine kinases treated with 20 µM of clusianone determine using the DiscoverX scanTK kinase panel. The panel uses an active site-directed competition assay, which does not require the use of ATP to assess kinase function. Data is presented as a percentage of function after treatment as compared to a vehicle control. A kinase with a remaining function of 30% or less is considered to be significantly inhibited. The significantly inhibited kinases, JAK3 and ALK(C1156Y), are highlighted.

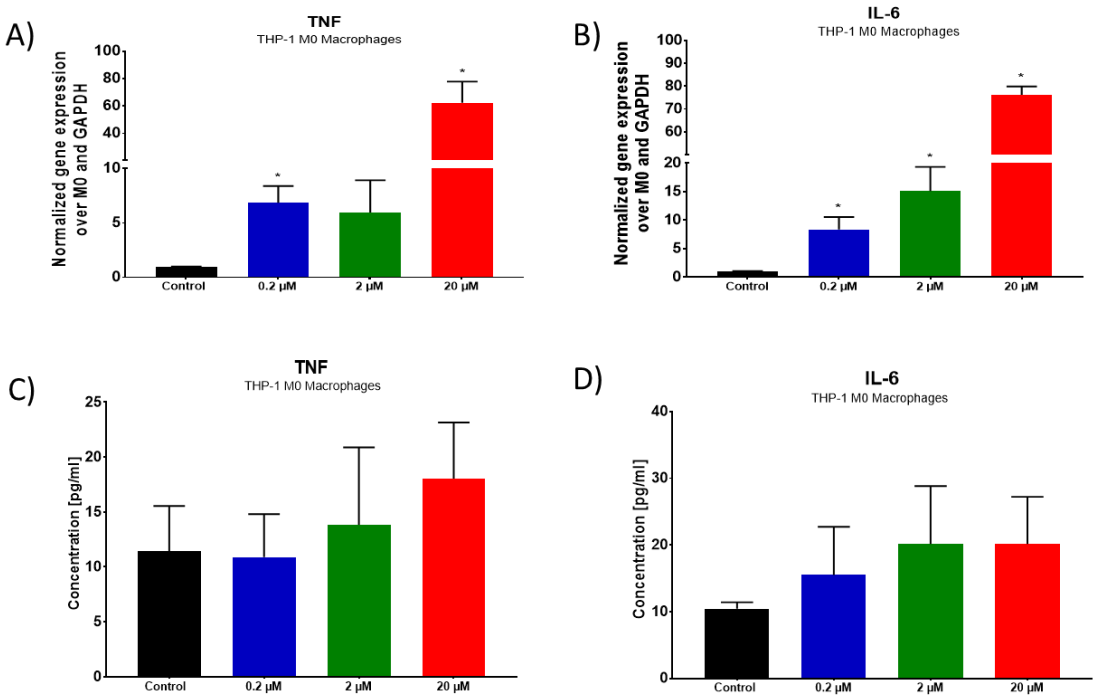

Figure 4.11. Gene and cytokine expression of macrophages treated with clusianone. RNA expression of THP-1 M0 Macrophage was determined after 72 hours of treatment with clusianone for A) TNFα and B) IL-6 by quantitative real-time PCR. Gene expression was normalized to the housekeeping gene GAPDH and the control group, non-treated THP-1 M0 macrophages (2-ΔΔC). Cytokine concentration in culture media was determined for C) TNFα and D) IL-6 by ELISA assay. P values of less than 0.05 were considered to be significant. (* denotes significant difference compared to the control group.)

CHAPTER 5

SUMMARY

Targeted cancer therapies are revolutionizing cancer treatment, but their full potential has not been realized due to the occurrence of treatment induced resistance, the limited number of patients they can treat, and the high cost often associated with them. Natural products may offer a safe, low cost solution to these problems in a number of ways. Biologically active natural products tend to influence multiple cellular pathways simultaneously, making them a source of compounds which can provide a multipronged attack on cancer cells. When combined with the treatment cocktails containing multiple targeted therapeutics and chemotherapeutics, natural products may be able to synergize with multiple components of the treatments in addition to interfering with other cancer related pathways, such as those responsible for resistance and metastasis.

One way in which natural products may increase the efficacy of targeted cancer therapies and chemotherapeutics is by inhibiting the growth and function of a small population of cells called cancer stem cells. These cells have been suggested to be responsible for acquired drug resistance, metastasis, and tumor recurrence after remission. A collection of natural products including polyphenols, alkaloids, flavonoids, and others, have been shown to reduce cancer stem cell populations within tumors,

reduce invasion and metastasis, and reduce the tumor initiating potential of isolated cancer cells. Many of these compounds have additionally been shown to target multiple cancer related cellular pathways from inducing cell cycle arrest and apoptosis to modulating inflammation. Using the lessons learned from the success of targeted therapeutics, natural products can be screened for their ability to influence combinations of cancer related pathways which will provide robust and effective treatment, especially when combined with currently used clinical treatments.

In this study, two natural products were screened for their multi-targeted effect on cancer pathways. The first compound was the abietane diterpenoid, deacetylnemorone. This compound was found to reduce growth inhibition in a wide array of cancer types in addition to selectively inducing cell deal in SK-OV-3 melanoma cells at 10 μM. The growth inhibitory properties of the compound were shown to be due, in at least part, to the ability of deacetylnemorone to delay progression of the cell cycle through the S and G2/M phases. Deacetylnemorone was also shown to increase the sensitivity of HCT 116/200 colorectal cancer cells to FdUrd, a chemotherapeutic agent which it had developed a resistance to. The compound was further shown to inhibit two pathways which lead to tumor growth and metastasis, namely invasion and angiogenesis, at concentrations as low as 0.3 μM. EMT inhibition was suggested from the invasion results by a reduced number of single cells found invading the cell free space. Deacetylnemorone's ability to reduce treatment induced resistance and inhibit EMT may suggest that the compound is capable of targeting cancer stem cells.

The second compound investigated was clusianone. Clusianone was demonstrated to induce dose dependent growth inhibition and cell death in cancers across 8 solid tumor cell lines. The compound was investigated further in the context of lung cancer due to the sensitivity of lung cancer cell lines to the compound in addition to the exceedingly poor prognoses of lung cancer patients to this day. Specifically, clusianone was shown to induce G1/G0 arrest followed by apoptotic cell death in NCI-H460 non-small cell lung cancer when used at 35 µM concentrations. Activation of the apoptotic cell death pathways was demonstrated using both Annexin V/propidium iodide expression flow cytometry and western blotting of caspases and PARP. At lower concentrations, from 0.2 to 20 µM, the multi-targeting compound was also shown to inhibit angiogenesis and invasion of NCI-H460 cells. For the first time, specific molecular targets of clusianone were also identified. The compound stabilized tubulin polymerization, similar to the chemotherapeutic paclitaxel, between 20 and 200 µM, potentially contributing to its growth inhibitory properties. Clusianone also significantly inhibited the function of the kinases ALK (C1156Y) and JAK3, suggesting the compound may target treatment resistant small-cell lung cancers as well as modulate the immune system. Indeed, immune modulating properties were demonstrated through the polarization of macrophages from an M2 to an M1 anticancer state, evidenced by an increased expression of TNF-α and IL-6, in response to exposure to the compound from 0.2 to 20 µM.

The results from this study have shown deacetylnemorone and clusianone to be compounds capable of influencing multiple cancer related pathways simultaneously,

including angiogenesis, immune regulation, invasion, cell growth, and apoptosis. Future studies will be necessary to fully determine the mechanism of action for each of these anticancer effects, in addition to screening of other cancer related pathways. More importantly, translation of these results to animal models of cancer will need to be performed. These *in vivo* experiments should include investigations of clusianone and deacetylnemorone used in combination with currently used targeted therapies and chemotherapeutics, to confirm their synergistic effects. By combining these compounds with currently used treatments, clusianone and deacetylnemorone may lower the hurdles of resistance to current therapies in addition to expanding the population of treatable patients.

REFERENCES

1. Siegel, R.L., Miller, K.D. & Jemal, A. Cancer statistics, 2018. CA Cancer J Clin 68, 7-30 (2018).
2. Lin, J.K. et al. Cost Effectiveness of Chimeric Antigen Receptor T-Cell Therapy in Relapsed or Refractory Pediatric B-Cell Acute Lymphoblastic Leukemia. J Clin Oncol, JCO2018790642 (2018).
3. Scott, L.J. Nivolumab: A Review in Advanced Melanoma. Drugs 75, 1413-1424 (2015).
4. Kwapisz, D. Cyclin-dependent kinase 4/6 inhibitors in breast cancer: palbociclib, ribociclib, and abemaciclib. Breast Cancer Res Treat 166, 41-54 (2017).
5. Giordani, E. et al. Old Tyrosine Kinase Inhibitors and Newcomers in Gastrointestinal Cancer Treatment. Curr Cancer Drug Targets 16, 175-185 (2016).
6. Lin, Z., Zhang, Q. & Luo, W. Angiogenesis inhibitors as therapeutic agents in cancer: Challenges and future directions. Eur J Pharmacol 793, 76-81 (2016).
7. Bonnet, D. & Dick, J.E. Human acute myeloid leukemia is organized as a hierarchy that originates from a primitive hematopoietic cell. Nat Med 3, 730-737 (1997).
8. Velasco-Velaquez, M.A., Homsi, N. & De La Fuente, M. Breast Cancer Stem Cells. The International Journal of Biochemistry & Cell Biology 44, 537-577 (2012).
9. Al-Hajj, M., Wicha, M.S., Benito-Hernandez, A., Morrison, S.J. & Clarke, M.F. Prospective identification of tumorigenic breast cancer cells. Proc Natl Acad Sci U S A 100, 3983-3988 (2003).
10. O'Brien, C.A., Pollett, A., Gallinger, S. & Dick, J.E. A human colon cancer cell capable of initiating tumour growth in immunodeficient mice. Nature 445, 106-110 (2007).
11. Prince, M.E. et al. Identification of a subpopulation of cells with cancer stem cell properties in head and neck squamous cell carcinoma. Proc Natl Acad Sci U S A 104, 973-978 (2007).
12. Suetsugu, A. et al. Characterization of CD133+ hepatocellular carcinoma cells as cancer stem/progenitor cells. Biochem Biophys Res Commun 351, 820-824 (2006).
13. Chiba, T. et al. Side population purified from hepatocellular carcinoma cells harbors cancer stem cell-like properties. Hepatology 44, 240-251 (2006).
14. Eramo, A. et al. Identification and expansion of the tumorigenic lung cancer stem cell population. Cell Death Differ 15, 504-514 (2008).
15. Szotek, P.P. et al. Ovarian cancer side population defines cells with stem cell-like characteristics and Mullerian Inhibiting Substance responsiveness. Proc Natl Acad Sci U S A 103, 11154-11159 (2006).

16. Patrawala, L. et al. Side population is enriched in tumorigenic, stem-like cancer cells, whereas ABCG2+ and ABCG2- cancer cells are similarly tumorigenic. Cancer Res 65, 6207-6219 (2005).
17. Li, C., Lee, C.J. & Simeone, D.M. Identification of human pancreatic cancer stem cells. Methods Mol Biol 568, 161-173 (2009).
18. Zhang, Q., Feng, Y. & Kennedy, D. Multidrug-resistant cancer cells and cancer stem cells hijack cellular systems to circumvent systemic therapies, can natural products reverse this? Cellular and Molecular Life Sciences (2016).
19. Lee, H.E. et al. An increase in cancer stem cell population after primary systemic therapy is a poor prognostic factor in breast cancer. Br J Cancer 104, 1730-1738 (2011).
20. Radisky, D.C. Epithelial-mesenchymal transition. J Cell Sci 118, 4325-4326 (2005).
21. Bao, S. et al. Glioma stem cells promote radioresistance by preferential activation of the DNA damage response. Nature 444, 756-760 (2006).
22. Phillips, T.M., McBride, W.H. & Pajonk, F. The response of CD24(-/low)/CD44+ breast cancer-initiating cells to radiation. J Natl Cancer Inst 98, 1777-1785 (2006).
23. Li, X. et al. Intrinsic resistance of tumorigenic breast cancer cells to chemotherapy. J Natl Cancer Inst 100, 672-679 (2008).
24. Clarke, M.F. et al. Cancer stem cells--perspectives on current status and future directions: AACR Workshop on cancer stem cells. Cancer Res 66, 9339-9344 (2006).
25. Hwang-Verslues, W.W. et al. Multiple lineages of human breast cancer stem/progenitor cells identified by profiling with stem cell markers. PLoS One 4, e8377 (2009).
26. Leishman, A. & Fairchild, P.J. Differentiation of Dendritic Cells from Human Induced Pluripotent Stem Cells. Stem Cells and Cancer Stem Cells 12, 29-37 (2013).
27. Rao, C.V. & Mohammed, A. New insights into pancreatic cancer stem cells. World J Stem Cells 7, 547-555 (2015).
28. Chan, K.S., Volkmer, J.P. & Weissman, I. Cancer stem cells in bladder cancer: a revisited and evolving concept. Curr Opin Urol 20, 393-397 (2010).
29. Orian-Rousseau, V. CD44, a therapeutic target for metastasising tumours. Eur J Cancer 46, 1271-1277 (2010).
30. Zöller, M. CD44: can a cancer-initiating cell profit from an abundantly expressed molecule? Nat Rev Cancer 11, 254-267 (2011).
31. Vira, D. et al. Cancer stem cells, microRNAs, and therapeutic strategies including natural products. Cancer Metastasis Rev 31, 733-751 (2012).
32. Cheng, J.X., Liu, B.L. & Zhang, X. How powerful is CD133 as a cancer stem cell marker in brain tumors? Cancer Treat Rev 35, 403-408 (2009).
33. Baba, T. et al. Epigenetic regulation of CD133 and tumorigenicity of CD133+ ovarian cancer cells. Oncogene 28, 209-218 (2009).
34. Ferrandina, G. et al. Expression of CD133-1 and CD133-2 in ovarian cancer. Int J Gynecol Cancer 18, 506-514 (2008).

35. Hermann, P.C. et al. Distinct populations of cancer stem cells determine tumor growth and metastatic activity in human pancreatic cancer. Cell Stem Cell 1, 313-323 (2007).
36. Horst, D. et al. The cancer stem cell marker CD133 has high prognostic impact but unknown functional relevance for the metastasis of human colon cancer. J Pathol 219, 427-434 (2009).
37. Yiming, L. et al. CD133 overexpression correlates with clinicopathological features of gastric cancer patients and its impact on survival: a systematic review and meta-analysis. Oncotarget 6, 42019-42027 (2015).
38. Hurt, E.M., Kawasaki, B.T., Klarmann, G.J., Thomas, S.B. & Farrar, W.L. CD44+ CD24(-) prostate cells are early cancer progenitor/stem cells that provide a model for patients with poor prognosis. Br J Cancer 98, 756-765 (2008).
39. Fang, X., Zheng, P., Tang, J. & Liu, Y. CD24: from A to Z. Cell Mol Immunol 7, 100-103 (2010).
40. Kristiansen, G. et al. CD24 is an independent prognostic marker of survival in nonsmall cell lung cancer patients. Br J Cancer 88, 231-236 (2003).
41. Kwon, M.J. et al. CD24 Overexpression Is Associated with Poor Prognosis in Luminal A and Triple-Negative Breast Cancer. PLoS One 10, e0139112 (2015).
42. Kristiansen, G. et al. CD24 is expressed in ovarian cancer and is a new independent prognostic marker of patient survival. Am J Pathol 161, 1215-1221 (2002).
43. Dalerba, P. et al. Phenotypic characterization of human colorectal cancer stem cells. Proc Natl Acad Sci U S A 104, 10158-10163 (2007).
44. Osta, W.A. et al. EpCAM is overexpressed in breast cancer and is a potential target for breast cancer gene therapy. Cancer Res 64, 5818-5824 (2004).
45. Armstrong, L. et al. Phenotypic characterization of murine primitive hematopoietic progenitor cells isolated on basis of aldehyde dehydrogenase activity. Stem Cells 22, 1142-1151 (2004).
46. Corti, S. et al. Identification of a primitive brain-derived neural stem cell population based on aldehyde dehydrogenase activity. Stem Cells 24, 975-985 (2006).
47. Huang, E.H. et al. Aldehyde dehydrogenase 1 is a marker for normal and malignant human colonic stem cells (SC) and tracks SC overpopulation during colon tumorigenesis. Cancer Res 69, 3382-3389 (2009).
48. Charafe-Jauffret, E. et al. Aldehyde dehydrogenase 1-positive cancer stem cells mediate metastasis and poor clinical outcome in inflammatory breast cancer. Clin Cancer Res 16, 45-55 (2010).
49. Chen, Y.C. et al. Aldehyde dehydrogenase 1 is a putative marker for cancer stem cells in head and neck squamous cancer. Biochem Biophys Res Commun 385, 307-313 (2009).
50. Landen, C.N. et al. Targeting aldehyde dehydrogenase cancer stem cells in ovarian cancer. Mol Cancer Ther 9, 3186-3199 (2010).
51. Jiang, F. et al. Aldehyde dehydrogenase 1 is a tumor stem cell-associated marker in lung cancer. Mol Cancer Res 7, 330-338 (2009).

52. Goodell, M.A., Brose, K., Paradis, G., Conner, A.S. & Mulligan, R.C. Isolation and functional properties of murine hematopoietic stem cells that are replicating in vivo. J Exp Med 183, 1797-1806 (1996).
53. Ho, M.M., Ng, A.V., Lam, S. & Hung, J.Y. Side population in human lung cancer cell lines and tumors is enriched with stem-like cancer cells. Cancer Res 67, 4827-4833 (2007).
54. Dave, B., Mittal, V., Tan, N.M. & Chang, J.C. Epithelial-mesenchymal transition, cancer stem cells and treatment resistance. Breast Cancer Res 14, 202 (2012).
55. Ponti, D. et al. Isolation and in vitro propagation of tumorigenic breast cancer cells with stem/progenitor cell properties. Cancer Res 65, 5506-5511 (2005).
56. Cao, L. et al. Sphere-forming cell subpopulations with cancer stem cell properties in human hepatoma cell lines. BMC Gastroenterol 11, 71 (2011).
57. Beier, D. et al. CD133(+) and CD133(-) glioblastoma-derived cancer stem cells show differential growth characteristics and molecular profiles. Cancer Res 67, 4010-4015 (2007).
58. Dallas, N.A. et al. Chemoresistant colorectal cancer cells, the cancer stem cell phenotype, and increased sensitivity to insulin-like growth factor-I receptor inhibition. Cancer Res 69, 1951-1957 (2009).
59. Moitra, K. Overcoming Multidrug Resistance in Cancer Stem Cells. Biomed Res Int 2015, 635745 (2015).
60. Moitra, K., Lou, H. & Dean, M. Multidrug efflux pumps and cancer stem cells: insights into multidrug resistance and therapeutic development. Clin Pharmacol Ther 89, 491-502 (2011).
61. Daflon-Yunes, N. et al. Characterization of a multidrug-resistant chronic myeloid leukemia cell line presenting multiple resistance mechanisms. Mol Cell Biochem 383, 123-135 (2013).
62. Nakanishi, T. et al. Novel 5' untranslated region variants of BCRP mRNA are differentially expressed in drug-selected cancer cells and in normal human tissues: implications for drug resistance, tissue-specific expression, and alternative promoter usage. Cancer Res 66, 5007-5011 (2006).
63. Katayama, K., Noguchi, K. & Sugimoto, Y. Regulations of P-Glycoprotein/ABCB1/MDR1in Human Cancer Cells. New Journal of Science, 1-10 (2014).
64. Croker, A.K. & Allan, A.L. Inhibition of aldehyde dehydrogenase (ALDH) activity reduces chemotherapy and radiation resistance of stem-like ALDHhiCD44^{+} human breast cancer cells. Breast Cancer Res Treat 133, 75-87 (2012).
65. Zhou, J. et al. Activation of the PTEN/mTOR/STAT3 pathway in breast cancer stem-like cells is required for viability and maintenance. Proc Natl Acad Sci U S A 104, 16158-16163 (2007).
66. Cochrane, C.R., Szczepny, A., Watkins, D.N. & Cain, J.E. Hedgehog Signaling in the Maintenance of Cancer Stem Cells. Cancers (Basel) 7, 1554-1585 (2015).
67. Clevers, H. The cancer stem cell: premises, promises and challenges. Nat Med 17, 313-319 (2011).

68. Borst, P. Cancer drug pan-resistance: pumps, cancer stem cells, quiescence, epithelial to mesenchymal transition, blocked cell death pathways, persisters or what? Open Biol 2, 120066 (2012).
69. Petrovska, B.B. Historical review of medicinal plants' usage. Pharmacogn Rev 6, 1-5 (2012).
70. Solecki, R.S. Shanidar IV, a Neanderthal Flower Burial in Northern Iraq. Science 190, 880-881 (1975).
71. Robinson, M.M. & Zhang, X. Traditional Medicines: Global Situation, Issues and Challenges, in The World Medicines Situation 2011 (WHO Press, Geneva, Switzerland; 2011).
72. Newman, D.J. & Cragg, G.M. Natural products as sources of new drugs over the last 25 years. J Nat Prod 70, 461-477 (2007).
73. Weaver, B.A. How Taxol/paclitaxel kills cancer cells. Mol Biol Cell 25, 2677-2681 (2014).
74. Balunas, M.J. & Kinghorn, A.D. Drug discovery from medicinal plants. Life Sci 78, 431-441 (2005).
75. Jantan, I., Bukhari, S.N.A., Mohamed, M.A.S., Wai, L.K. & Mesaik, M.A. The Evolving Role of Natural Products from the Tropical Rainforests as a Replenishable Source of New Drug Leads, in Drug Discovery and Development - From Molecules to Medicine. (ed. P.O. Vallisuta) (InTech, 2015).
76. Basmadjian, C. et al. Cancer wars: natural products strike back. Front Chem 2, 20 (2014).
77. Szymański, P., Markowicz, M. & Mikiciuk-Olasik, E. Adaptation of high-throughput screening in drug discovery-toxicological screening tests. Int J Mol Sci 13, 427-452 (2012).
78. Mishra, B.B. & Tiwari, V.K. Natural products: an evolving role in future drug discovery. Eur J Med Chem 46, 4769-4807 (2011).
79.Arya, R., Bhutkar, S., Dhulap, S. & Hirwani, R.R. Patent analysis as a tool for research planning: study on natural based therapeutics against cancer stem cells. Recent Pat Anticancer Drug Discov 10, 72-86 (2015).
80. Marucci, C. et al. Natural Products and Cancer Stem Cells. Curr Pharm Des 21, 5547-5557 (2015).
81. Weng, C.J. & Yen, G.C. Chemopreventive effects of dietary phytochemicals against cancer invasion and metastasis: phenolic acids, monophenol, polyphenol, and their derivatives. Cancer Treat Rev 38, 76-87 (2012).
82. Scarlatti, F. et al. Resveratrol induces growth inhibition and apoptosis in metastatic breast cancer cells via de novo ceramide signaling. FASEB J 17, 2339-2341 (2003).
83. Opipari, A.W. et al. Resveratrol-induced autophagocytosis in ovarian cancer cells. Cancer Res 64, 696-703 (2004).
84. Shankar, S. et al. Resveratrol inhibits pancreatic cancer stem cell characteristics in human and KrasG12D transgenic mice by inhibiting pluripotency maintaining factors and epithelial-mesenchymal transition. PLoS One 6, e16530 (2011).

85. Pandey, P.R. et al. Resveratrol suppresses growth of cancer stem-like cells by inhibiting fatty acid synthase. Breast Cancer Res Treat 130, 387-398 (2011).
86. Singh, C.K., Ndiaye, M.A. & Ahmad, N. Resveratrol and cancer: Challenges for clinical translation. Biochim Biophys Acta 1852, 1178-1185 (2015).
87. Amri, A., Chaumeil, J.C., Sfar, S. & Charrueau, C. Administration of resveratrol: What formulation solutions to bioavailability limitations? J Control Release 158, 182-193 (2012).
88. Bisht, S. et al. Polymeric nanoparticle-encapsulated curcumin ("nanocurcumin"): a novel strategy for human cancer therapy. J Nanobiotechnology 5, 3 (2007).
89. Epelbaum, R., Vizel, B. & Bar-Sela, G. Phase II study of curcumin and gemcitabine in patients with advanced pancreatic cancer. Journal of Clinical Oncology 26 (2008).
90. Kakarala, M. et al. Targeting breast stem cells with the cancer preventive compounds curcumin and piperine. Breast Cancer Res Treat 122, 777-785 (2010).
91. Lin, L. et al. Targeting colon cancer stem cells using a new curcumin analogue, GO-Y030. Br J Cancer 105, 212-220 (2011).
92. Yu, Y. et al. Elimination of Colon Cancer Stem-Like Cells by the Combination of Curcumin and FOLFOX. Transl Oncol 2, 321-328 (2009).
93. Wahlström, B. & Blennow, G. A study on the fate of curcumin in the rat. Acta Pharmacol Toxicol (Copenh) 43, 86-92 (1978).
94. Pan, M.H., Huang, T.M. & Lin, J.K. Biotransformation of curcumin through reduction and glucuronidation in mice. Drug Metab Dispos 27, 486-494 (1999).
95. Aggarwal, B.B. & Sung, B. Pharmacological basis for the role of curcumin in chronic diseases: an age-old spice with modern targets. Trends Pharmacol Sci 30, 85-94 (2009).
96. Galati, G. & O'Brien, P.J. Potential toxicity of flavonoids and other dietary phenolics: significance for their chemopreventive and anticancer properties. Free Radic Biol Med 37, 287-303 (2004).
97. Middleton, E., Kandaswami, C. & Theoharides, T.C. The effects of plant flavonoids on mammalian cells: implications for inflammation, heart disease, and cancer. Pharmacol Rev 52, 673-751 (2000).
98. Lamson, D.W. & Brignall, M.S. Antioxidants and cancer, part 3: quercetin. Altern Med Rev 5, 196-208 (2000).
99. Atashpour, S. et al. Quercetin induces cell cycle arrest and apoptosis in CD133(+) cancer stem cells of human colorectal HT29 cancer cell line and enhances anticancer effects of doxorubicin. Iran J Basic Med Sci 18, 635-643 (2015).
100. Tang, S.N. et al. The dietary bioflavonoid quercetin synergizes with epigallocathechin gallate (EGCG) to inhibit prostate cancer stem cell characteristics, invasion, migration and epithelial-mesenchymal transition. J Mol Signal 5, 14 (2010).
101. Cai, X., Fang, Z., Dou, J., Yu, A. & Zhai, G. Bioavailability of quercetin: problems and promises. Curr Med Chem 20, 2572-2582 (2013).
102. Lu, J.J., Bao, J.L., Chen, X.P., Huang, M. & Wang, Y.T. Alkaloids isolated from natural herbs as the anticancer agents. Evid Based Complement Alternat Med 2012, 485042 (2012).

103. Beljanski, M. & Beljanski, M.S. Selective inhibition of in vitro synthesis of cancer DNA by alkaloids of beta-carboline class. Exp Cell Biol 50, 79-87 (1982).
104. Oh, S.H. et al. Dihydrocapsaicin (DHC), a saturated structural analog of capsaicin, induces autophagy in human cancer cells in a catalase-regulated manner. Autophagy 4, 1009-1019 (2008).
105. Yaffe, P.B., Power Coombs, M.R., Doucette, C.D., Walsh, M. & Hoskin, D.W. Piperine, an alkaloid from black pepper, inhibits growth of human colon cancer cells via G1 arrest and apoptosis triggered by endoplasmic reticulum stress. Mol Carcinog 54, 1070-1085 (2015).
106. Samykutty, A. et al. Piperine, a Bioactive Component of Pepper Spice Exerts Therapeutic Effects on Androgen Dependent and Androgen Independent Prostate Cancer Cells. PLoS One 8, e65889 (2013).
107. Kunnumakkara, A.B., Anand, P. & Aggarwal, B.B. Curcumin inhibits proliferation, invasion, angiogenesis and metastasis of different cancers through interaction with multiple cell signaling proteins. Cancer Lett 269, 199-225 (2008).
108. Meeran, S.M., Katiyar, S. & Katiyar, S.K. Berberine-induced apoptosis in human prostate cancer cells is initiated by reactive oxygen species generation. Toxicol Appl Pharmacol 229, 33-43 (2008).
109. Iizuka, N. et al. Inhibitory effect of Coptidis Rhizoma and berberine on the proliferation of human esophageal cancer cell lines. Cancer Lett 148, 19-25 (2000).
110. Ma, X. et al. Modulation of drug-resistant membrane and apoptosis proteins of breast cancer stem cells by targeting berberine liposomes. Biomaterials 34, 4452-4465 (2013).
111. Gillis, J.C. & Goa, K.L. Tretinoin. A review of its pharmacodynamic and pharmacokinetic properties and use in the management of acute promyelocytic leukaemia. Drugs 50, 897-923 (1995).
112. Gudas, L.J. & Wagner, J.A. Retinoids regulate stem cell differentiation. J Cell Physiol 226, 322-330 (2011).
113. Ginestier, C. et al. Retinoid signaling regulates breast cancer stem cell differentiation. Cell Cycle 8, 3297-3302 (2009).
114. Wallen, E., Sellers, R.G. & Peehl, D.M. Brefeldin A induces p53-independent apoptosis in primary cultures of human prostatic cancer cells. J Urol 164, 836-841 (2000).
115. Shao, R.G., Shimizu, T. & Pommier, Y. Brefeldin A is a potent inducer of apoptosis in human cancer cells independently of p53. Exp Cell Res 227, 190-196 (1996).
116. Tseng, C.N. et al. Brefeldin A reduces anchorage-independent survival, cancer stem cell potential and migration of MDA-MB-231 human breast cancer cells. Molecules 19, 17464-17477 (2014).
117. Tseng, C.N. et al. Brefeldin a effectively inhibits cancer stem cell-like properties and MMP-9 activity in human colorectal cancer Colo 205 cells. Molecules 18, 10242-10253 (2013).
118. Kimiz-Gebologlu, I., Gulce-Iz, S. & Biray-Avci, C. Monoclonal antibodies in cancer immunotherapy. Mol Biol Rep (2018).

119. Berraondo, P. et al. Cytokines in clinical cancer immunotherapy. Br J Cancer (2018).
120. van Willigen, W.W. et al. Dendritic Cell Cancer Therapy: Vaccinating the Right Patient at the Right Time. Front Immunol 9, 2265 (2018).
121. Jackson, H.J., Rafiq, S. & Brentjens, R.J. Driving CAR T-cells forward. Nat Rev Clin Oncol 13, 370-383 (2016).
122. Chae, Y.K. et al. Current landscape and future of dual anti-CTLA4 and PD-1/PD-L1 blockade immunotherapy in cancer; lessons learned from clinical trials with melanoma and non-small cell lung cancer (NSCLC). J Immunother Cancer 6, 39 (2018).
123. Mayer, I.A. & Arteaga, C.L. The PI3K/AKT Pathway as a Target for Cancer Treatment. Annu Rev Med 67, 11-28 (2016).
124. Moghadam, S.E. et al. Wound Healing Potential of Chlorogenic Acid and Myricetin-3-O-β-Rhamnoside Isolated from Parrotia persica. Molecules 22 (2017).
125. Hu, R., George, D.J. & Zhang, T. What is the role of sipuleucel-T in the treatment of patients with advanced prostate cancer? An update on the evidence. Ther Adv Urol 8, 272-278 (2016).
126. Liu, D. & Zhao, J. Cytokine release syndrome: grading, modeling, and new therapy. J Hematol Oncol 11, 121 (2018).
127. Cogdill, A.P., Andrews, M.C. & Wargo, J.A. Hallmarks of response to immune checkpoint blockade. Br J Cancer 117, 1-7 (2017).
128. Cascone, T. et al. Upregulated stromal EGFR and vascular remodeling in mouse xenograft models of angiogenesis inhibitor-resistant human lung adenocarcinoma. J Clin Invest 121, 1313-1328 (2011).
129. Shojaei, F. et al. G-CSF-initiated myeloid cell mobilization and angiogenesis mediate tumor refractoriness to anti-VEGF therapy in mouse models. Proc Natl Acad Sci U S A 106, 6742-6747 (2009).
130. von Tell, D., Armulik, A. & Betsholtz, C. Pericytes and vascular stability. Exp Cell Res 312, 623-629 (2006).
131. Semenza, G.L. Oxygen sensing, hypoxia-inducible factors, and disease pathophysiology. Annu Rev Pathol 9, 47-71 (2014).
132. Jain, R.K. Antiangiogenesis strategies revisited: from starving tumors to alleviating hypoxia. Cancer Cell 26, 605-622 (2014).
133. Troselj, K.G. & Kujundzic, R.N. Curcumin in combined cancer therapy. Curr Pharm Des 20, 6682-6696 (2014).
134. Wang, Y. et al. Anti-tumor effect of emodin on gynecological cancer cells. Cell Oncol (Dordr) 38, 353-363 (2015).
135. Iwanowycz, S. et al. Emodin Inhibits Breast Cancer Growth by Blocking the Tumor-Promoting Feedforward Loop between Cancer Cells and Macrophages. Mol Cancer Ther 15, 1931-1942 (2016).
136. Li, L., Hou, X., Xu, R., Liu, C. & Tu, M. Research review on the pharmacological effects of astragaloside IV. Fundam Clin Pharmacol 31, 17-36 (2017).
137. Auyeung, K.K., Mok, N.L., Wong, C.M., Cho, C.H. & Ko, J.K. Astragalus saponins modulate mTOR and ERK signaling to promote apoptosis through the extrinsic pathway in HT-29 colon cancer cells. Int J Mol Med 26, 341-349 (2010).

138. Jiao, D. et al. Curcumin inhibited HGF-induced EMT and angiogenesis through regulating c-Met dependent PI3K/Akt/mTOR signaling pathways in lung cancer. Mol Ther Oncolytics 3, 16018 (2016).
139. Bråkenhielm, E., Cao, R. & Cao, Y. Suppression of angiogenesis, tumor growth, and wound healing by resveratrol, a natural compound in red wine and grapes. FASEB J 15, 1798-1800 (2001).
140. Wang, Z. et al. Broad targeting of angiogenesis for cancer prevention and therapy. Semin Cancer Biol 35 Suppl, S224-S243 (2015).
141. Lu, K., Bhat, M. & Basu, S. Plants and their active compounds: natural molecules to target angiogenesis. Angiogenesis 19, 287-295 (2016).
142. Ai, B., Bie, Z., Zhang, S. & Li, A. Paclitaxel targets VEGF-mediated angiogenesis in ovarian cancer treatment. Am J Cancer Res 6, 1624-1635 (2016).
143. Choudhary, M.I. et al. Anticancer and α-chymotrypsin inhibting diterpenes and triterpenes from Salvia leriifolia. Phytochemistry Letters 6, 5 (2013).
144. Vol. 2018 (National Cancer Institute, dtp.cancer.gov; 2015).
145. Shoemaker, R.H. The NCI60 human tumour cell line anticancer drug screen. Nat Rev Cancer 6, 813-823 (2006).
146. Berger, S.H., Barbour, K.W. & Berger, F.G. A naturally occurring variation in thymidylate synthase structure is associated with a reduced response to 5-fluoro-2'-deoxyuridine in a human colon tumor cell line. Mol Pharmacol 34, 480-484 (1988).
147. Taylor, W.F. & Jabbarzadeh, E. The use of natural products to target cancer stem cells. Am J Cancer Res 7, 1588-1605 (2017).
148. Edinger, A.L. & Thompson, C.B. Death by design: apoptosis, necrosis and autophagy. Curr Opin Cell Biol 16, 663-669 (2004).
149. Chen, T., Stephens, P.A., Middleton, F.K. & Curtin, N.J. Targeting the S and G2 checkpoint to treat cancer. Drug Discov Today 17, 194-202 (2012).
150. Chaffer, C.L., San Juan, B.P., Lim, E. & Weinberg, R.A. EMT, cell plasticity and metastasis. Cancer Metastasis Rev 35, 645-654 (2016).
151. Gotwals, P. et al. Prospects for combining targeted and conventional cancer therapy with immunotherapy. Nat Rev Cancer 17, 286-301 (2017).
152. Heron, M. Deaths: Leading Causes for 2016. Natl Vital Stat Rep 67, 1-77 (2018).
153. Zugazagoitia, J. et al. Current Challenges in Cancer Treatment. Clin Ther 38, 1551-1566 (2016).
154. Yang, L. & Zhang, Y. Tumor-associated macrophages, potential targets for cancer treatment. Biomark Res 5, 25 (2017).
155. Griffin, M. et al. BRAF inhibitors: resistance and the promise of combination treatments for melanoma. Oncotarget 8, 78174-78192 (2017).
156. Liu, D., Jenkins, R.W. & Sullivan, R.J. Mechanisms of Resistance to Immune Checkpoint Blockade. Am J Clin Dermatol (2018).
157. Huang, Y., Cai, T., Xia, X., Cai, Y. & Wu, X.Y. Research Advances in the Intervention of Inflammation and Cancer by Active Ingredients of Traditional Chinese Medicine. J Pharm Pharm Sci 19, 114-126 (2016).

158. Yu, G.J. et al. Anti-inflammatory potential of saponins derived from cultured wild ginseng roots in lipopolysaccharide-stimulated RAW 264.7 macrophages. Int J Mol Med 35, 1690-1698 (2015).
159. Zhang, X., Zhang, S., Sun, Q., Jiao, W. & Yan, Y. Compound K Induces Endoplasmic Reticulum Stress and Apoptosis in Human Liver Cancer Cells by Regulating STAT3. Molecules 23 (2018).
160. Castro, A.P. et al. In vivo schistosomicidal activity of 7-epiclusianone and its quantification in the plasma of healthy and Schistosoma mansoni infected mice using UPLC-MS/MS. Phytomedicine 38, 66-73 (2018).
161. Almeida, L.S. et al. Antimicrobial activity of Rheedia brasiliensis and 7-epiclusianone against Streptococcus mutans. Phytomedicine 15, 886-891 (2008).
162. de Barros, M. et al. Antibacterial Activity of 7-Epiclusianone and Its Novel Copper Metal Complex on Streptococcus spp. Isolated from Bovine Mastitis and Their Cytotoxicity in MAC-T Cells. Molecules 22 (2017).
163. Santa-Cecília, F.V. et al. Antinociceptive and anti-inflammatory properties of 7-epiclusianone, a prenylated benzophenone from Garcinia brasiliensis. Eur J Pharmacol 670, 280-285 (2011).
164. Murata, R.M. et al. Antiproliferative effect of benzophenones and their influence on cathepsin activity. Phytother Res 24, 379-383 (2010).
165. Simpkins, N.S., Holtrup, F., Rodeschini, V., Taylor, J.D. & Wolf, R. Comparison of the cytotoxic effects of enantiopure PPAPs, including nemorosone and clusianone. Bioorg Med Chem Lett 22, 6144-6147 (2012).
166. Sales, L. et al. Anticancer activity of 7-epiclusianone, a benzophenone from Garcinia brasiliensis, in glioblastoma. BMC Complement Altern Med 15, 393 (2015).
167. Ionta, M. et al. 7-Epiclusianone, a Benzophenone Extracted from Garcinia brasiliensis (Clusiaceae), Induces Cell Cycle Arrest in G1/S Transition in A549 Cells. Molecules 20, 12804-12816 (2015).
168. Reis, F.H. et al. Clusianone, a naturally occurring nemorosone regioisomer, uncouples rat liver mitochondria and induces HepG2 cell death. Chem Biol Interact 212, 20-29 (2014).
169. Boyce, J.H. & Porco, J.A. Asymmetric, stereodivergent synthesis of (-)-clusianone utilizing a biomimetic cationic cyclization. Angew Chem Int Ed Engl 53, 7832-7837 (2014).
170. Horwitz, S.B. Taxol (paclitaxel): mechanisms of action. Ann Oncol 5 Suppl 6, S3-6 (1994).
171. Vašíková, A. [EML4-ALK fusion gene in patients with lung carcinoma: biology, diagnostics and targeted therapy]. Klin Onkol 25, 434-439 (2012).
172. Malemud, C.J. The role of the JAK/STAT signal pathway in rheumatoid arthritis. Ther Adv Musculoskelet Dis 10, 117-127 (2018).
173. Simbulan-Rosenthal, C.M., Rosenthal, D.S., Iyer, S., Boulares, H. & Smulson, M.E. Involvement of PARP and poly(ADP-ribosyl)ation in the early stages of apoptosis and DNA replication. Mol Cell Biochem 193, 137-148 (1999).
174. Ghobrial, I.M., Witzig, T.E. & Adjei, A.A. Targeting apoptosis pathways in cancer therapy. CA Cancer J Clin 55, 178-194 (2005).

175. Folkman, J. Role of angiogenesis in tumor growth and metastasis. Semin Oncol 29, 15-18 (2002).
176. Somasundaram, A. & Burns, T.F. The next generation of immunotherapy: keeping lung cancer in check. J Hematol Oncol 10, 87 (2017).
177. Jinushi, M. & Komohara, Y. Tumor-associated macrophages as an emerging target against tumors: Creating a new path from bench to bedside. Biochim Biophys Acta 1855, 123-130 (2015).
178. Brown, J.M., Recht, L. & Strober, S. The Promise of Targeting Macrophages in Cancer Therapy. Clin Cancer Res 23, 3241-3250 (2017).

APPENDIX A

SUPPLEMENTARY TABLES AND FIGURES

Table A.1: Primers used for quantitative real-time polymerase chain reaction.

Gene	**5'-3' primer sequences: (F: forward R: reverse)**
TNFα	F: CTG CTG CAC TTT GGA GTG AT
	R: AGA TGA TCT GAC TGC CTG GG
IL-6	F: AGC CAC TCA CCT CTT CAG AAC
	R: GCC TCT TTG CTG CTT TCA CAC
GAPDH	F: GTG GAC CTG ACC TGC CGT CT
	F: GGA GGA GTG GGT GTC GCT GT

Table A.2: Percent growth of the 60 cell lines examined in the NCI-60 five dose screening method. The cancer cell lines are organized by tissue type.

Leukemia (% Growth)					
CCRF-CEM	103	102	103		-7
HL-60(TB)	94	94	95	-43	-38
K-562	98	91	96	10	15
MOLT-4	95	96	89	-4	-1
RPMI-8226	96	101	90	-33	-34
SR	94	99	100	5	1
Concentration (logM)	-8.0	-7.0	-6.0	-5.0	-4.0

Non-Small Cell Lung Cancer (% Growth)					
A549/ATCC	96	103	101	6	-70
EKVX	87	90	85	-7	-34
HOP-62	92	95	96	-10	-44
HOP-92	98	102	89	-29	-57
NCI-H226	98	104	96	-12	-44
NCI-H23	96	95	92	-5	-36
NCI-H322M	96	94	94	-10	-57
NCI-H460	107	110	103	-28	-69
NCI-H522	93	86	81	-12	-21
Concentration (logM)	-8.0	-7.0	-6.0	-5.0	-4.0

Colon Cancer (% Growth)					
COLO 205	97	98	94	-22	-42
HCC-2998	94	103	97	-26	-73
HCT-116	92	94	87	-44	-71
HCT-15	94	97	90	1	-64
HT29	98	97	97	-7	-51
KM12	100	101	99	4	-40
SW-620	106	106	104	12	-41
Concentration (logM)	-8.0	-7.0	-6.0	-5.0	-4.0

CNS Cancer (% Growth)					
SF-268	97	95	94	-29	-75
SF-295	85	91	89	-39	-51
SF-539	88	93	99	-38	-80
SNB-19	98	104	100	3	-20
SNB-75	72	79	75	3	-48
U251	106	104	102	2	-54
Concentration (logM)	-8.0	-7.0	-6.0	-5.0	-4.0

Melanoma (% Growth)					
LOX IMVI	95	96	96	-22	-55
MALME-3M	89	95	83	-47	-79
M14	90	95	90	-23	-67
MDA-MB-435	92	96	95	-5	-70
SK-MEL-2	93	92	82	-23	-38
SK-MEL-28	90	95	92	-21	-80
SK-MEL-5	94	96	85	-86	-92
UACC-257	100	108	102	-14	-32
UACC-62	96	96	85	-57	-73
Concentration (logM)	-8.0	-7.0	-6.0	-5.0	-4.0

Ovarian Cancer (% Growth)					
IGROV1	102	98	97	6	-33
OVCAR-3	103	100	97	-22	-70
OVCAR-4	89	99	80	-9	5
OVCAR-5	88	91	87	10	-37
OVCAR-8	107	106	106	1	-8
NCI/ADR-RES	100	99	99	2	-31
SK-OV-3	95	100	99	-11	-8
Concentration (logM)	-8.0	-7.0	-6.0	-5.0	-4.0

Renal Cancer (% Growth)					
786-0	86	93	83	-33	-38
A498	100	103	98	-60	-51
ACHN	93	99	93	1	-13
CAKI-1	88	93	92	3	-37
RXF 393	101	101	97	-35	-77
SN12C	101	99	96	2	-31
TK-10	92	88	93	5	-21
UO-31	88	88	85	-1	-18
Concentration (logM)	-8.0	-7.0	-6.0	-5.0	-4.0

Prostate Cancer (% Growth)					
PC-3	93	94	88	-6	-60
DU-145	100	100	97	-12	-57
Concentration (logM)	-8.0	-7.0	-6.0	-5.0	-4.0

Breast Cancer (% Growth)					
MCF7	86	88	88	1	-11
MDA-MB-231/ATCC	102	110	103	-9	-42
HS 578T	101	106	105	-3	-18
BT-549	94	100	88	-64	-80
T-47D	79	89	85	-8	-14
MDA-MB-468	99	100	96	-21	-44
Concentration (logM)	-8.0	-7.0	-6.0	-5.0	-4.0

A)

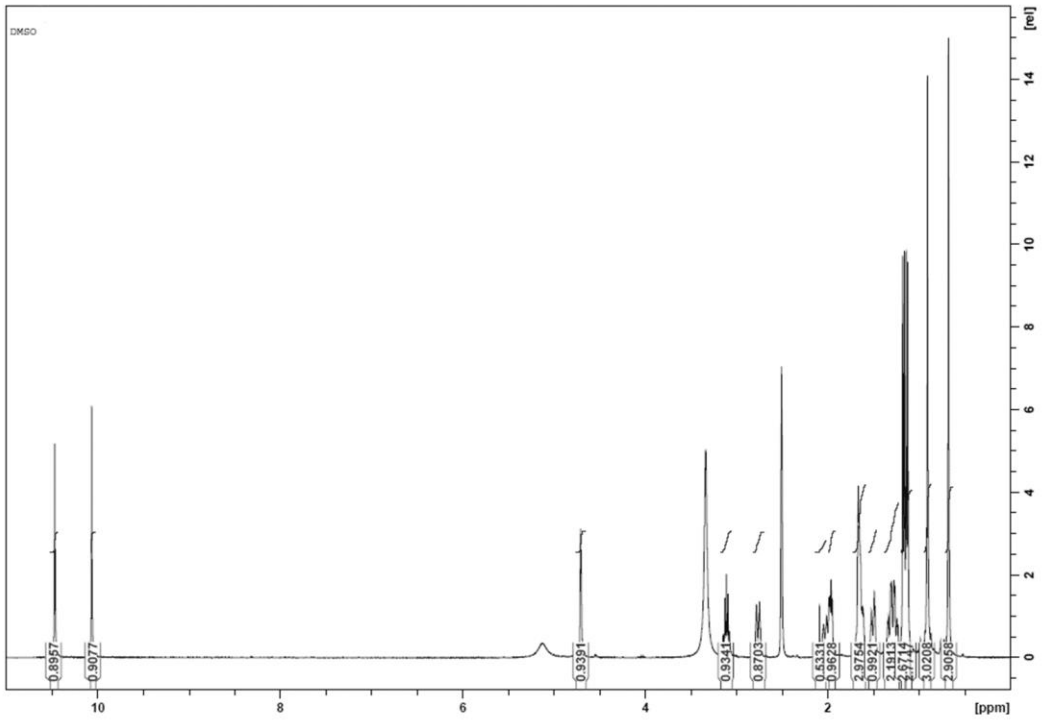
DMSO
[rel]
[ppm]
0.8957
0.9077
0.9391
0.9341
0.8703
0.6331
0.9628
2.9754
0.9921
2.1913
2.0714
3.0206
2.9058

B)

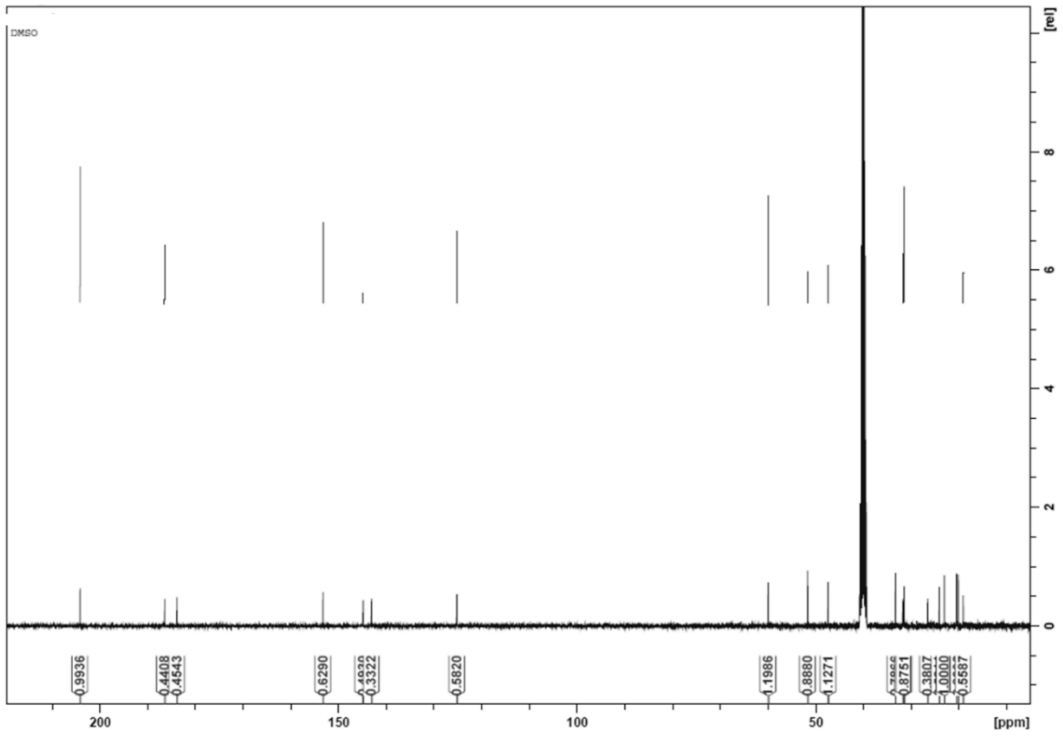
DMSO
[rel]
[ppm]
0.9936
0.4408
0.4543
0.6290
0.3322
0.5820
1.1986
0.8880
1.1271
0.8751
0.3807
1.0000
0.5587

C)

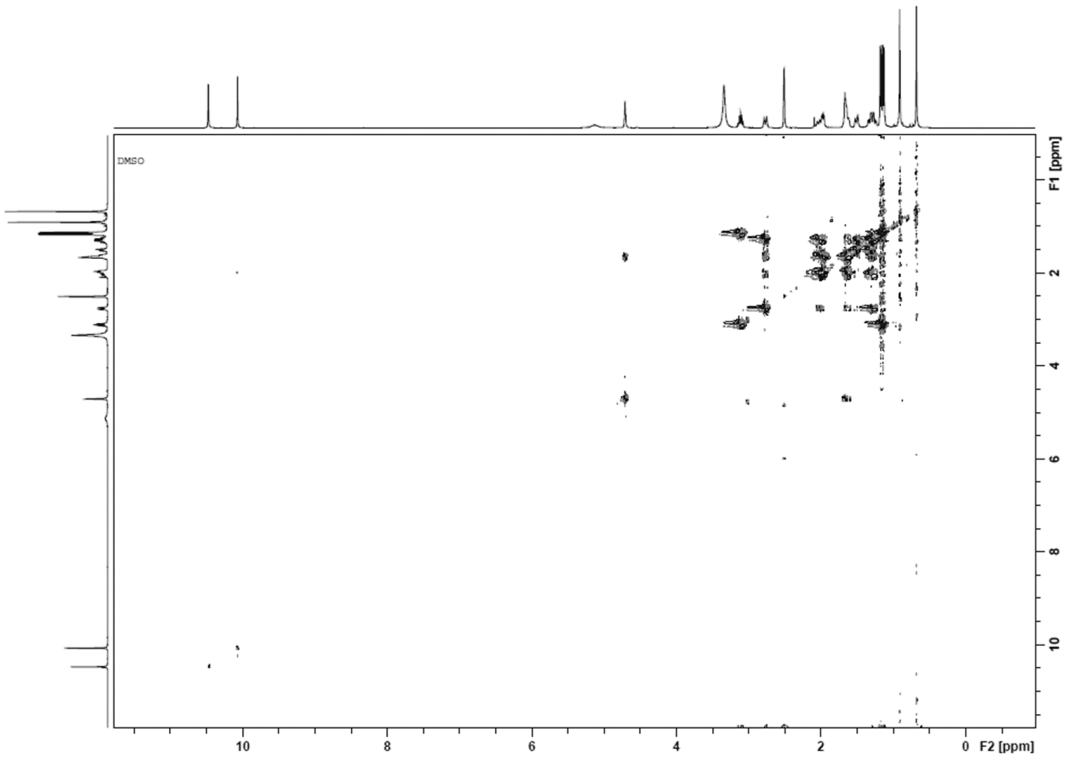

D)

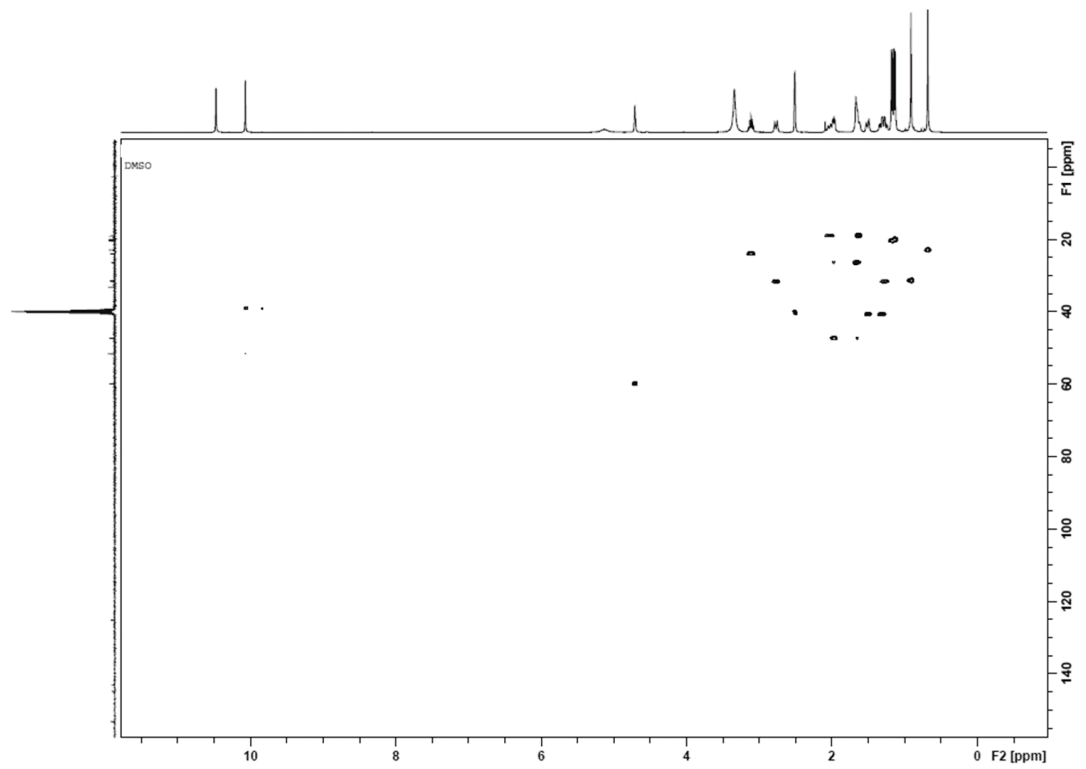

E)

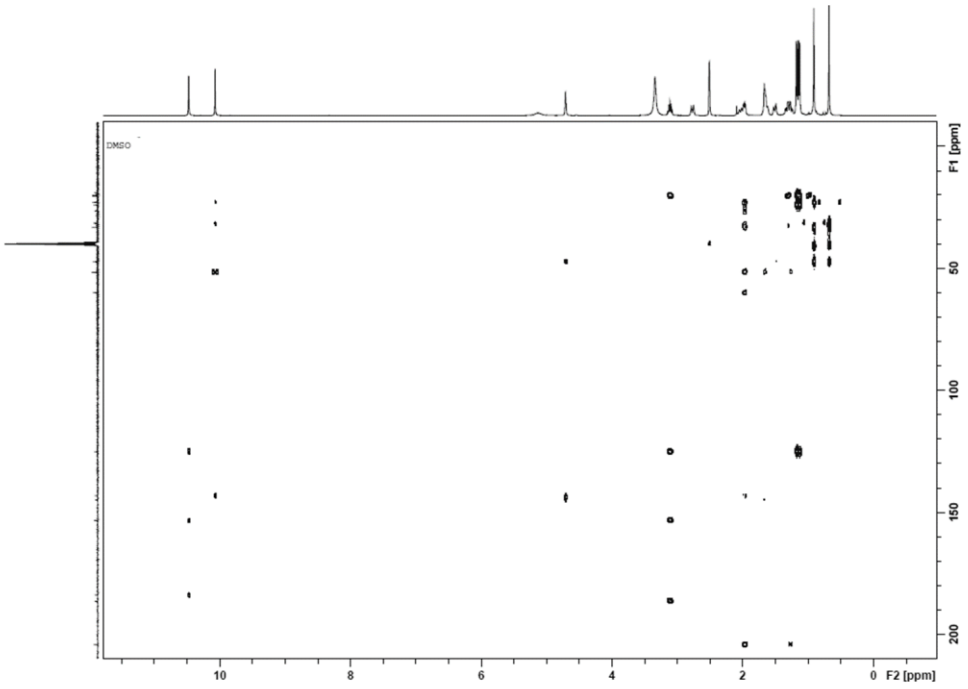

Figure A.1: The A) ^{1}H-NMR, B) ^{13}C-NMR, C) H-H COSY, D.) HSQC, and E) HMBC spectra of the abietane diterpenoid, deacetylnemorone (in DMSO-d6).

A)

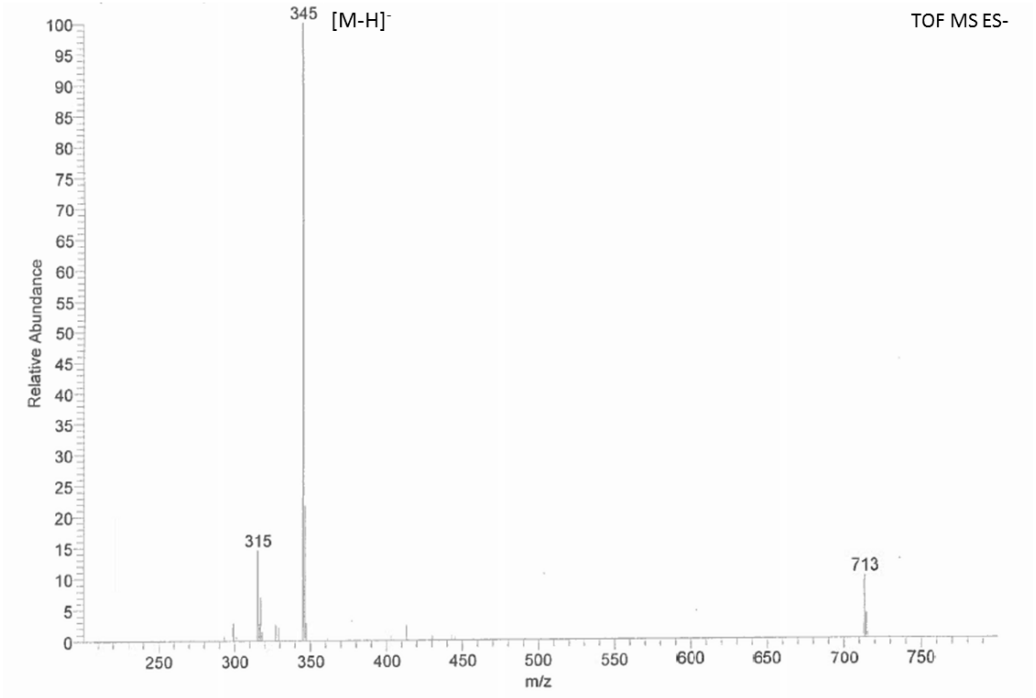

B)

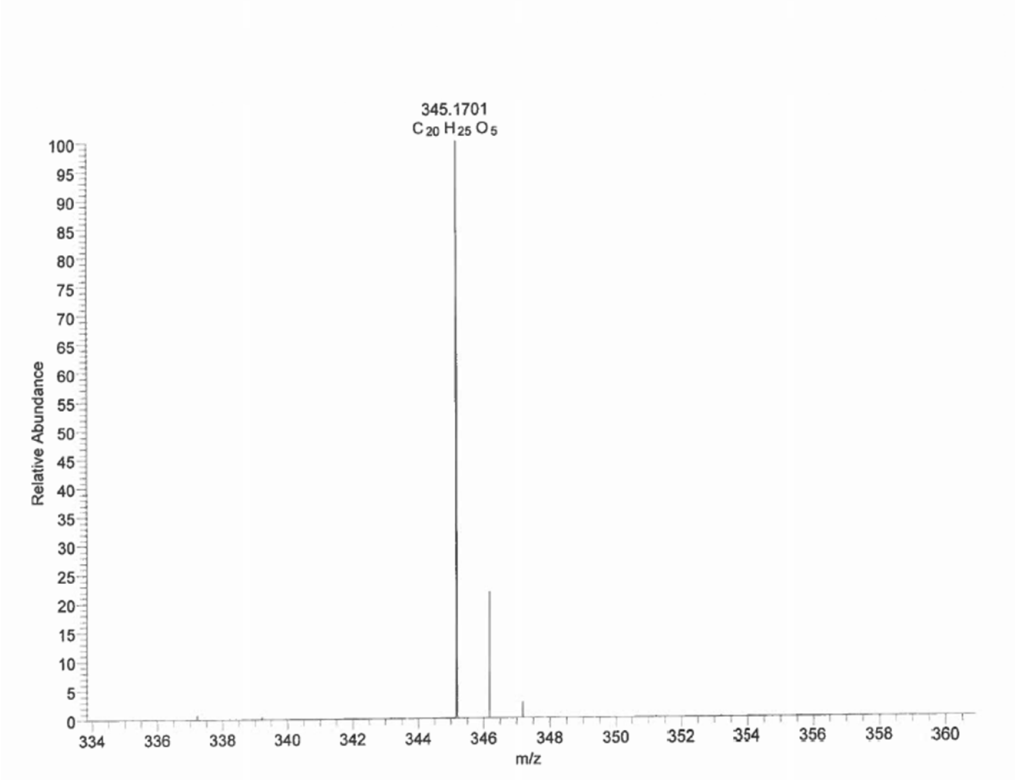

Figure A.2: The A) negative ion mode time of flight-mass spectrometry and B) negative mode HR-MS spectra of deacetylnemorone used to determine molecular weight.

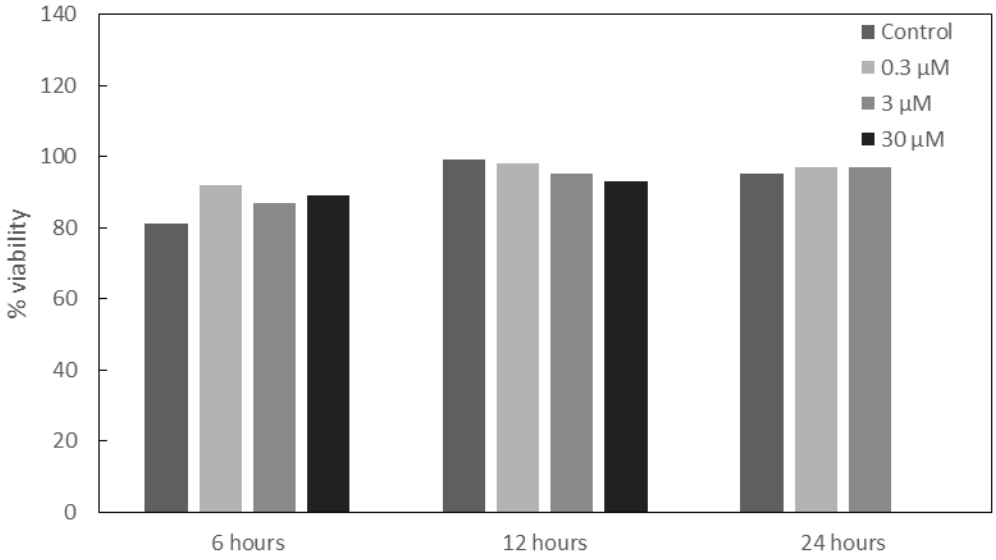

Figure A.3: Viability of SK-MEL-5 cells after 6, 12, or 24 hours of incubation with deacetylnemorone. The cells were seeded in 2 well culture inserts within 12 well culture plates and allowed to reach confluency before being treated with deacetylnemorone. Viability was determine by manually counting cells excluding trypan blue using a hemocytometer. (Note no data was collected for the 30µM concentration at 24 hours).

A)

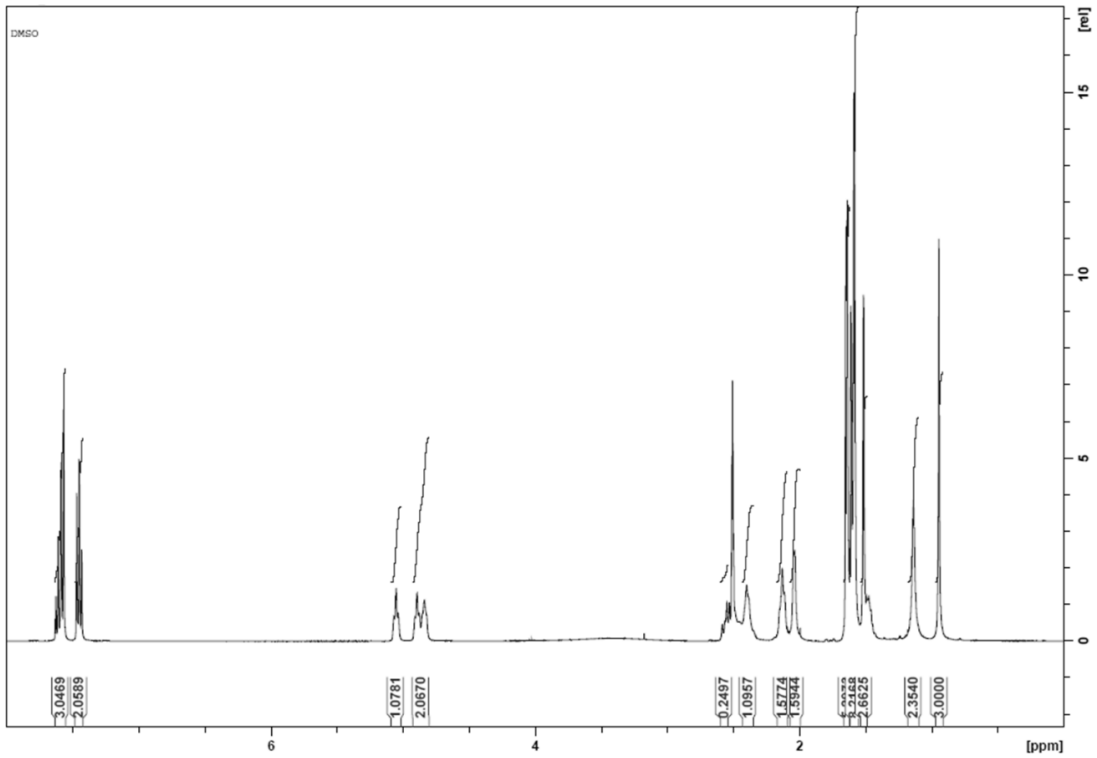
DMSO
[rel]
15
10
5
0
3.0469
2.0589
1.0781
2.0670
0.2497
1.0957
1.5774
1.5944
2.6625
2.3540
3.0000
6
4
2
[ppm]

B)

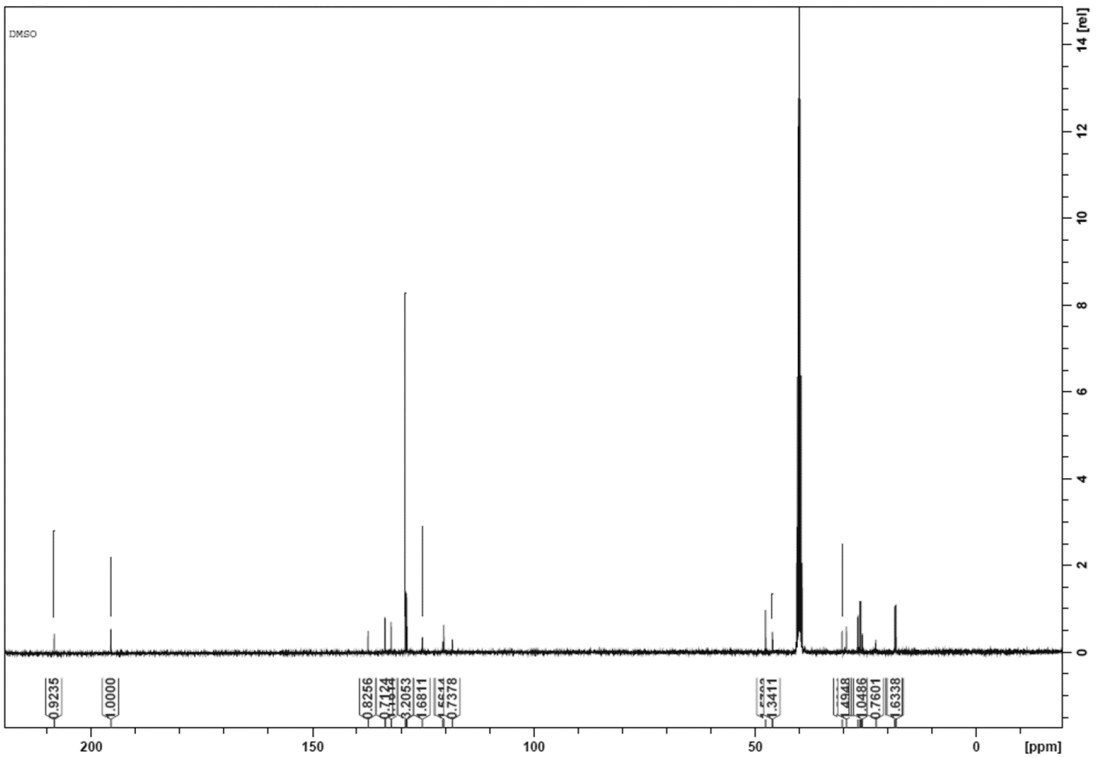
DMSO
14 [rel]
12
10
8
6
4
2
0
0.9235
1.0000
0.8256
0.7144
3.2053
1.6811
0.7378
1.3411
1.0486
0.7601
1.6338
200
150
100
50
0
[ppm]

C)

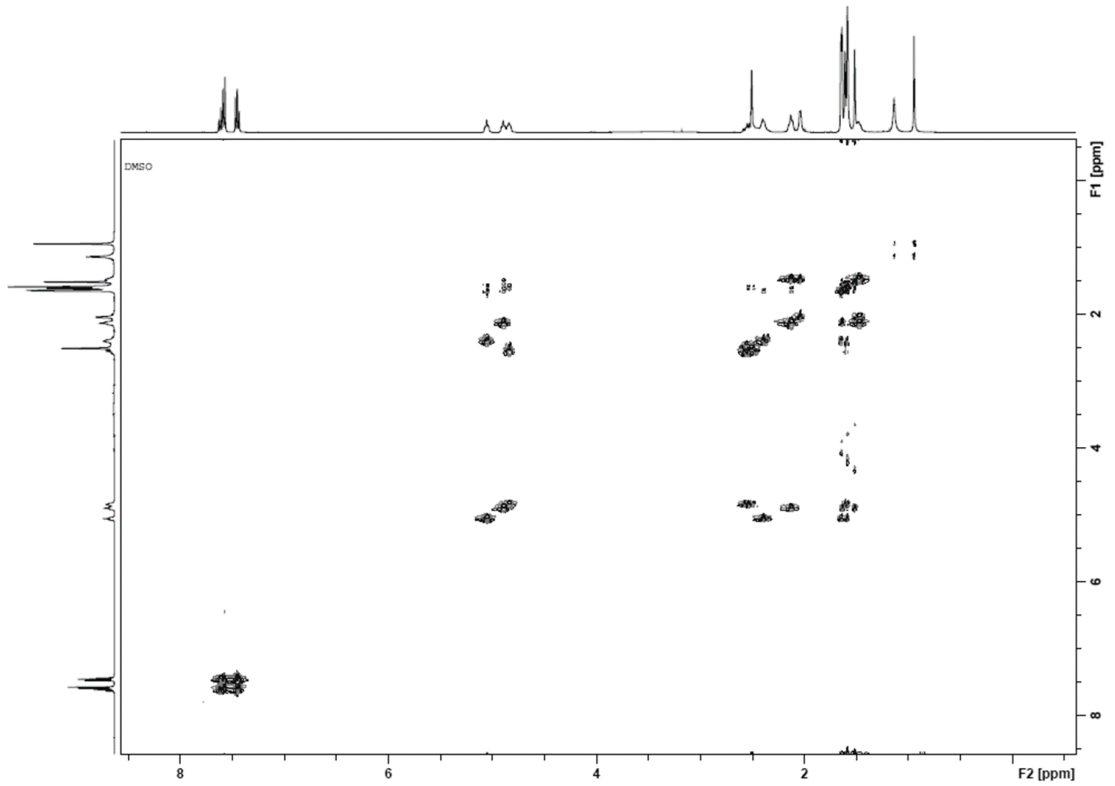

D)

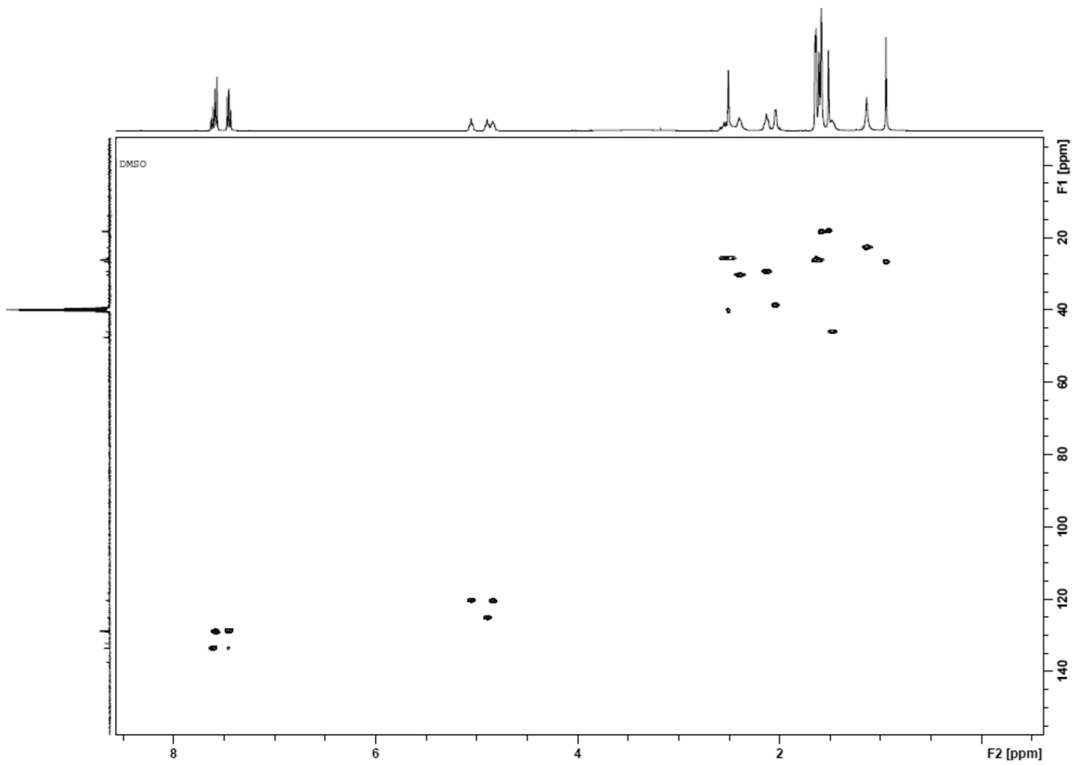

E)

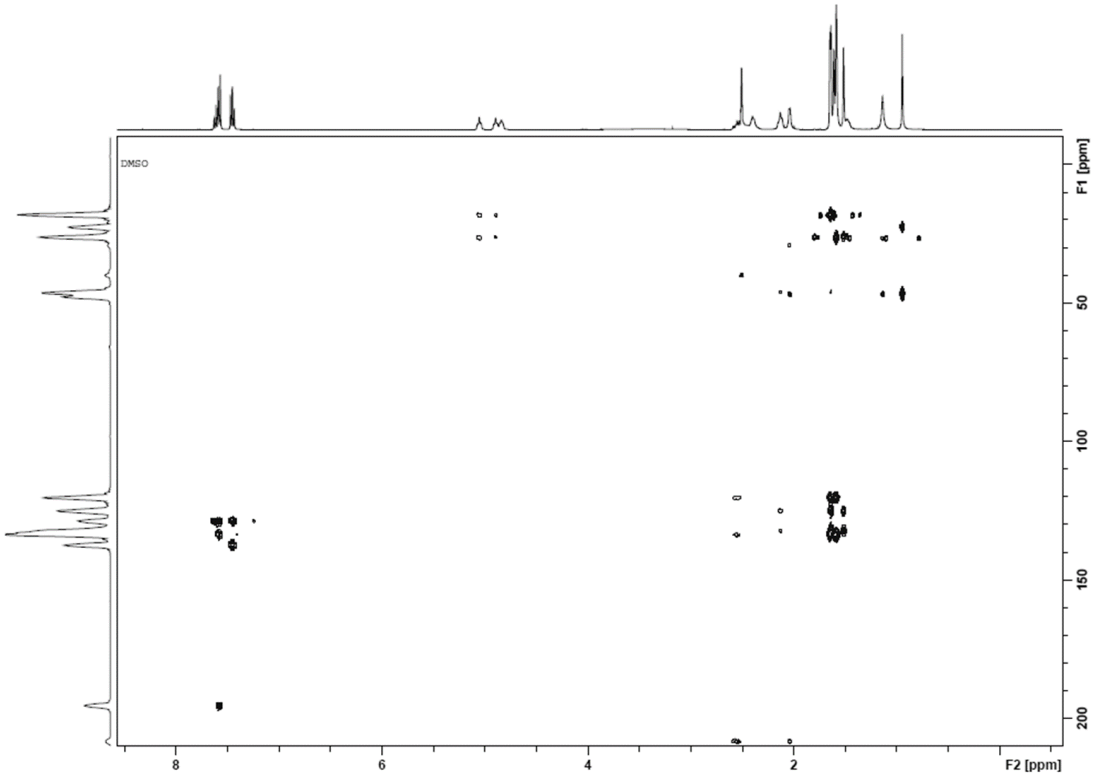

Figure A.4: The A) 1H-NMR spectrum, B) 13C-NMR spectrum, C) H-H COSY spectrum, D) HSQC spectrum, and E) HMBC spectrum of clusianone in DMSO.

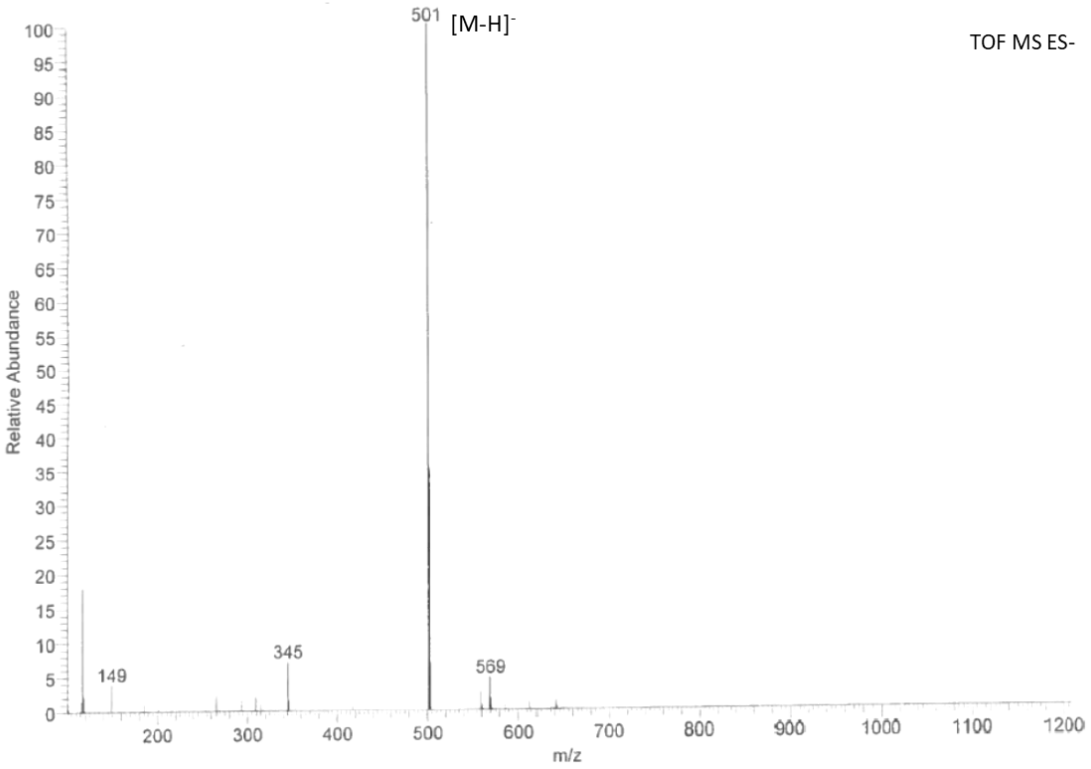

Figure A.5: Time of flight mass spectrum determination of molecular weight for clusianone.

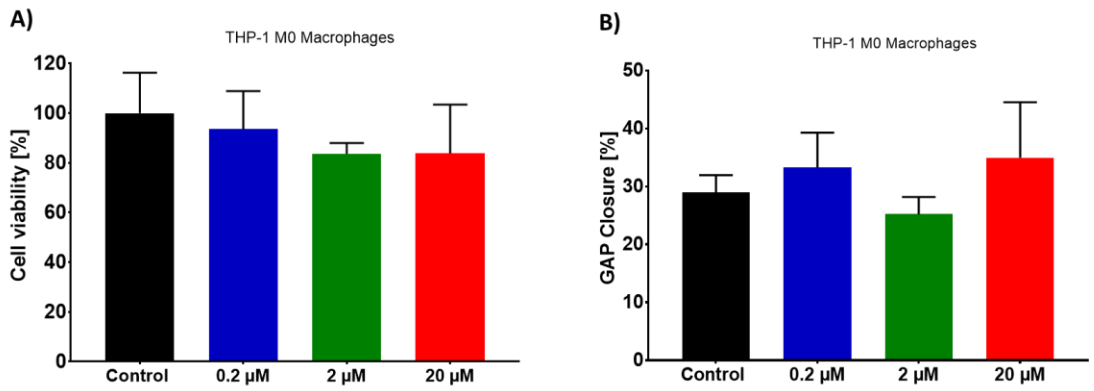

Figure A.6: Cell viability and invasion of macrophages in response to incubation with clusianone. The effect clusianone on A) the viability of THP-1 macrophages, as determined by the MTS assay, after 72 hours of exposure to a vehicle control or 0.2, 2, or 20 µM of clusianone, and B) the percent wound closure of THP-1 macrophages into a cell-free gap after 24-hour exposure to a vehicle control or 0.2, 2, or 20 µM of clusianone are shown.

APPENDIX B

PERMISSION TO REPRINT

The following screenshot from the website for *American Journal of Cancer Research* is provided for proof of permission to reprint "The use of natural products to target cancer stem cells" as a chapter of this thesis.

Copyright Policy

By submitting a manuscript to any of e-Century Publishing Corporation journal, all authors agree that all copyrights of all materials included in the submitted manuscript will be exclusively transferred to the publisher, e-Century Publishing Corporation once the manuscript is accepted.

Once the paper is published, the copyright will be released by the publisher under the "Creative Commons Attribution Noncommercial License", enabling the unrestricted non-commercial use, distribution, and reproduction of the published article in any medium, provided that the original work is properly cited. **If the manuscript contains a figure or table reproduced from a book or another journal article, the authors should obtain permission from the copyright holder before submitting the manuscript,** and be fully responsible for any legal and/or financial consequences if such permissions are not obtained.

All PDF, XML and html files for all articles published in this journal are the property of the publisher, e-Century Publishing Corporation (www.e-Century.org). Authors and readers are granted the right to freely use these files for all academic purposes. In addition, **the author has the right to reuse any materials in his/her own paper for any purpose without getting the permission from the publisher** provided that the original work is properly cited.By publishing paper in this journal, the authors grant the permanent right to the publisher to use any articles published in this journal without any restriction including, but not limited to academic and/or commercial purposes.

If you are interested in using PDF, html, XML files or any art works published in this journal for **any commercial purposes**, please contact the publisher at business@e-century.org.